LASER DAMAGE STUDY OF THIN FILMS

Final Technical Report

for the period

1 April 1965 - 1 April 1966

DEPARTMENT OF THE NAVY

OFFICE OF NAVAL RESEARCH

WASHINGTON, D.C. 20360

RESEARCH AND DEVELOPMENT

BAUSCH & LOMB INCORPORATED

ROCHESTER, NEW YORK 14602

Contract No. Nonr-4717(00)

1 April 1965

LASER DAMAGE STUDY OF THIN FILMS

Final Technical Report

for the period

1 April 1965 - 1 April 1966

Laser Damage Study of Thin Films

Contract No.	Nonr-4717 (00)
Order No.	ARPA Order 306
Project Code No.	4730
Name of Contractor	Bausch & Lomb Inc. Rochester, N.Y.
Date of Contract	1 April 1965
Amount of Contract	$28,520.00
Contract Expiration Date	31 March 1966
Project Scientist	Dr. A. F. Turner 716-232-2000 Ext. 296

Final Technical Report

For the period: 1 April 1965 - 1 April 1966

Report prepared by: J. Becker, W.F. Coombs and A.F. Turner

Table of Contents

List of Illustrations

List of Tables

LASER DAMAGE STUDY OF THIN FILMS

1.0 Introduction

Damage to optical surfaces and materials is often experienced in high intensity laser beams. The threshold values above which this damage occurs are of interest for both optical engineering and theoretical purposes. Information on thresholds in the literature appears very meager Cullom and Waynant[1] give values for internal damage in different glasses ranging from 0.2×10^{10} to 71×10^{10} watts/cm^2 for a pulse duration of 70 nsec. Atwood et al[2] report coated optical surfaces being damaged by 65 nsec. pulses with energy density thresholds in the range from 5 to 50 joules/cm^2 for different interference film coatings and coating materials.

Further work on damage thresholds for vacuum evaporated interference film coatings is important in view of their general use in high intensity laser instrumentation as anti-reflection films, beam dividers and so on. In the present work energy density thresholds were determined for single quarterwave and halfwave films vacuum evaporated on glass and quartz substrates. Using a 6 microsec. ruby laser pulse films of the following dielectric materials were studied: ThF_4, MgF_2, Al_2O_3, $5NaF.3AlF_3$, SiO_2, ZrO_2, TiO_2, CeO_2 and ZnS. Aluminum and Inconel films were also included. The latter were found to have thresholds around .05 joules/cm^2, whereas thresholds for the dielectrics covered the range from 50 down to 0.5 joules/cm^2, roughly in the sequence of the preceding listing.

1.1 Experimental Technique

The experimental technique for determing the damage threshold of a coated surface stems from the observation that the damage spots caused by a laser beam focused accurately

on the surface decrease in size with decreasing laser output. A plot of the radii of the spots against the energy incident is a smooth curve which can be extrapolated to zero radius to give the threshold value. The decrease in spot damage radius as threshold is approached is due to the shape of the energy density profile of the laser beam. It is peaked on-axis, about which it is roughly rotationally symmetrical, and falls of sharply with angle of divergence. The relative slope of the profile is maintained constant by holding the operating conditions for the laser constant. The total energy of a pulse incident on the sample is varied by use of density filters. At the rim of a damage spot the energy density is assumed to have the threshold value. Therefore, as the total energy focused on the surface is decreased with filters, the threshold value is found at intersections with the profile having smaller radii. Knowing the total energy under the curve from a monitoring calorimeter the experimental energy density profile can be analyzed to give the on-axis or peak energy density. This is the threshold for a damage spot of radius zero, as found by extrapolation from the sequence of radii.

This technique has the advantage of an averaging effect, making threshold determinations more objective and less dependent, we believe, on the subjective factors entailed in visual examinations of a surface for the last trace of damage. This is especially important in work with ruby laser beams which are characterized by inhomogeneities and sporadic filamentary energy spikes.

2.0 Test Equipment

2.1 List of Equipment

The major pieces of equipment used in this study were as follows:

1) LS-2 Lear-Siegler ruby laser installation
2) MH-1 Lear-Siegler Q-switch
3) MI-2 Lear-Siegler laser energy monitor
4) 585 Tektronix oscilloscope
5) C-27 Tektronix ultra-high rate oscilloscope camera

2.2 Description of Laser and Output

The Lear-Siegler ruby laser installation utilizes a 3" long by ¼" diameter ruby rod with a TIR end. The ruby is pumped by a helical flash lamp which is concentric with a cylindrical reflector. The ruby, flash tube and reflector have a common axis. The laser cavity is formed by the TIR end on the ruby and the dielectric mirror of the rotating Q-switch when the mirror moves into optical alignment. The Q-switch rotates at 3600 RPM. A schematic of the set-up is shown in Fig. 1. This arrangement produces a laser burst which consists of a series of spikes with a total duration of approximately 6 microseconds. Figure 2 shows a typical burst. Usually, a high initial spike (100 to 200 KW peak) is followed by a train of spikes much lower in intensity. The total energy of a burst is nominally 0.1 joule. The interval between bursts is several minutes, and the capacitor bank is charged to 2500 joules.

2.3 Sample Testing Arrangement and Procedure

The unfocused laser beam is not of sufficient intensity to damage the dielectric coatings studied. To increase the intensity sufficiently, a simple lens of 40mm focal length is used. The radii of curvature of the two surfaces of

this lens are in the ratio of about 8:1 to minimize spherical aberration. Its surfaces are anti-reflection coated. The surface of a sample to be tested is placed at the focus of this lens by auto collimation and kept in focus by focusing the microscope on the surface. The microscope is sensitive to axial motion of about 0.2 mm, so when the sample is moved laterally, an axial error in the sample position can be corrected by moving the sample back into focus in the microscope. The sample holder provides independent lateral and axial adjustments.

When testing a sample, it is normally placed at the focus with the coated side toward the laser. A different position of the sample is irradiated for each laser burst. Density filters are inserted in the beam ahead of the lens to control the total amount of energy falling on the sample The filters are used to reduce the intensity of the beam so that the firing conditions of the laser can be held as constant as possible. This procedure allows a series of damage spots to be obtained which provide data for plotting damage spot curves such as those in Figs. 8 through 40.

It is to be noted that power and energy could not be varied independently. The total energy incident on the sample was monitored for each burst.

3.0 Thermal Diffusivity

Thermal calculations indicate that the energy in the laser pulse is more than sufficient to vaporize all the film material within the observed damage spots. This is true of any film tested. The validity of the assumption that the threshold energy density for damage occurs at the periphery of the observed damage spot depends on the velocity of the thermal wave spreading outward from the damage spot.

The rate of energy input to the film is so high that a cloud of vapor at high temperature and pressure is formed by the leading edge of the laser pulse. This vapor cloud above the damage area may act as a specular reflector[3]. During most of the laser pulse the energy is being reflected by this vapor cloud. The film at the periphery of the damage area is raised to the vaporization temperature of this material at the very beginning of the pulse.

In the case of inconel and aluminum films the heat conduction radially outward in the film is the principal means by which the heat is carried away from the periphery of the damaged area. According to Jakob[4]

$$T = \frac{H}{4\pi L k T} \; e^{-r^2/4\alpha t}$$

where

T = temperature rise at a distance r away from a point source of heat.

L = film thickness

t = time

H = heat input

$\alpha = k/\rho c_\rho$

k = thermal conductivity

ρ = density

c_ρ = heat capacity

The maximum temperature at a given radius is obtained by maximizing T as a function of time at that radius. This yields

$$t(T_{max}) = r^2/4\alpha \qquad \text{and}$$

$$T_{max}(r) \quad \frac{\alpha H}{e\pi L k r^2}$$

The radial velocity of propagation of the temperature maximum T_{max} is

$$v = \frac{dr}{dt} = 4\alpha/r$$

At the outset the periphery of the damage spot is at T_{max} equal to the vaporization temperature of the material. This can be taken as the initial condition and the outward propagation can be determined.

Table 1 gives the cgs, bulk constant values of k, c_p, and ρ [5] for various film materials and the derived values of α.

TABLE 1

	k	c_p	ρ	α
Inconel	0.02	0.15	8.5	0.016
Aluminum	0.5	0.3	2.7	0.6
Al_2O_3	0.08	0.2	4.0	0.1
SiO_2	0.015	0.2	2.65	0.03
TiO_2	0.017	0.16	4.0	0.03
Zr_2O_3	0.004	0.11	5.7	0.006

The measured transmittances of the inconel and aluminum films were 0.07 and 0.30 respectively. Calculated thicknesses are 0.043 microns for inconel and 0.006 microns for aluminum. The velocities for the thermal wave obtained using the above formula were 0.13 microns per

microsecond for aluminum assuming a typical 100 microns damage spot radius. The inverse square dropoff of maximum temperature with radius implies that points close to the damage spot are subjected to relatively small temperature increase after the laser pulse.

The radial velocity of the thermal wave at 50 micron radii in various dielectric materials ranges from 0.8 microns per microsecond in aluminum to 0.05 microns per microsecond in zirconium dioxide. The velocity of the thermal wave in the substrate was calculated in a similar fashion and found comparable to the dielectric film velocities. During a pulse of several microseconds durations thermal spreading is negligible.

Thermal radiation from a black body disc the size of a typical damage spot (100 micron diameter) amounts to only 0.07 microjoules per microsecond at 3000°K. Thus, it appears that for pulses up to several microseconds duration, the heat loss from the damage area during the pulse is negligible. On the other hand, a laser without a Q-switch usually produces pulses of several millisecond duration. A Q-switched laser is needed for these measurements; but, a pulse duration as short as a few microseconds is sufficient.

4.0 Preparation and Properties of Evaporated Film Samples

4.1 Sample Preparation

The samples specially prepared for this study were made using glass and fused quartz substrates. These samples were single layer coatings with nominal optical thicknesses of $\lambda/4$ and $\lambda/2$ at 6943Å. Both electron beam evaporation and resistance heating were used. The details of preparation of the samples are given in Tables 2 and 3. Some samples were prepared using an oxygen bleed during evaporation. Oxygen pressure and substrate temperature are indicated in the tables.

TABLE 2

High Threshold Sample Preparation Details and Thresholds

Film Material	Sample	Film Thickness*	Substrated Material	O_2 bleed Pressure (Torr)	Method of Evaporation	Substrate Temp. (°C)	Threshold (joules/cm^2)
ThF_4	6-11-65, #3A	λ/4	glass	---	electron beam	370	47.0
n = 1.54	Thick ThF_4	λ/4 @ 6u	glass	---	e.b.		3.0
MgF_2	6-9-65, #2A	λ/4	glass	---	e.b.	370	42.0
n = 1.38	2-11-66,#1	λ/4	silica	---	e.b.	370	20.0
	6-9-65, #2	λ/4	glass	---	e.b.	370	16.0
	2-3-66, #21	λ/2	glass	---	e.b.	370	17.0
	2-17-66,#53	λ/2	silica	---	e.b.	370	7.5
Al_2O_3	6-25-65, #2	λ/4	silica	2.0×10^{-4}	e.b.	370	25.0
n = 1.62	12-27-65,#2	λ/4	glass	1.8	e.b.	370	26.0
	12-27-65.#2+	λ/4	glass	1.8	e.b.	370	21.0
	12-28-65,#2	λ/2	glass	No bleed	e.b.	370	43.0
	2-21-66,#34	λ/2	silica	1.8	e.b.	370	6.5
Chiolite	2-14-66,#81	λ/4	glass	---	resistance heating	85	21.0
n = 1.35	2-10-66,#71	λ/4	glass	---	r.h.	85	10.0
	10-18-65,#1C	λ/4 @ 2u	glass	---	r.h.	100	4.8
SiO_2	6-24-65,#4	λ/4	silica	---	e.b.	370	20.0
n = 1.45	12-28-65,#1	λ/2	silica	---	e.b.	370	38.0
	2-21-66,#23	λ/2	silica	---	e.b.	370	22.0

* minal optical thickness at 6943A unless otherwise specified.

+ Baked for 2 hours in air at 260° C.

TABLE 3

Low Threshold Sample Preparation Details and Thresholds

Low Threshold Sample Preparation Details and Thresholds

Film Material	Sample	Film Thickness*	Substrated Material	O_2 bleed Pressure (Torr)	Method of Evaporation	Substrate Temp. (°C)	Threshold (joules/cm^2)
ZrO_2	6-10-66, #1	$\lambda/4$	glass	2.0×10^{-4}	electron beam	370	14.0
	6-25-65, #1	$\lambda/4$	silica	2.0	e.b.	370	13.0
n = 1.95	2-22-66,#34	$\lambda/2$	silica	1.8	e.b.	370	8.5
	2-22-66,#42	$\lambda/2$	silica	1.8	e.b.	370	5.5
TiO_2	12-23-65, #3	$\lambda/4$	glass	1.8	e.b.	370	2.8
	12-23-65,#3A+	$\lambda/4$	glass	1.8	e.b.	370	10.0
n = 2.3	6-24-65, #3	$\lambda/4$	silica	2.0	e.b.	370	3.0
	12-22-65,#2A+	$\lambda/2$	glass	1.8	e.b.	370	3.5
	12-22-65, #2	$\lambda/2$	glass	1.8	e.b.	370	1.0
	12-22-65,#1A+	$\lambda/2$	glass	1.8	e.b.	370	3.5
	12-22-65,#1B	$\lambda/2$	glass	1.8	e.b.	370	3.5
	12-16-65,#54	$\lambda/2$	silica	1.8	e.b.	370	0.65
CeO_2 n = 1.74	6-11-65, #1	$\lambda/4$	glass	2.0	e.b.	370	10.0
ZnS	2-10-66,#62	$\lambda/4$	glass	---	resistance heating	85	3.0
n = 2.3	2-8-66, #12	$\lambda/2$	glass	---	r.h.	85	2.0
	2-10-66,#61	$\lambda/2$	glass	---	r.h.	85	1.5
Inconel	9-13-65,#1In.		glass	---	production	20	0.05
	2-23-66,#2In.		glass	---	production	20	0.06
Aluminum	1-26-66, #1		glass	---	r.h.	20	0.04

* Nominal optical thickness at 6943Å unless otherwise specified.

\+ Baked for 5 hours in air at 425°C.

4.2 Film Absorption

The amount of energy absorbed in a halfwave film compared with that absorbed in a quarterwave film is of interest. Because of multiple reflections this ratio is by no means 2 for films with identical absorption coefficients, despite the 2:1 ratio of physical thicknesses. Let there be a film of index n, and thickness h, between a substrate of index n_0 and a medium of incidence of index n. The Fresnel amplitude reflectance at the first film interface will be r_1, and at the second r_0. The absorption in the film is assumed weak with the intensity decreasing by the fraction $a = \exp(-\alpha h)$ upon passage through a distance h, in the material of the film. The absorptance in the film is given by A = 1-R-T where R and T are the measured reflectance and transmittance. For a halfwave film:

$$A_{hw} = N/(1+r_1 r_0 a)^2$$

and for a quarterwave film:

$$A_{qw} = N/(1-r_1 r_0 a)^2$$

where

$$N = (1-r_1^2)(1-a)(1+a r_0^2).$$

The absorptance ratio $A_{h/q}$ is then

$$A_{h/q} \equiv A_{hw}/A_{qw} = \left(\frac{1-r_1 r_0 a}{1+r_1 r_0 a}\right)^2.$$

This is identical with the ratio of the (measured) transmittance of a halfwave to a quarterwave film, since:

$$T_{hw} = \frac{a(1-r_1^2)(1-r_0^2)}{(1+r_1 r_0 a)^2}$$

$$T_{qw} = \frac{a(1-r^2)(1-r_0^2)}{(1-r_1 r_0 a)^2}$$

In the limiting case of no absorption, a = 1, this transmittance ratio can be evaluated in terms of the refractive indices:

$$A_{h/q} = \frac{T_{hw}}{T_{qw}} = \frac{1}{n_1^2}\left(\frac{n n_0 + n_1^2}{n + n_0}\right)^2 .$$

When the film absorption is very weak this expression gives the ratio of the energy absorbed in a halfwave film to that absorbed in a film one half as thick.

Example 1. Anti-reflection film with $n_0 > n_1 > n$.

Let n = 1.0
n_0 = 1.52
n_1 = 0.38
$A_{h/q}$ = 0.98

There is less absorption in the halfwave film despite its thickness being double that of the quarterwave film.

Example 2. Beam divider coating with $n_0 < n_1 > n$.

Let n = 1.0
n_0 = 1.52
n_1 = 2.4
$A_{h/q}$ = 1.45

The halfwave film absorbs only 45% more than the quarterwave film despite its double thickness.

Threshold measurements are probably not yet refined sufficiently to reflect these results accurately. Superficially they would indicate that the thresholds of halfwave films should be higher than of quarterwave films of identical materials, because there is less average absorption per unit volume of material in the former. This conclusion may however need to be modified after an analysis of the distribution of absorption within a film. It is non-uniform because of the standing wave component of the electric field.

4.3 Absorption Requirements for Thermal Damage

That portion of field damage which is due to thermal causes must depend on the coupling between the radiation and the film material via the absorption coefficient α, where $a = \exp(-\alpha h_1)$ as in the preceding section. By the Lambert-Beer law, the decrease in radiation power (intensity) W after traversing a distance dz is

$$\frac{dW}{W} = -\alpha\, dz .$$

The energy transferred to the film material in the path dz is $dE = -\tau\, dW$ where τ is the pulse duration. To ablate this amount of material the energy dE must at least equal dE_v, the energy required for vaporization:

$$dE_v = \left[\frac{\rho}{M} A \Delta H\right] dz$$

where ρ = density
M = gram molecular weight
A = cross sectional area of laser beam
ΔH = heat of vaporization per gram molecular weight

Equating $dE = dE_v$ we find

$$-a \ln a = \frac{1}{J}\left[\frac{\rho}{M} A \Delta H\right] h_1$$

where J is the total energy of the laser pulse.

This equation relates the material and thermodynamic constants of the film to the minimum absorption for vaporization. It is necessary but not a sufficient condition. The energy level to produce the required temperature rise must also be taken into account. This will not be done here since only the thermal energy balance and its demand on the absorption in the film is considered.

The heats of vaporization of ZnS and ZrO_2 are 63 k cal/mole and 165 k cal/mole respectively. Assuming an energy density of 100 joules/cm^2, which lies within the experimentally determined threshold range of values, it is found that a = .999 for a quarterwave ZnS film and a = .997 for a quarterwave ZrO_2 film. Film absorptances of only a few tenths percent thus need be involved in a thermal energy damage process. The determination of such minute trances of absorption would require precision spectrophotometry of the films of a very advanced nature and many "perfectly transparent" films could in reality be absorbing to this extent.

4.4 Spectrophotometric Transmittance Curves

The measured spectrophotometric transmittance curves of several of the film samples are given in Figs. 3 through 5. An absorption-free halfwave film on a substrate will have a transmittance equal to that of the uncoated substrate. A lower transmittance indicates absorption (when dealing with homogeneous films) and the film absorption is approximately equal to the difference in transmittance. Thus the halfwave TiO_2 shown in Fig. 3 has an absorptance of about 2% at 6943$\mathring{A}$.

The onset of strong ultraviolet absorption in the films is of interest because an apparent correlation was found between it and the laser damage thresholds, the more laser

resistant films having their cutoff wavelengths farther in the ultraviolet. The approximate wavelength positions for the beginning of this absorption are, from Figs. 4 and 5:

ZnS	3500A
CeO_2	3400A
TiO_2	3300A
ZrO_2	2300A
SiO_2	2100A
Al_2O_3	2000A
MgF_2	1200A

5.0 Beam Profile and Energy Density

Energy density incident at a point on the film is the basic quantity computed. The total energy in each laser pulse was measured by using a Lear Siegler MI-2 Laser Energy Monitor. The amount of this energy reaching the film was estimated by subtracting the reflections from the two surfaces of the focusing lens and applying the known optical densities of the filters.

The distribution of energy within the transverse section of the laser pulse is extremely complex as can be seen in Fig. 7. The major features of this beam profile are preserved from pulse to pulse. The following method was designed to obtain the iso-energy density contours within the beam profile and to provide the ratio of peak energy density to total pulse energy.

The method is based on the assumption that the damage observed at a point on the periphery of a damaged area is due only to the laser beam energy impinging on that point. The threshold energy density for damage occurs at all points on the periphery of the damage area on the film.

To assure repeatability of the beam profile from pulse to pulse, the operating conditions of the laser were the same for each pulse. The pulse energy at the film was varied by inserting neutral density filters in the laser beam after the energy monitor, but before the focusing lens. A series of damage spots similar to those shown in Fig. 7 were obtained using inconel and aluminum films. The actual energy density which would have been present at the periphery of the damage spot without the filter was obtained by dividing the threshold energy density by the transmittance of the filter used. In this way a series of iso-energy density beam profile contours was obtained. The energy density levels associated with these contours were in terms of threshold energy density.

A graphical integration of the energy density over the transverse beam cross section approximates the total pulse energy. This integration was accomplished by multiplying each incremental area between successive energy density contours by the arithmetic mean of the two energy densities associated with the two bounding contours. These products of incremental areas and average energy densities were then summed over the entire beam transverse section. This sum was then equated to the total pulse energy.

The limiting energy density contour for the graphical integration was the periphery of the damage spot obtained when no filter was used. The size of this damage spot was approximately the same as that obtained using blackened film as the target. The assumption used is that all the pulse energy is contained within this limiting energy density contour.

The pulse energy varied slightly from shot to shot; so, for this integration, the energies were normalized to 0.1 joules. The integration resulted in a ratio between the threshold energy density and the total pulse energy. The energy density associated with the highest iso-energy contour was assumed to be the peak energy density. It is expressed in terms of a constant times the threshold energy density. To obtain the ratio of peak energy density to total pulse energy, it was only necessary to multiply the ratio of threshold energy to total pulse energy by this factor.

The following quantities were used in the actual calculations:

E = energy density at the film
J = energy at the film
J_s = standard energy
E_t = threshold energy density
E_p = peak energy density
ΔA_i = incremental area between contours (i) and (i+1)
$K = E_p / E_t$

The average normalized energy density in ΔA_i is

$$\frac{1}{2}\left[\frac{E_t J_s}{J_i T_i} + \frac{E_t J_s}{J_{i+1} T_{i+1}}\right]$$

The energy in ΔA_i is

$$\frac{1}{2}\left[\frac{E_t J_s}{J_i T_i} + \frac{E_t J_s}{J_{i+1} T_{i+1}}\right] \Delta A_i$$

and the total energy incident on the sample is

$$J_s = \sum_{i=1}^{n} \frac{1}{2}\left[\frac{E_t J_s}{J_i T_i} + \frac{E_t J_s}{J_{i+1} T_{i+1}}\right] \Delta A_i$$

The ratio of peak energy density to total energy is

$$\frac{E_p}{J_s} = \frac{K E_t}{J_s} = \frac{K}{\sum_{i=1}^{n} \frac{1}{2}\left[\frac{J_s}{J_i T_i} + \frac{J_s}{J_{i+1} T_{i+1}}\right] \Delta A_i}$$

The calculated value is

$$\frac{E_p}{J_s} = 72.5 \quad \frac{\text{joules/cm}^2}{\text{joule}}$$

and the ratio

K = 1440

TABLE 4

Beam Profile Data

(obtained from aluminum film sample 1-26-66, #1)

Spot No.	i	Area (cm^2)	ΔA_i (cm^2)	$\frac{J_s}{J_i T_i}$	$\frac{1}{2}\left[\frac{J_s}{J_i T_i}+\frac{J_s}{J_{i+1} T_{i+1}}\right]$	$\frac{1}{2}\left[\frac{J_s}{J_i T_i}+\frac{J_s}{J_{i+1} T_{i+1}}\right] \times \Delta A_i$
28-28	1	9.0×10^{-4}	39.2×10^{-4}	0.935	1.21	47.4×10^{-4}
28-32	2	54.8	19.2	1.49	2.18	41.9
28-36	3	35.6	13.5	2.87	5.77	78.0
28-38	4	12.1	2.1	8.65	12.5	26.3
28-44	5	10.0	1.2	16.5	19.1	22.9
31-28	6	8.8	1.4	21.7	25.1	35.1
31-30	7	7.4	1.5	28.5	38.3	57.4
31-35	8	5.9	1.9	48.2	75.1	143.0
31-37	9	3.7	1.2	102	137	164.5
31-42	10	2.8	1.5	173	227	340.0
34-29	11	1.30	0.45	282	338	152.0
34-31	12	0.85	0.54	395	627	337.5
34-39	13	0.312	0.234	860	1010	236.0
34-45	14	0.078	0.052	1160	1300	67.7
34-46	15	1.026	0.026	1440	1440	36.9
no damage	16	0.000	---	1440	---	---

$$\sum_{i=1}^{15} = 1786.6 \times 10^{-4} \text{ cm}^2$$

6.0 Experimental Determinations of Damage Thresholds E_t

6.1 Damage Spot Curves

The experimental damage spot curves for all films tested are shown in Figs. 8 - 40. The spot radii are plotted as ordinates against peak energy densities as abscissae. The best curve was drawn through the experimental points and extrapolated to zero radius to give the threshold value E_t. Summaries of the values thus obtained are contained in Fig. 41 for the quarterwave films, and in Fig. 42 for the halfwave films. Thresholds range from 2 joules/cm^2 for Zns to 50 joules/cm^2 for ThF_4.

6.2 Qualitative Description of Low Threshold Damage Spots

The most thoroughly investigated material was TiO_2. One quarter and one half wave samples on both glass and fused silica substrates were tested. TiO_2 films have a relatively low threshold, and typify the damage which occurs to films classified as low threshold in this report.

The most salient feature of low threshold films is that damage seems purely thermal. The heating effects cause melting and vaporization. Examination of damage under high magnification reveals much evidence which points to this, for example: 1) debris scattered around high energy shots is often found in the form of beads oriented in a radial direction, 2) the pattern of the beam spot is always "burned" into the substrate in the center of a damage spot where all the film material has been removed, 3) removal of absorption in TiO_2 films by baking in air causes a pronounced corresponding increase in damage thresholds.

The damage (at incident energy levels near threshold) which occurs on low threshold films is in general simpler to describe than that on high threshold films. With the former it consists of an irregularly shaped spot with a fairly

definite boundary. The film is removed from the substrate in the central area and the surface of the substrate is disfigured. This disfigured surface reveals the complex cross sectional pattern of the beam spot.

The description of damage at the periphery of the spot varies somewhat between samples of the same or different materials. This is especially true of TiO_2 when comparing samples which have been baked in air for five hours at 425°C to unbaked samples. Figs. 43 and 44 illustrate this difference. At the periphery of spots on unbaked samples, there is a relatively narrow region where the film has been removed without damage to the substrate. This is most pronounced in high energy shots. The edges of damage spots on baked samples do not contain this region, whether or not measurable absorption was initially present before baking.

TiO_2 films initially with a measurable amount of absorption at the ruby wavelength demonstrated a dependence of threshold on baking. Absorbing films showed less absorption at the ruby wavelength (6943Å after baking and also a corresponding increase in threshold. This suggests that if there is a two photon process involved in film damage, for low threshold films it is outweighed by absorption at 6943Å. Half the ruby wavelength is at a point in the ultraviolet cutoff region of TiO_2, where there is a considerable amount of absorption. On a percentage basis, the absorption of a TiO_2 film hardly changes at half the ruby wavelength, but changes a great deal (several hundred per cent in some cases) at the ruby wavelength.

Film materials categorized as low threshold in this study are TiO_2, ZrO_2, CeO_2, ZnS, aluminum and inconel. The thresholds of aluminum and inconel. The thresholds of aluminum and inconel films are an order of magnitude lower than those of low threshold dielectrics; they also are absorbing to a relatively great extent.

Damage to films of ZrO_2 and CeO_2 appears to be identical to damage to TiO_2 films except for threshold.

The appearance of damage in ZnS films varies somewhat from that in TiO_2 films. ZnS films have a lower threshold and appear to have poorer adherence than the other low threshold films. Poorer adherence properties are evidenced by flaking at the periphery of damage spots and by the fact that large irregularly shaped damage spots are produced by high energy shots. (See Fig. 47).

6.3 Qualitative Description of High Threshold Damage Spots

Film materials classified as high threshold in this report are: ThF_4, MgF_2, Al_2O_3, Chiolite and SiO_2. The type of damage produced on high threshold films varies somewhat and is more inconsistent than that of low threshold films. The most typical type of damage to high threshold films occurs in damage spots where much of the film is removed from the substrate without damaging it. Apparently more than simple thermal damage is involved here because damage spots show evidence of film having been torn off without first melting and vaporizing. This may explain the steeper slope of most high threshold damage curves, since film material can be torn away to greater radii than vaporization would occur. Fig. 49 shows a typical example of this type of damage. Fig. 50 shows removal of a relatively thick film with little damage to the substrate. Cracking and lifting of the film at the edge of the damage spot is evident. The size of a damage spot is less predictable on a high threshold film than on a low threshold film.

The process by which damage occurs may be partly acoustical. That an acoustic process does enter the picture is supported by the fact that chipping often occurs at the rear of the substrate. Chipping is relatively rare on substrates of low threshold coatings.

6.4 Correlation of Ultraviolet Cutoff with Threshold

An interesting observation is that the position of the ultraviolet cutoff of the dielectric film materials tested, cf Section 4.6, correlates in general with their maximum thresholds. It is true that the closer the ultraviolet cutoff is to the visible region, the more residual absorption there is for that material in the visible region. It is true also that only a slight amount of absorption is needed (by calculation and by extrapolation of data from inconel and aluminum damage) to produce vaporization. Therefore it would not be surprising that damage threshold correlates with the ultraviolet cutoff if no other factors affect absorption. It may be possible to ascribe the erratic behavior of the high threshold films to slight amounts of absorption (undetectable by conventional spectrophotometric measurements) due to extraneous causes (e.g. contamination on the substrate underneath the coating). Some samples do show damage which suggests this. (See Figs. 48 and 51.)

7.0 Conclusions

A. Using a 6 microsecond pulse the damage thresholds of quarterwave films on glass and quartz to ruby laser radiation were found to be:

ZnS	3 joules/cm^2
CeO_2	10 joules/cm^2
TiO_2	11 joules/cm^2
ZrO_2	12 joules/cm^2
SiO_2	20 joules/cm^2
$5NaF.3AlF_3$	20 joules/cm^2
Al_2O_3	25 joules/cm^2
MgF_2	40 joules/cm^2
ThF_4	45 joules/cm^2

For comparison, the damge thresholds for semitransparent films of Aluminum and Inconel were approximately 0.05 joules/cm^2.

B. The quoted threshold values may not be intrinsic to the material of the films, but rather be characteristic of the film-substrate combination, including any special characteristics of the substrate surface such as could be due to polishing, cleaning and vacuum coating preparation.

C. Halfwave films of the same materials tended to have slightly lower thresholds.

D. The damage threshold sequence parallels to some extent the sequence of ultraviolet cutoff wavelengths of the materials, the highest thresholds being obtained in films with the shortest wavelengths of their ultraviolet absorption edges.

C. Absorptances of a few tenths percent would account for sufficient energy absorption from the laser beam to produce damage by thermal vaporization.

References

1. J.H. Cullom and R.W. Waynant, "Determination of Laser Damage Thresholds for Various Glasses," Appl. Optics 5, 539 (1964).

2. The Perkin-Elmer Corporation, Electro-Optical Division, Norwalk, Connecticut; TR-7945, Final Report, "Research into the Causes of Laser Damage to Optical Components".

3. R.W. Minck and W.G. Rado, "Optical Frequency Plasma Resonance in Gasses," J. Appl.Phys. 37, 355 (1966).

4. M. Jakob, Heat Transfer, Vol. I, (Wiley and Sons, New York, 1949), p. 341.

5a. Goldsmith, Waterman,and Hirschhorn, Handbook of Thermo Physical Properties of Physical Materials, (MacMillan, New York, 1961).

5b. "Properties of Some Metals and Alloys" (Int. Nickel Co. publication).

6. D.W. Harper "Laser Damage in Glasses," Brit. J. Appl. Phys. 16, 751 (1965).

7. C.R. Giuliano, "Laser Induced Damage to Transparent Dielectric Materials," Appl. Phys. Letters 5, 137 (1964).

TEST SET-UP

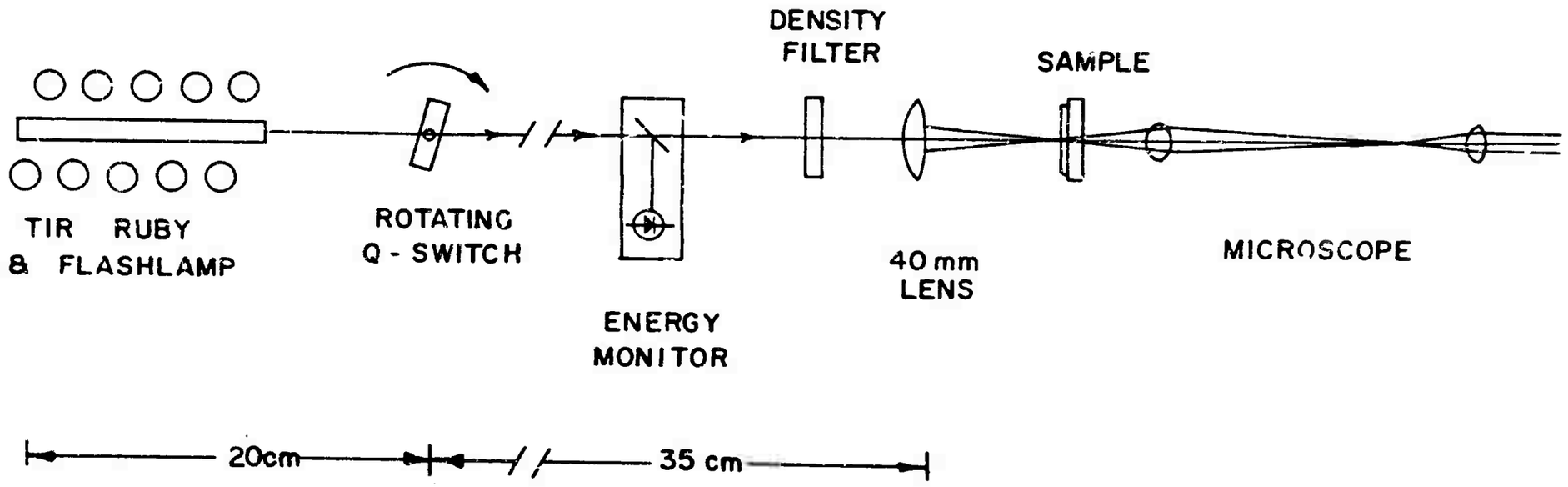

FIG. 1

SPIKING PATTERN

(typical pulse)

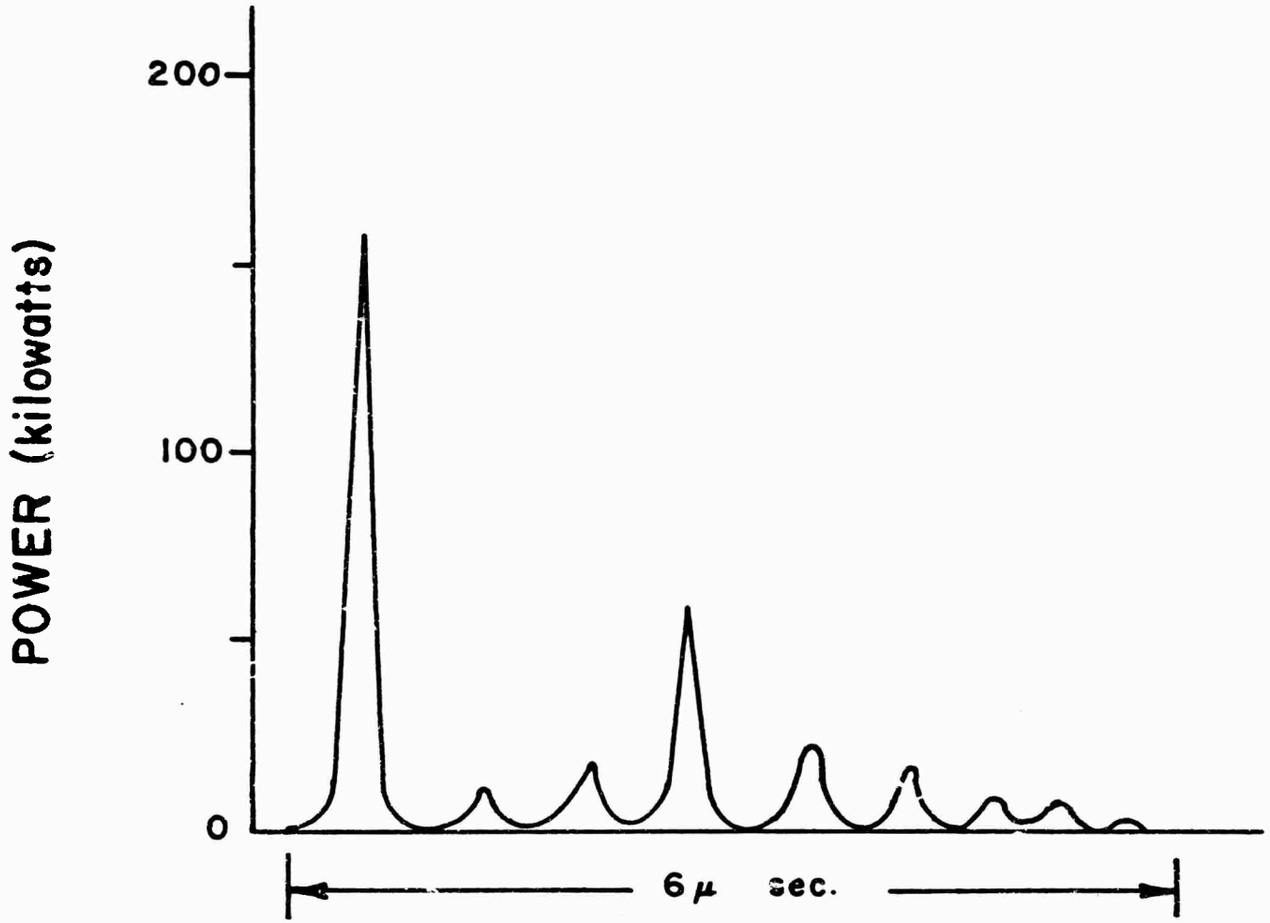

FIG. 2

TRANSMISSION OF $\lambda/4$ AND $\lambda/2$ THICKNESSES OF TiO_2 FILMS ON SILICA SUBSTRATES

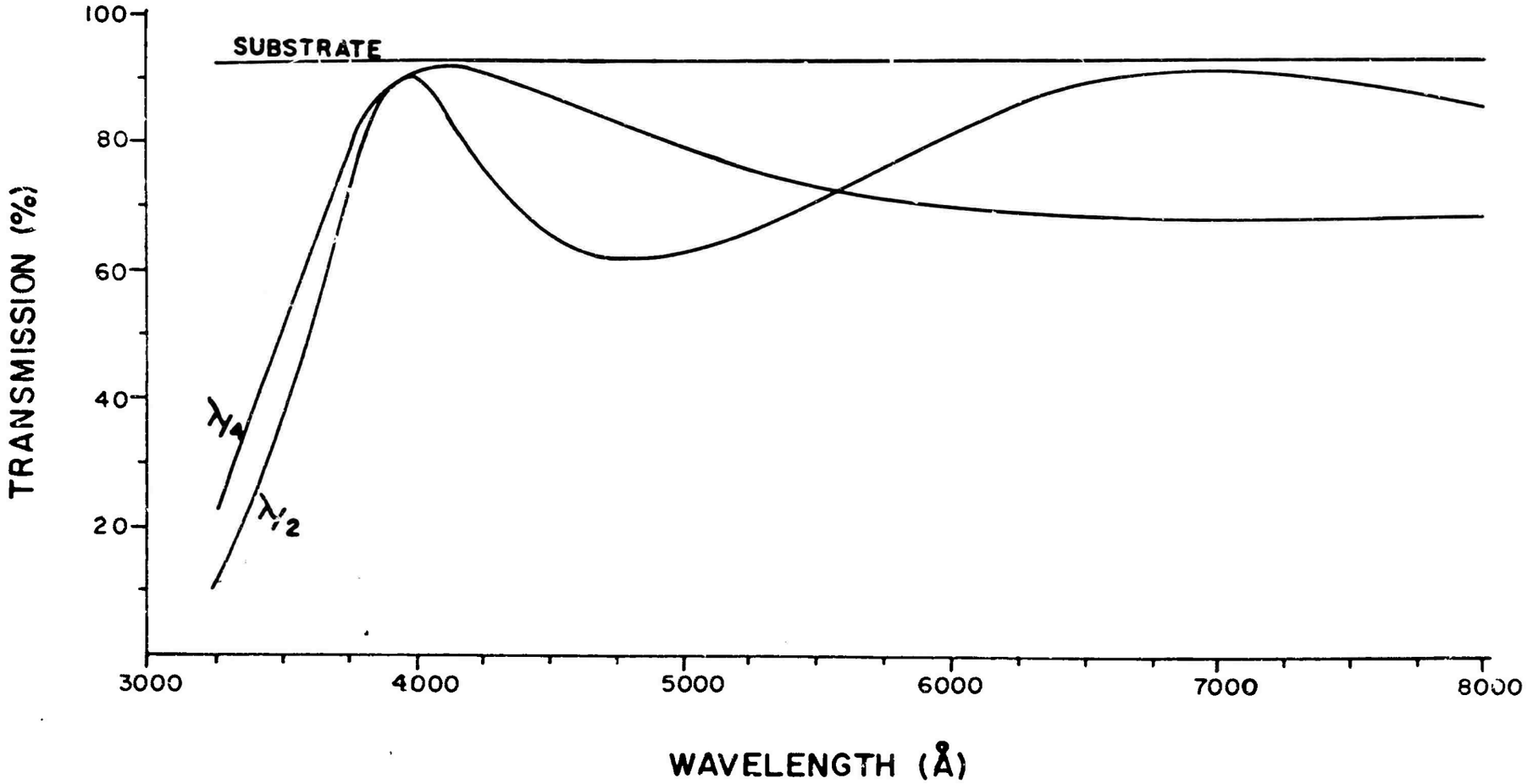

FIG. 3

TRANSMISSION OF $\lambda/2$ THICK FILMS ON SILICA SUBSTRATES

1 - 3mm THICK SILICA SUBSTRATE
2 - MgF_2; SAMPLE 2-17-66, # 53
3 - Al_2O_3; SAMPLE 2-17-66, # 34
4 - SiO_2; SAMPLE 2-21-66, # 23
5 - ZrO_2; SAMPLE 2-22-66, # 42

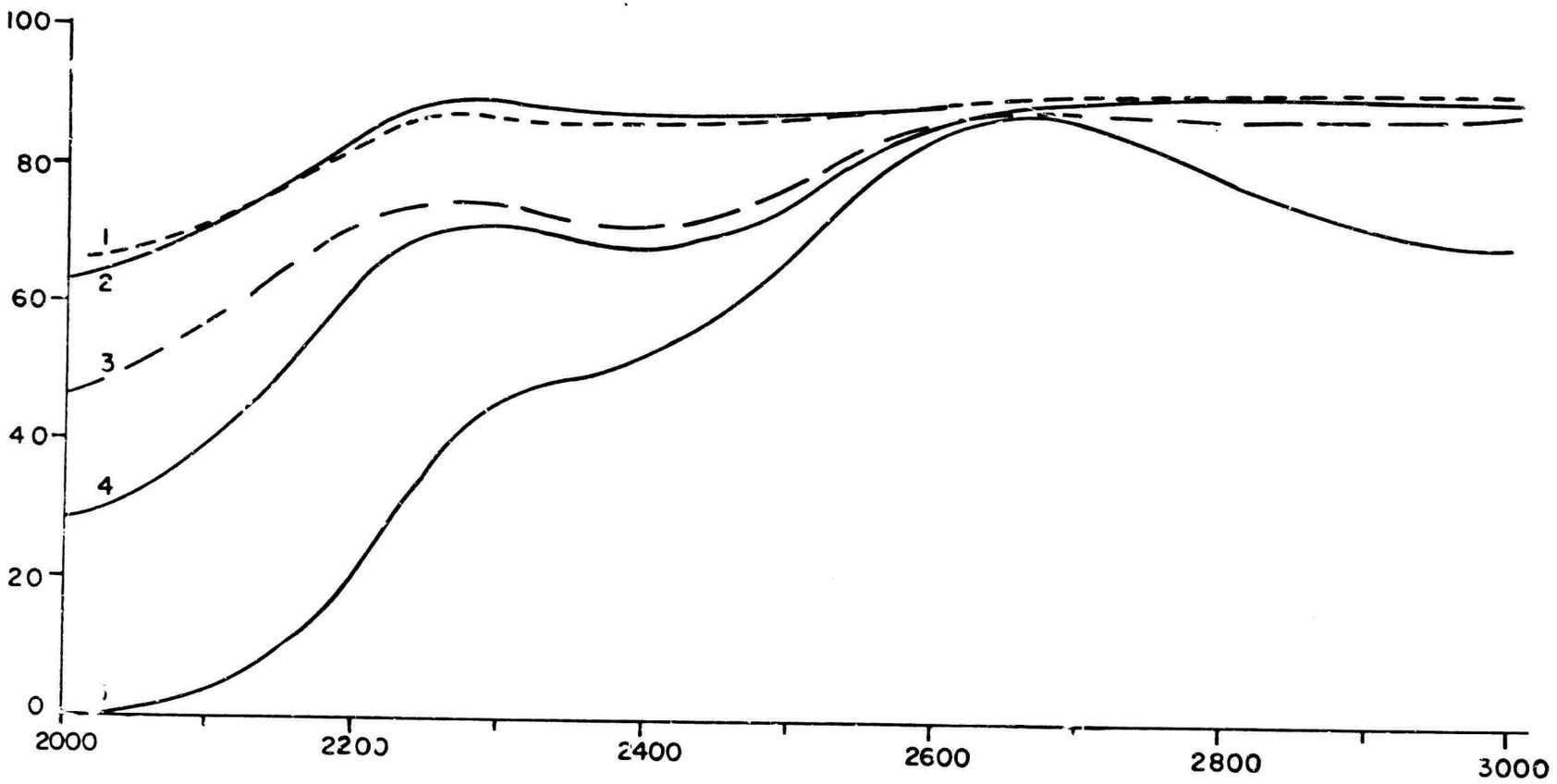

FIG. 4

TRANSMISSION OF $\lambda/4$ THICK FILM ON GLASS SUBSTRATES

1 - 2mm THICK GLASS SUBSTRATE
2 - CeO_2; SAMPLE 6-11-65, # 1
3 - TiO_2; SAMPLE 12-23-65, # 3A
4 - ZnS; SAMPLE 2-10-66, # 62

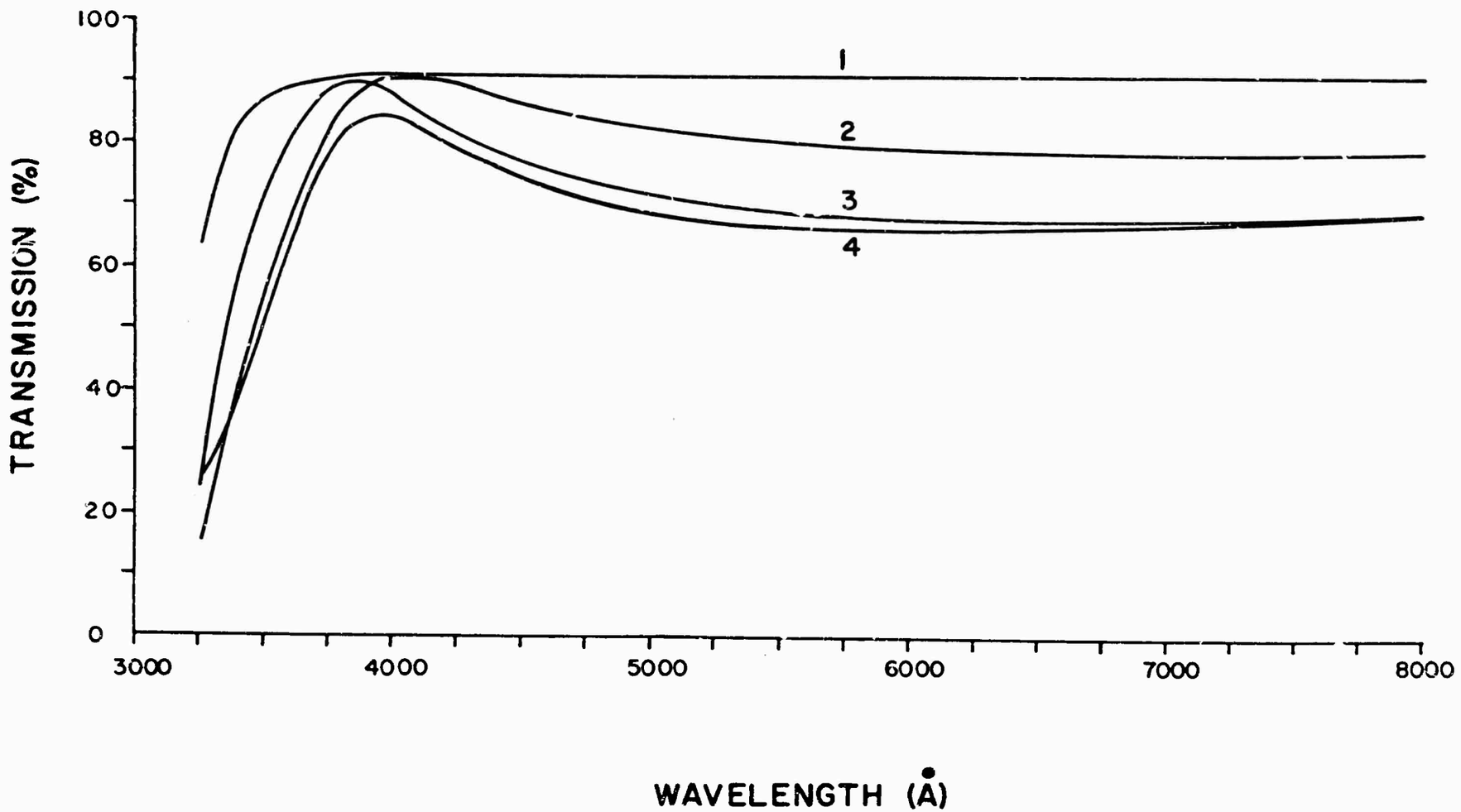

FIG. 5

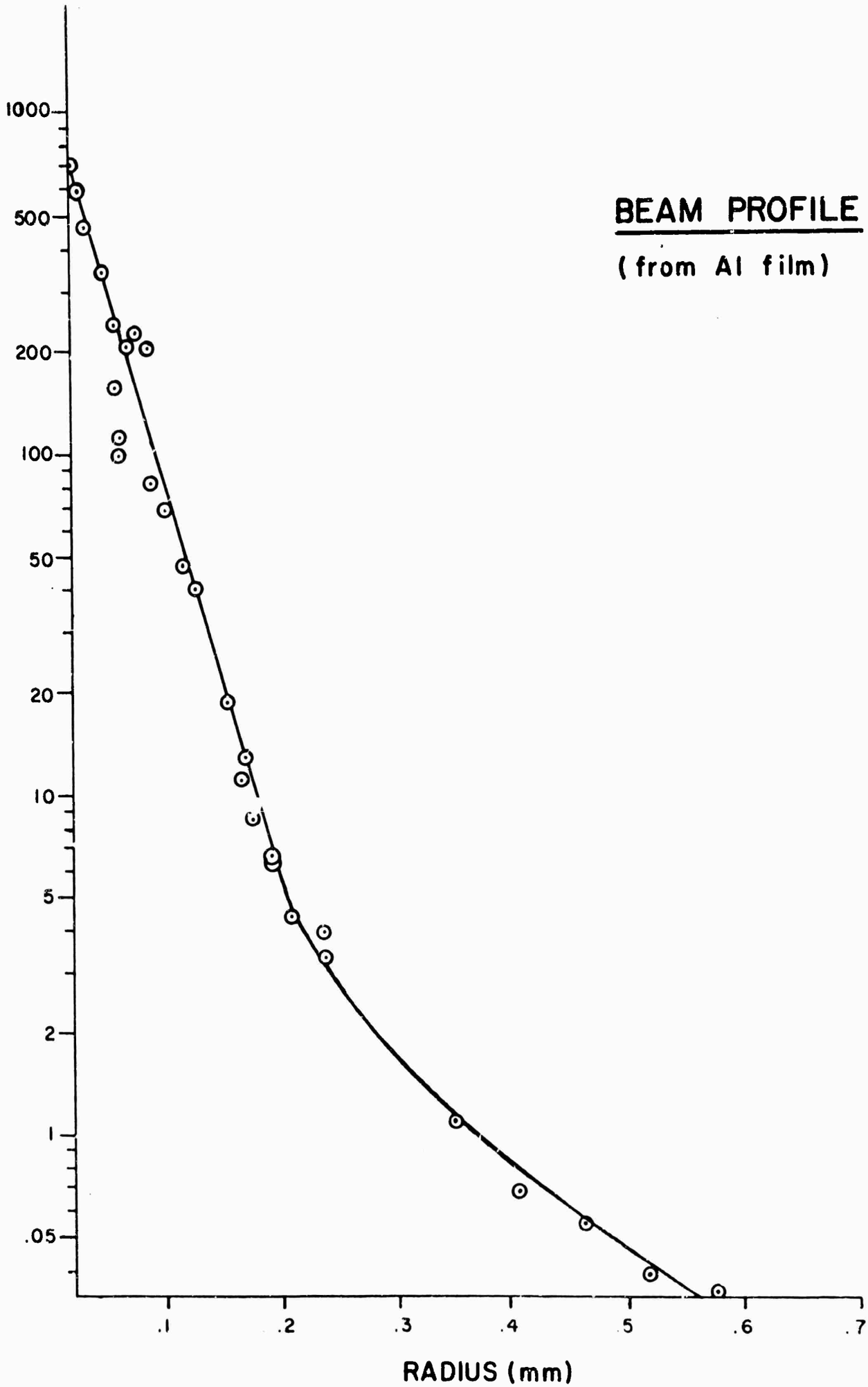
BEAM PROFILE
(from Al film)
1000
500
200
100
50
20
10
5
2
1
.05
.1
.2
.3
.4
.5
.6
.7
RADIUS (mm)

FIG. 6

ENERGY DENSITY CONTOURS

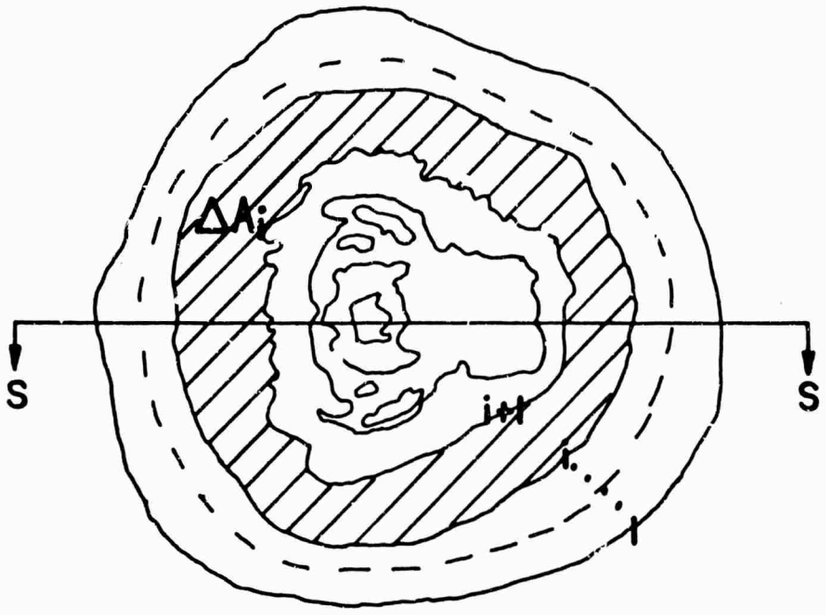

CROSS-SECTION S-S

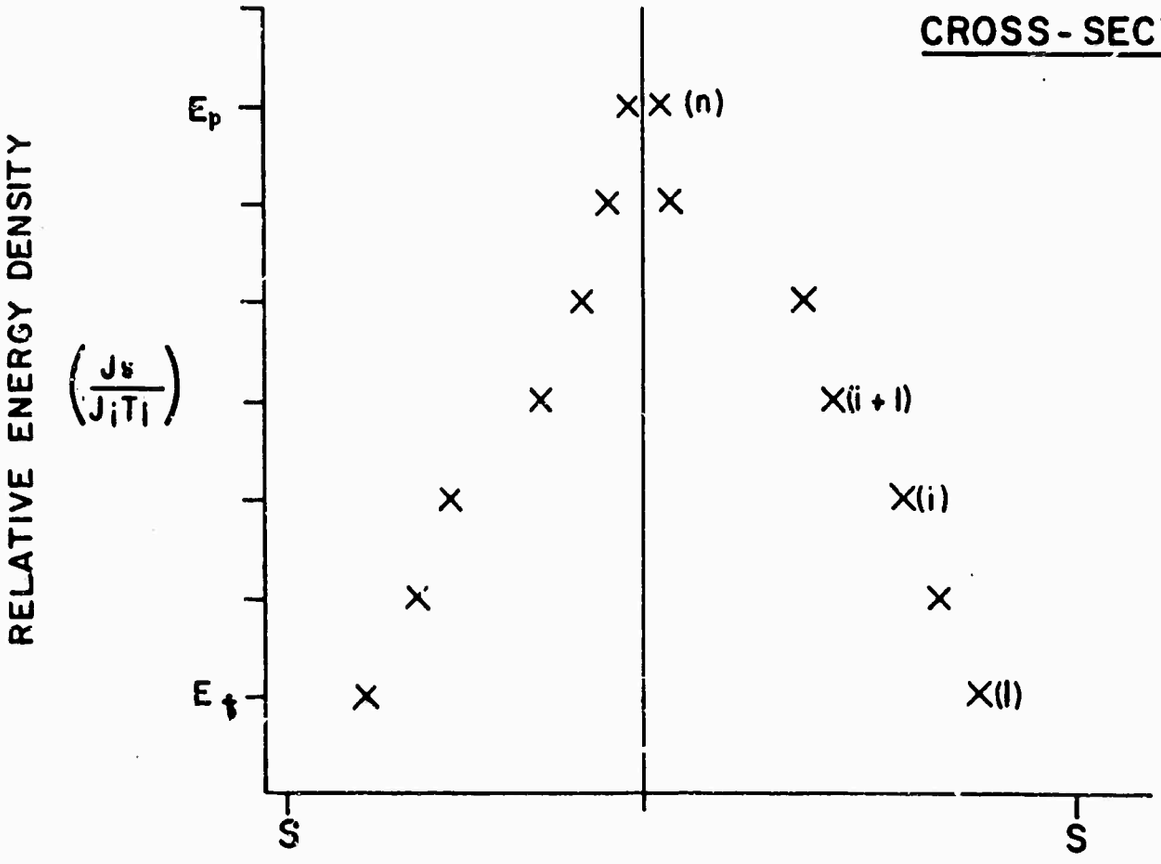

FIG. 7

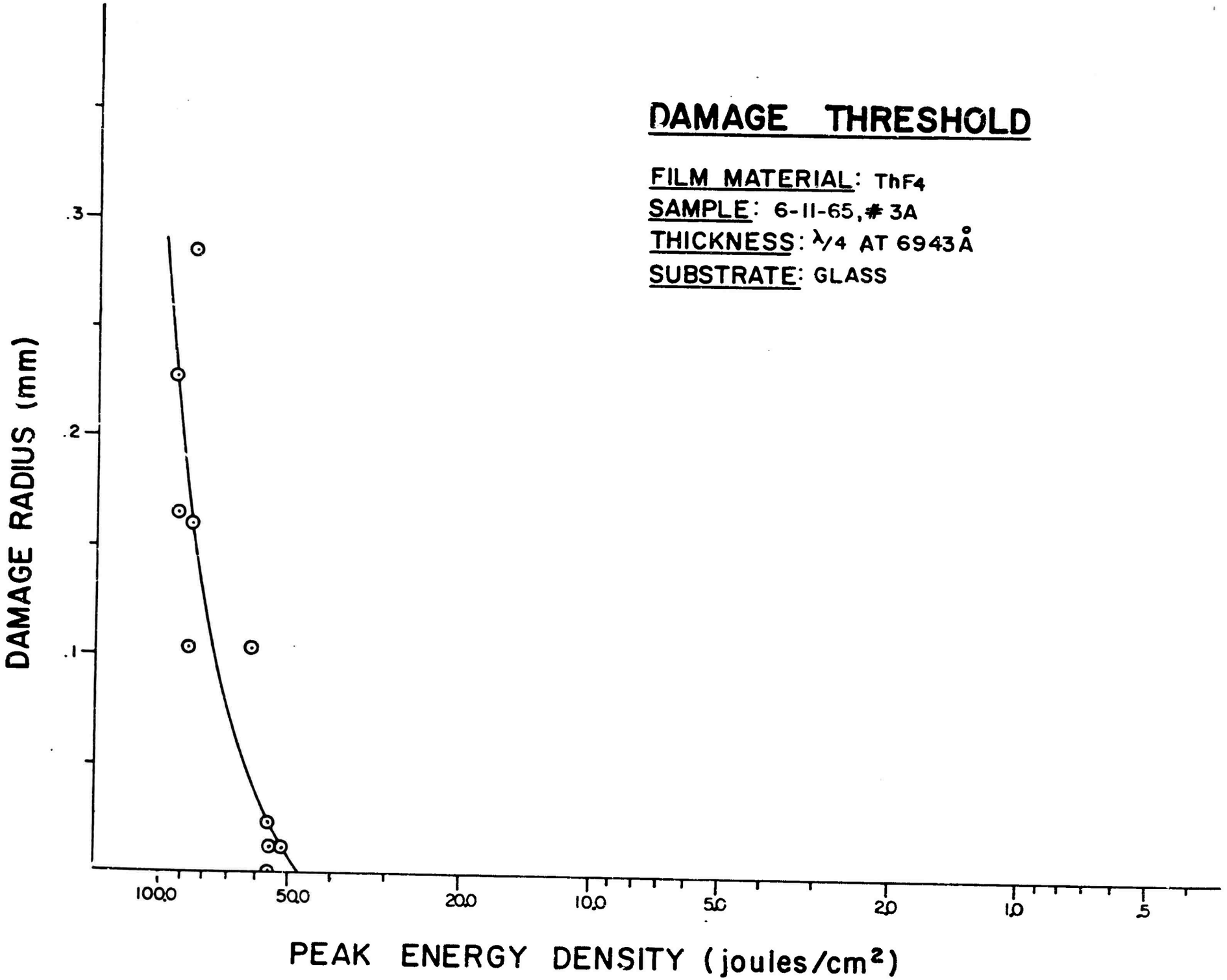
DAMAGE THRESHOLD
FILM MATERIAL: ThF4
SAMPLE: 6-11-65, # 3A
THICKNESS: λ/4 AT 6943Å
SUBSTRATE: GLASS
DAMAGE RADIUS (mm)
.3
.2
.1
100.0
50.0
20.0
10.0
5.0
2.0
1.0
.5
PEAK ENERGY DENSITY (joules/cm²)

FIG. 8

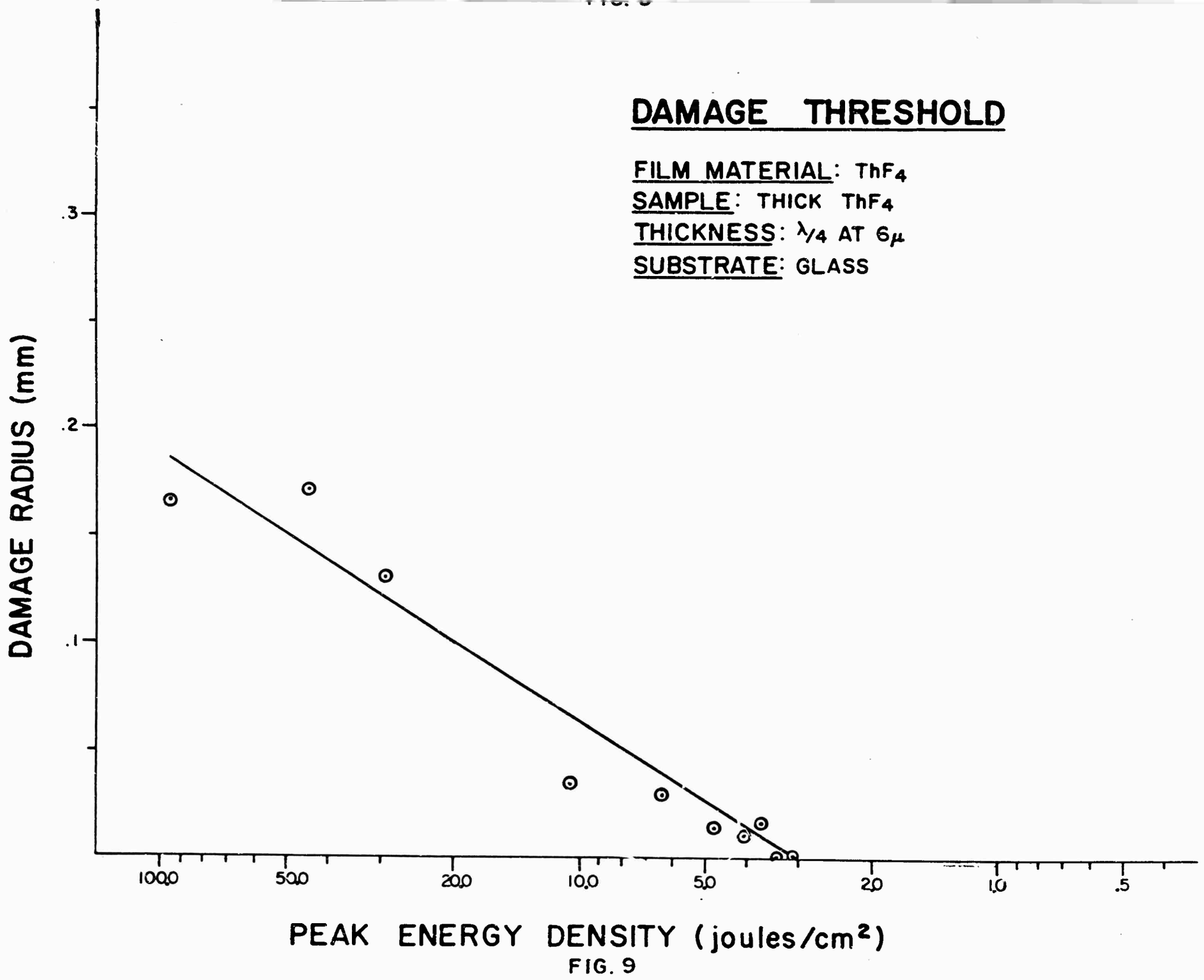
DAMAGE THRESHOLD
FILM MATERIAL: ThF4
SAMPLE: THICK ThF4
THICKNESS: λ/4 AT 6μ
SUBSTRATE: GLASS
DAMAGE RADIUS (mm)
.3
.2
.1
100.0
50.0
20.0
10.0
5.0
2.0
1.0
.5
PEAK ENERGY DENSITY (joules/cm²)

FIG. 9

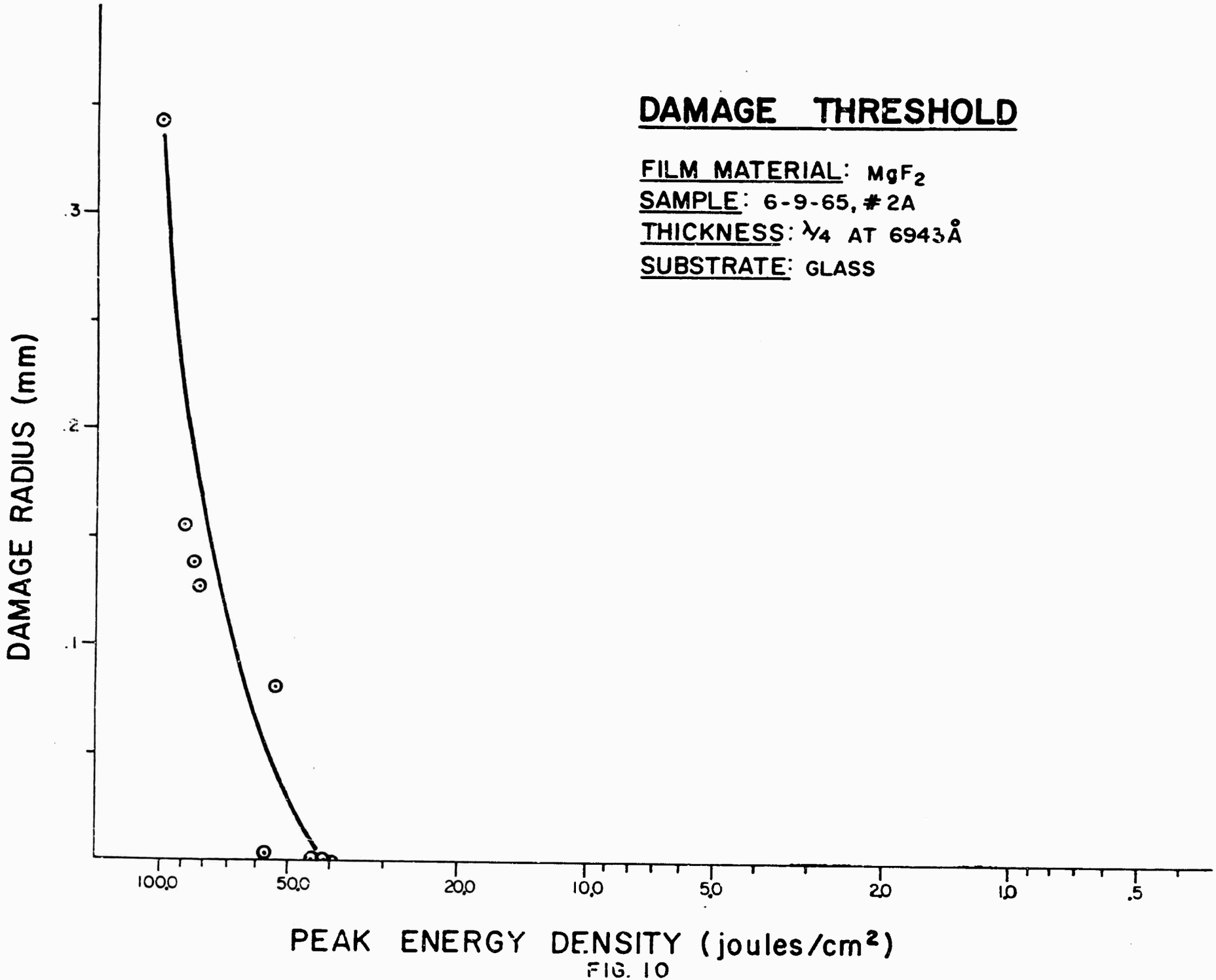
DAMAGE THRESHOLD
FILM MATERIAL: MgF_2
SAMPLE: 6-9-65, # 2A
THICKNESS: $\lambda/4$ AT 6943Å
SUBSTRATE: GLASS
DAMAGE RADIUS (mm)
.3
.2
.1
100.0
50.0
20.0
10.0
5.0
2.0
1.0
.5
PEAK ENERGY DENSITY (joules/cm²)

FIG. 10

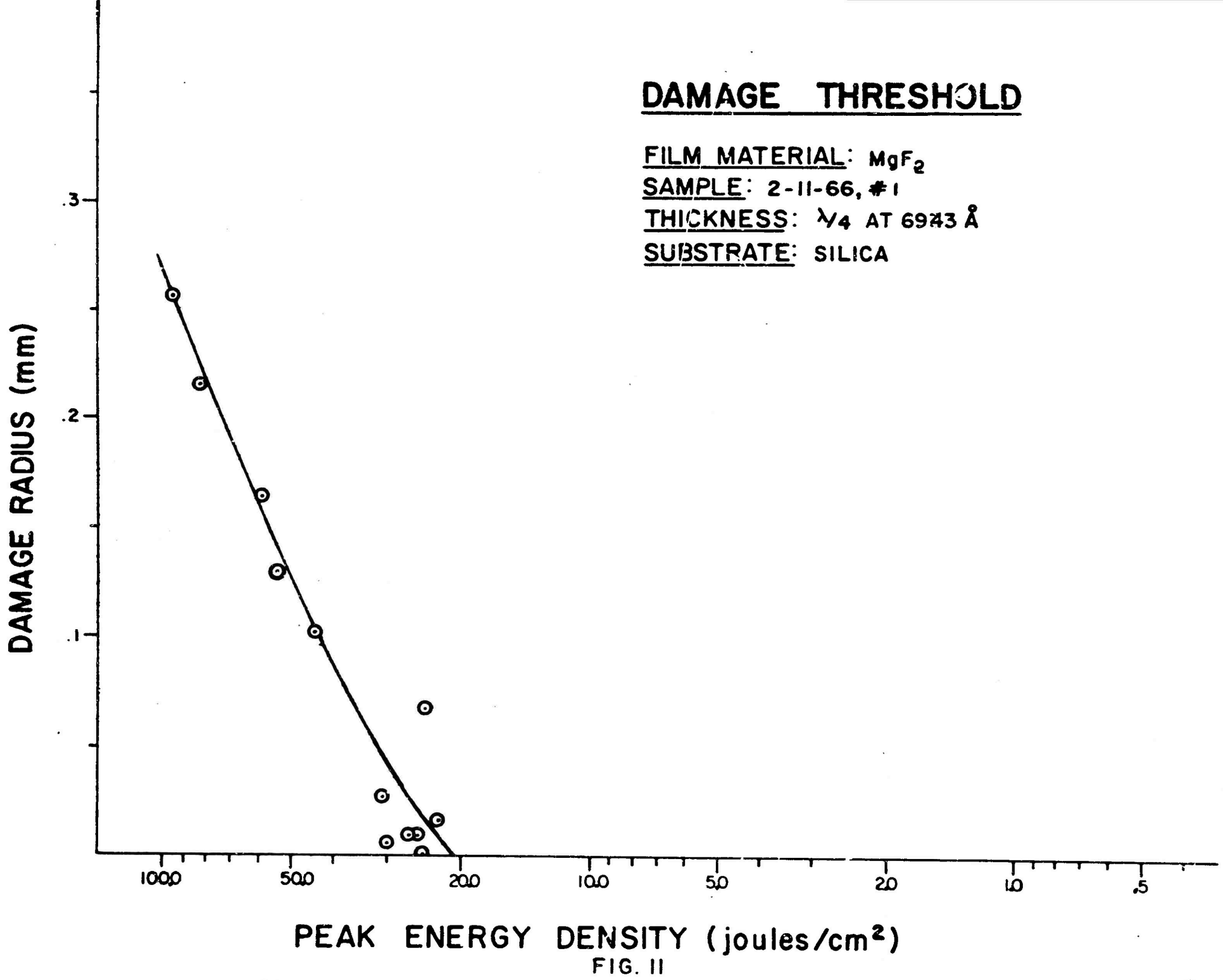
DAMAGE THRESHOLD
FILM MATERIAL: MgF_2
SAMPLE: 2-11-66, #1
THICKNESS: $\lambda/4$ AT 6943 Å
SUBSTRATE: SILICA
DAMAGE RADIUS (mm)
.3
.2
.1
1000
500
200
100
50
20
10
.5
PEAK ENERGY DENSITY (joules/cm²)

FIG. II

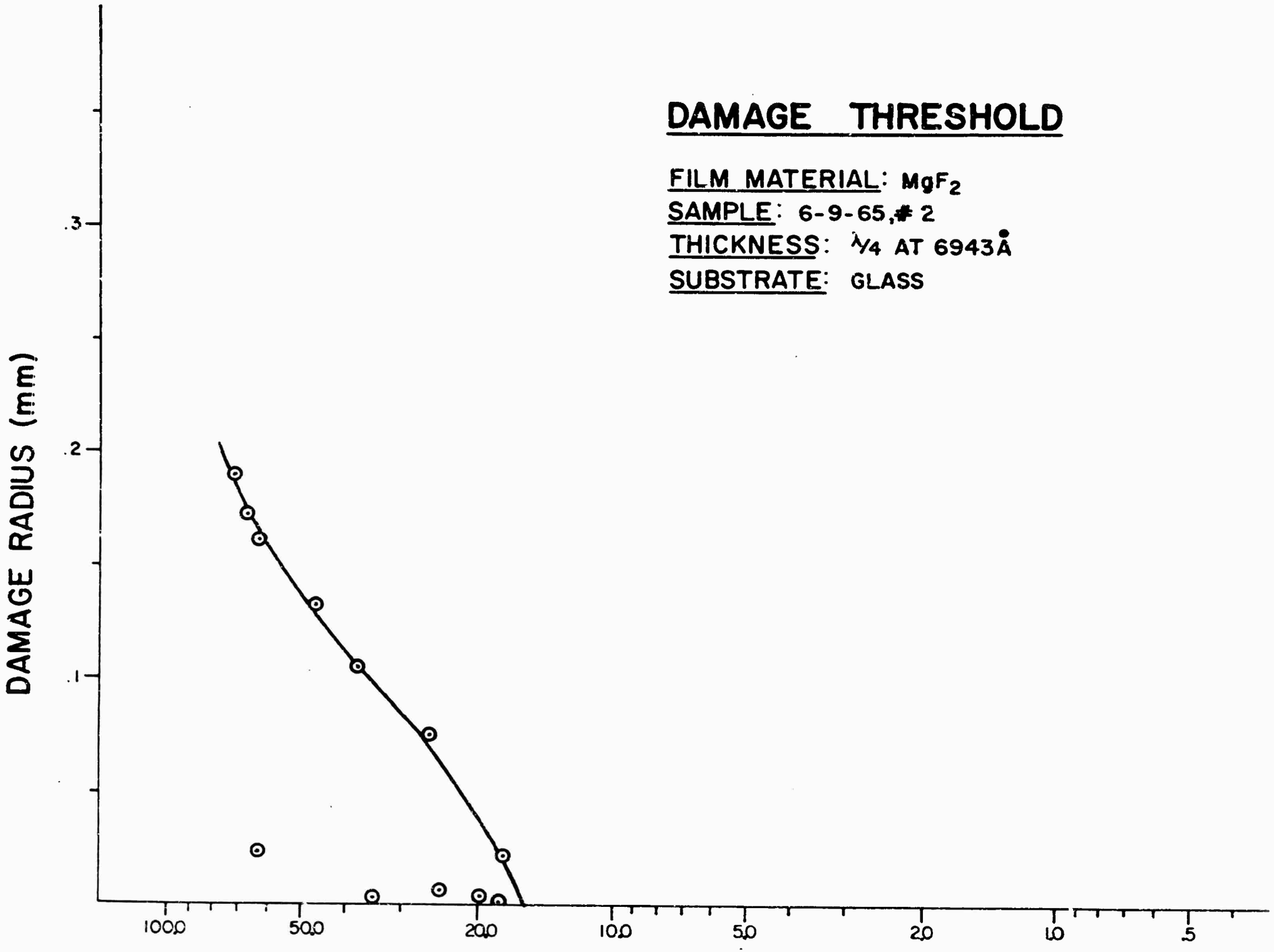
DAMAGE THRESHOLD
FILM MATERIAL: MgF_2
SAMPLE: 6-9-65, # 2
THICKNESS: λ/4 AT 6943Å
SUBSTRATE: GLASS
DAMAGE RADIUS (mm)
.3
.2
.1
100.0
50.0
20.0
10.0
5.0
2.0
1.0
.5
PEAK ENERGY DENSITY (joules/cm²)

FIG. 12

FIG. 12

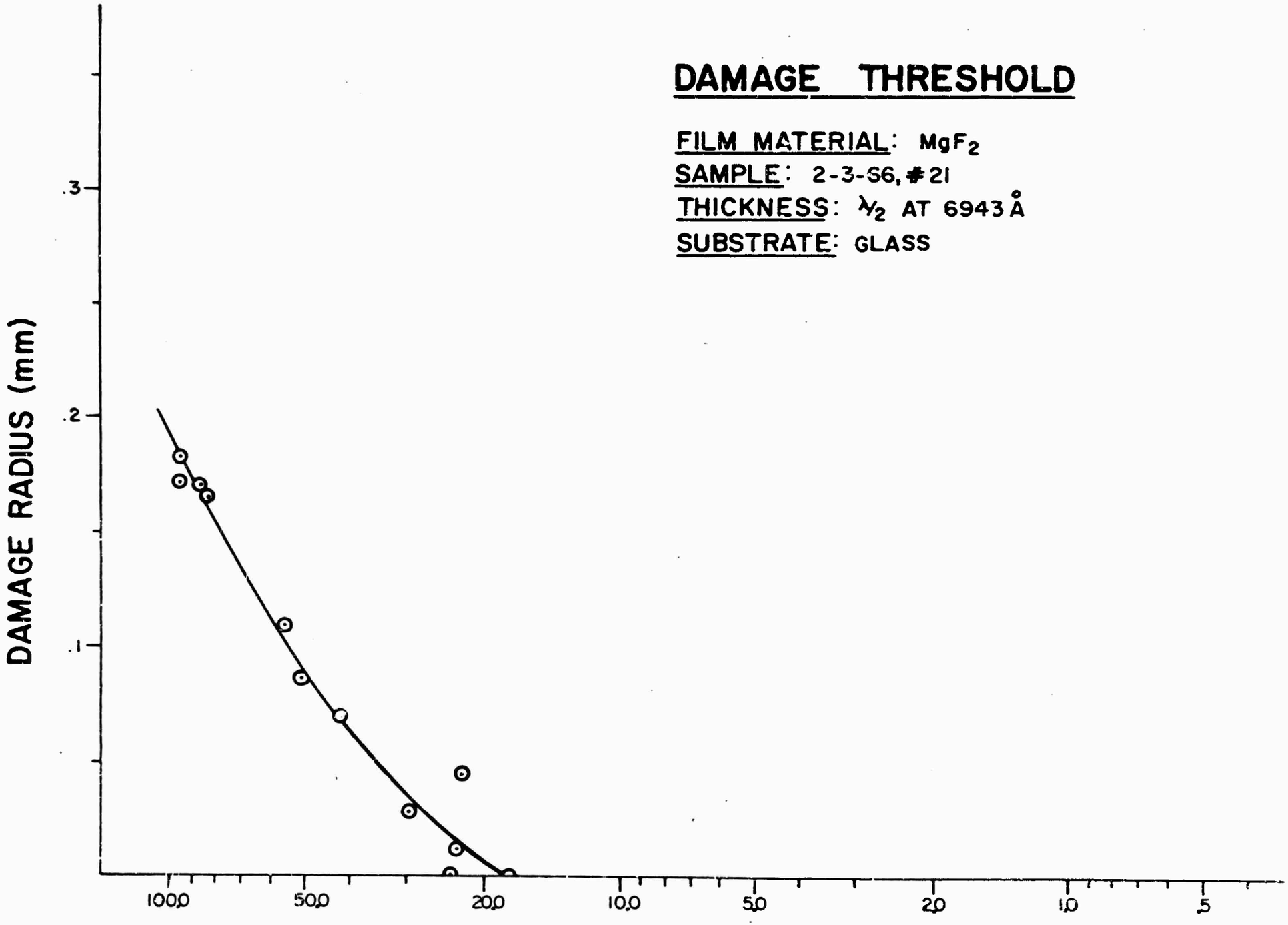
DAMAGE THRESHOLD
FILM MATERIAL: MgF_2
SAMPLE: 2-3-56, #21
THICKNESS: $\lambda/2$ AT 6943 Å
SUBSTRATE: GLASS
DAMAGE RADIUS (mm)
.3
.2
.1
100.0
50.0
20.0
10.0
5.0
2.0
1.0
.5
PEAK ENERGY DENSITY (joules/cm²)

FIG. 13

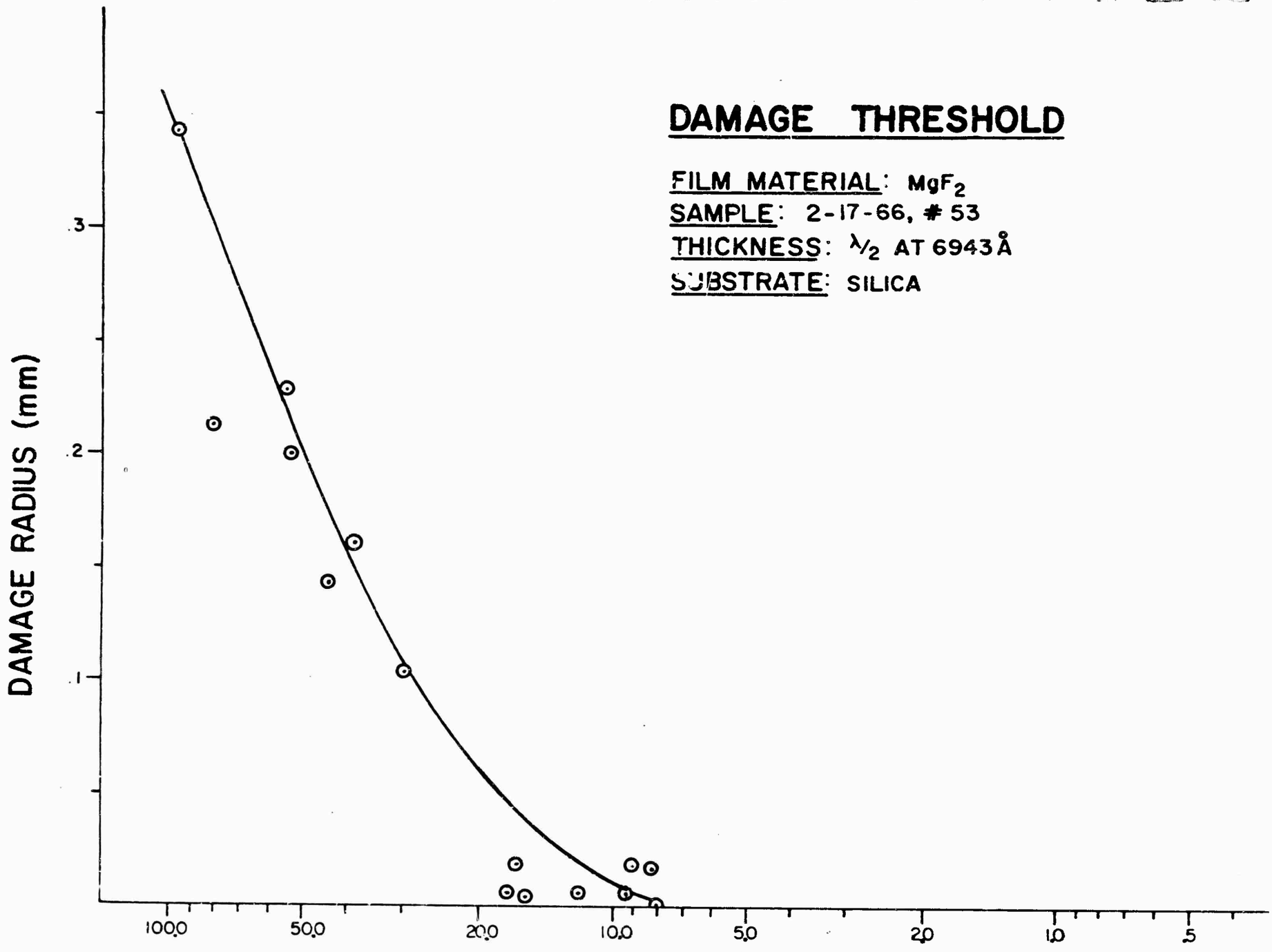
DAMAGE THRESHOLD
FILM MATERIAL: MgF_2
SAMPLE: 2-17-66, # 53
THICKNESS: $\lambda/2$ AT 6943Å
SUBSTRATE: SILICA
DAMAGE RADIUS (mm)
.3
.2
.1
100.0
50.0
20.0
10.0
5.0
2.0
1.0
.5
PEAK ENERGY DENSITY (joules/cm²)

FIG. 14

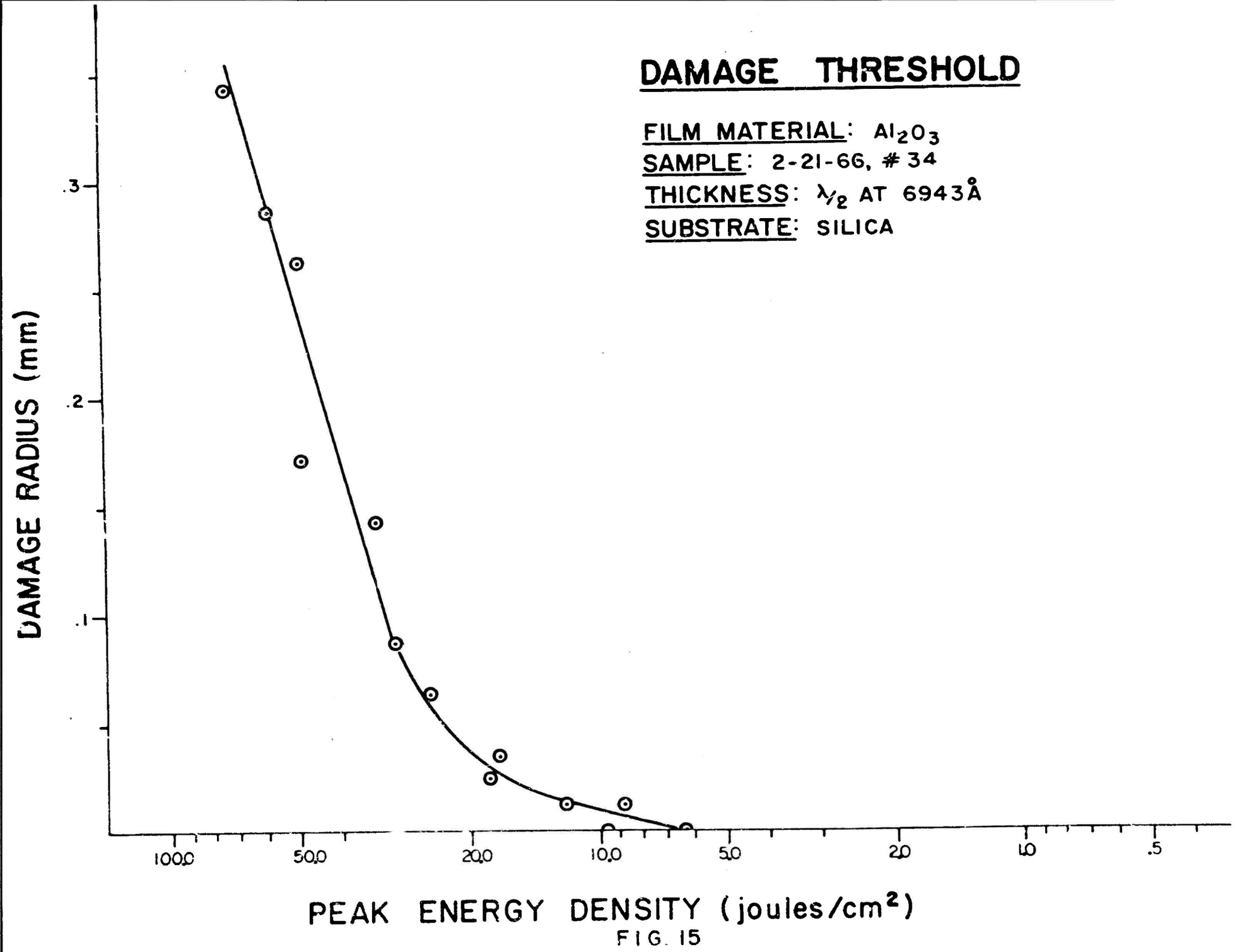
DAMAGE THRESHOLD
FILM MATERIAL: Al_2O_3
SAMPLE: 2-21-66, #34
THICKNESS: $\lambda/2$ AT 6943Å
SUBSTRATE: SILICA
DAMAGE RADIUS (mm)
.3
.2
.1
100.0
50.0
20.0
10.0
5.0
2.0
1.0
.5
PEAK ENERGY DENSITY (joules/cm²)

FIG. 15

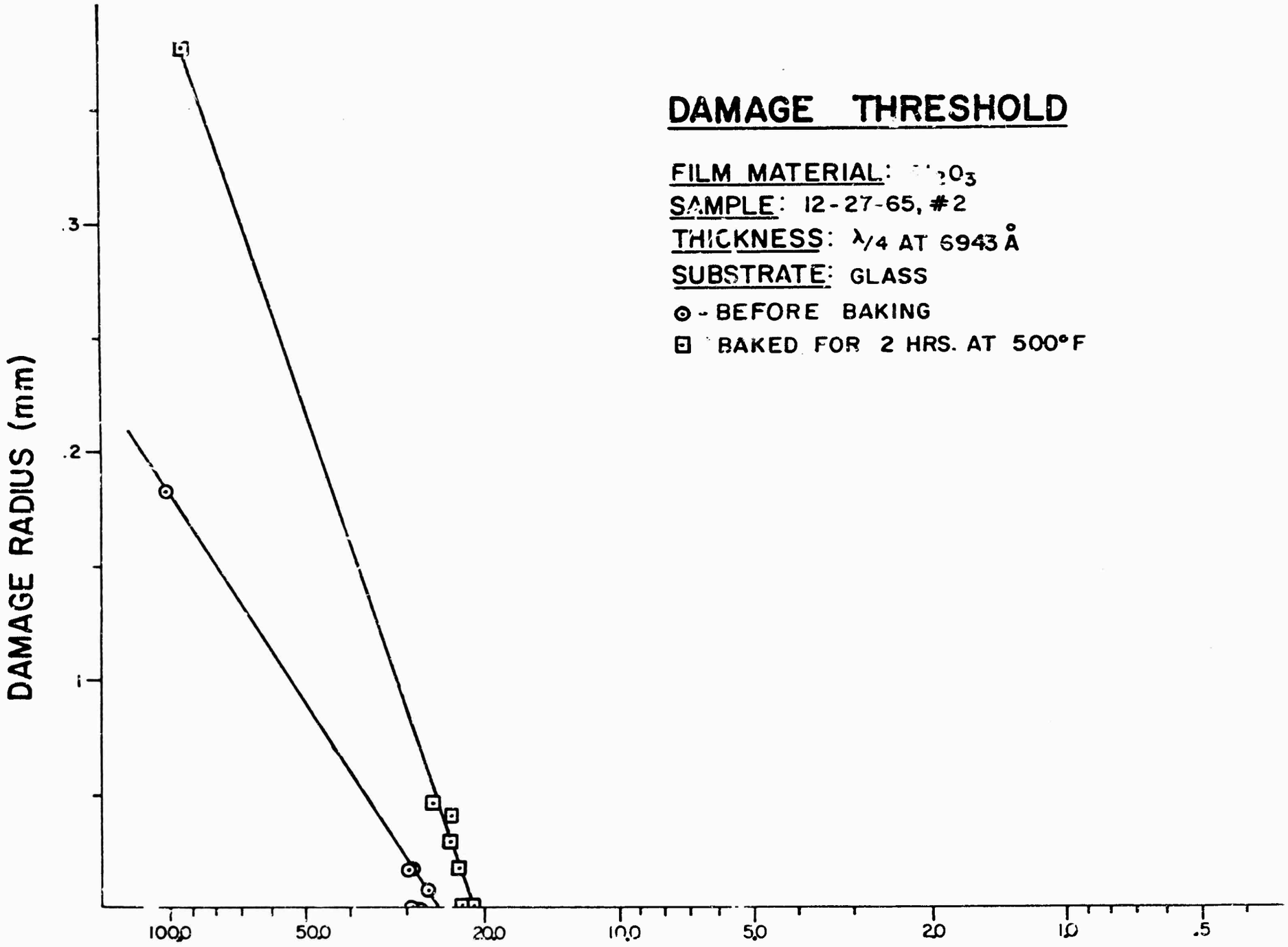
DAMAGE THRESHOLD
FILM MATERIAL: TiO_2
SAMPLE: 12-27-65, #2
THICKNESS: λ/4 AT 6943 Å
SUBSTRATE: GLASS
⊙ - BEFORE BAKING
⊡ BAKED FOR 2 HRS. AT 500°F
DAMAGE RADIUS (mm)
.3
.2
1
100.0
50.0
20.0
10.0
5.0
2.0
1.0
.5
PEAK ENERGY DENSITY (joules/cm²)

FIG. 16

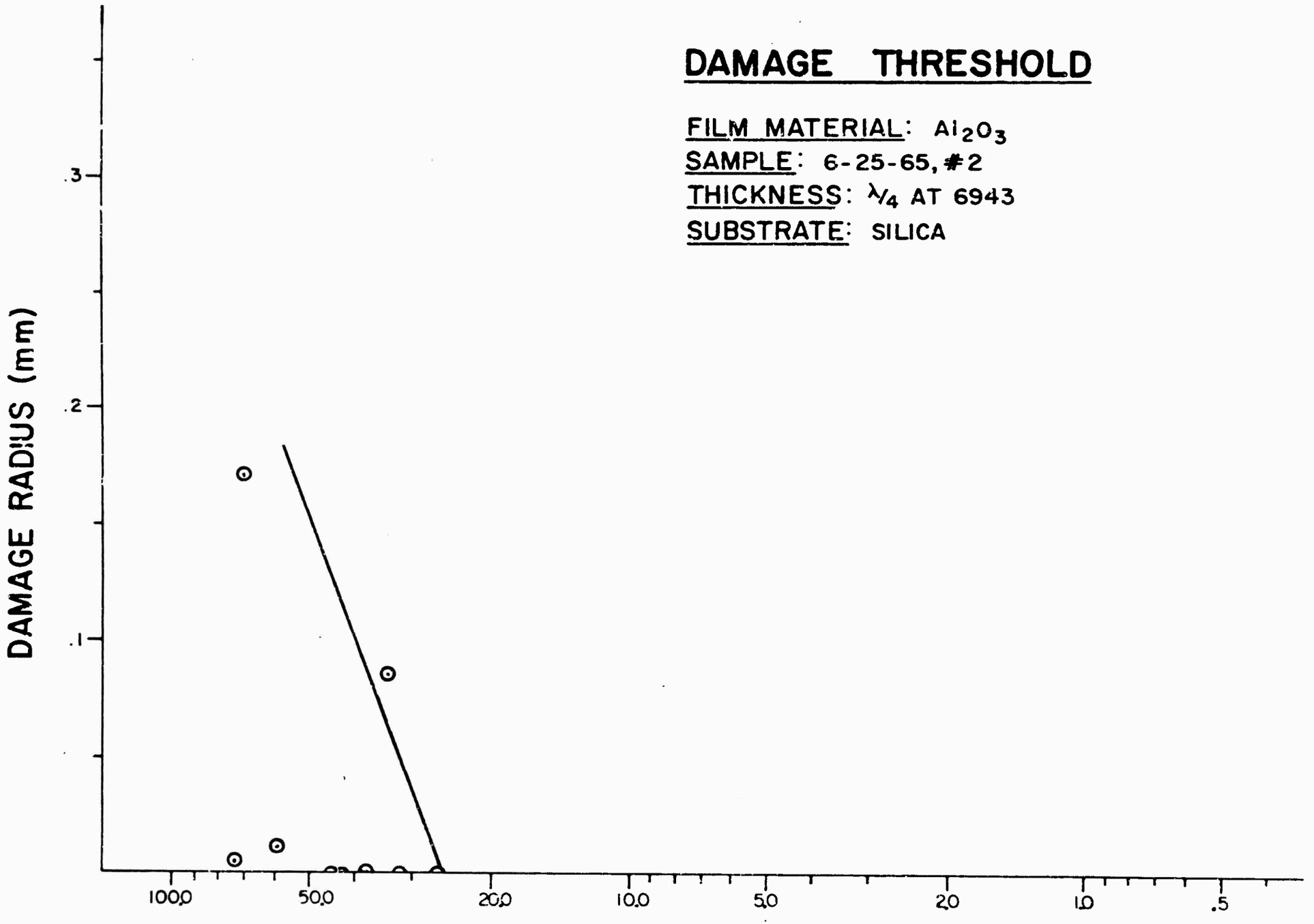
DAMAGE THRESHOLD
FILM MATERIAL: Al_2O_3
SAMPLE: 6-25-65, #2
THICKNESS: $\lambda/4$ AT 6943
SUBSTRATE: SILICA
DAMAGE RADIUS (mm)
.3
.2
.1
100.0
50.0
20.0
10.0
5.0
2.0
1.0
.5
PEAK ENERGY DENSITY (joules/cm²)

FIG. 17

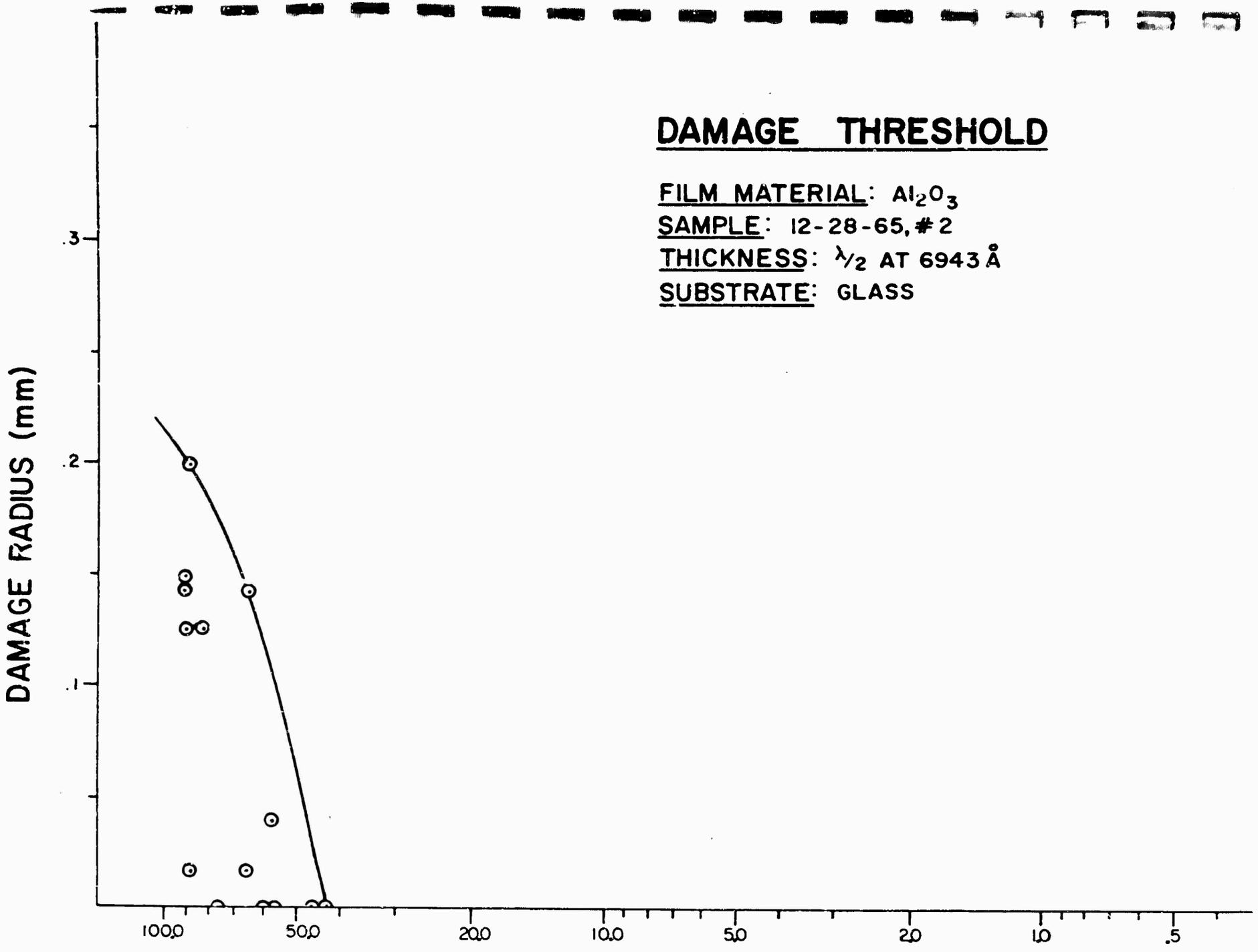
DAMAGE THRESHOLD
FILM MATERIAL: Al_2O_3
SAMPLE: 12-28-65, #2
THICKNESS: $\lambda/2$ AT 6943 Å
SUBSTRATE: GLASS
DAMAGE RADIUS (mm)
.3
.2
.1
100.0
50.0
20.0
10.0
5.0
2.0
1.0
.5
PEAK ENERGY DENSITY (joules/cm²)

FIG. 18

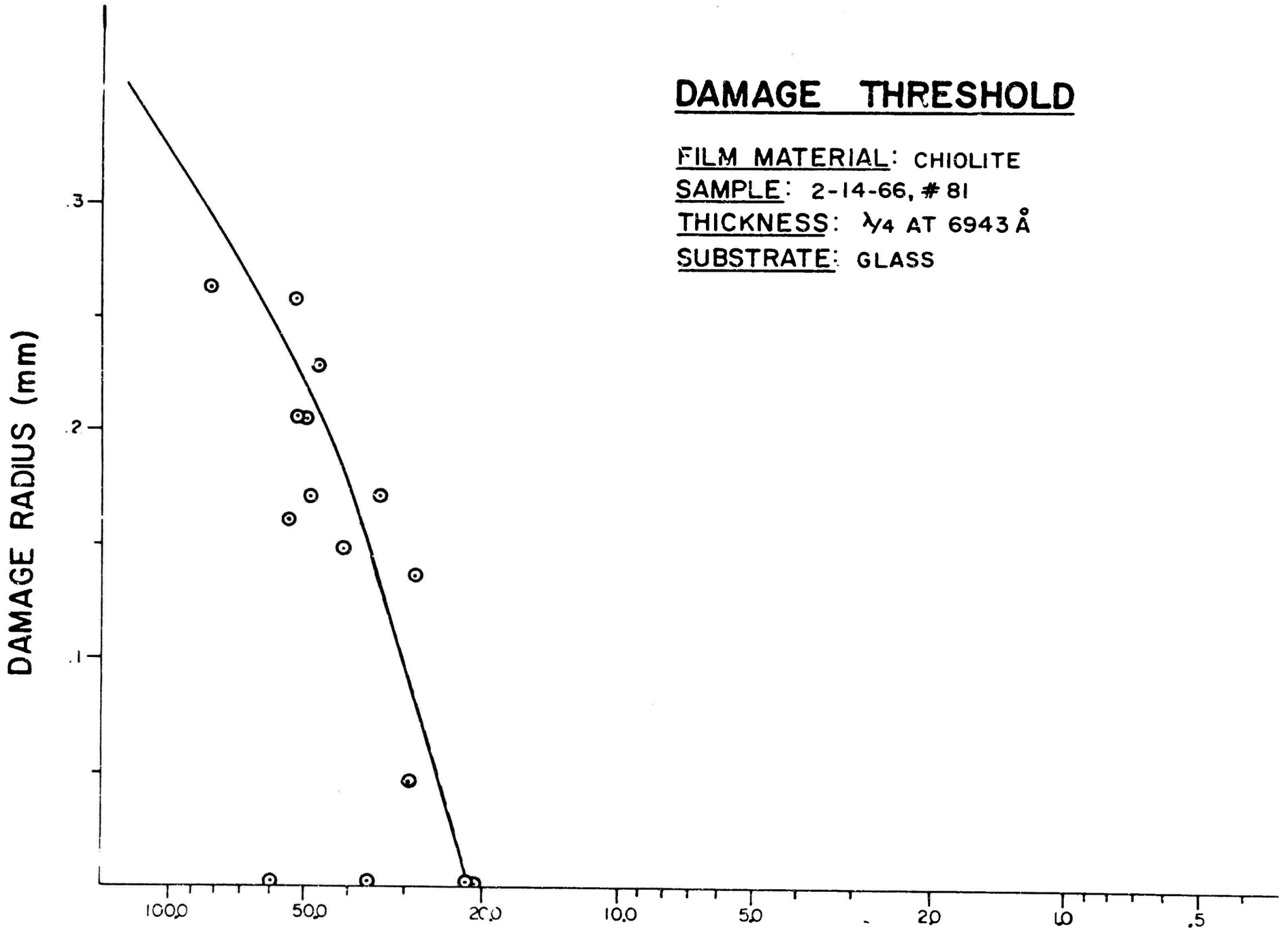
DAMAGE THRESHOLD
FILM MATERIAL: CHIOLITE
SAMPLE: 2-14-66, # 81
THICKNESS: λ/4 AT 6943 Å
SUBSTRATE: GLASS
DAMAGE RADIUS (mm)
.3
.2
.1
100.0
50.0
20.0
10.0
5.0
2.0
1.0
.5
PEAK ENERGY DENSITY (joules/cm²)

FIG. 19

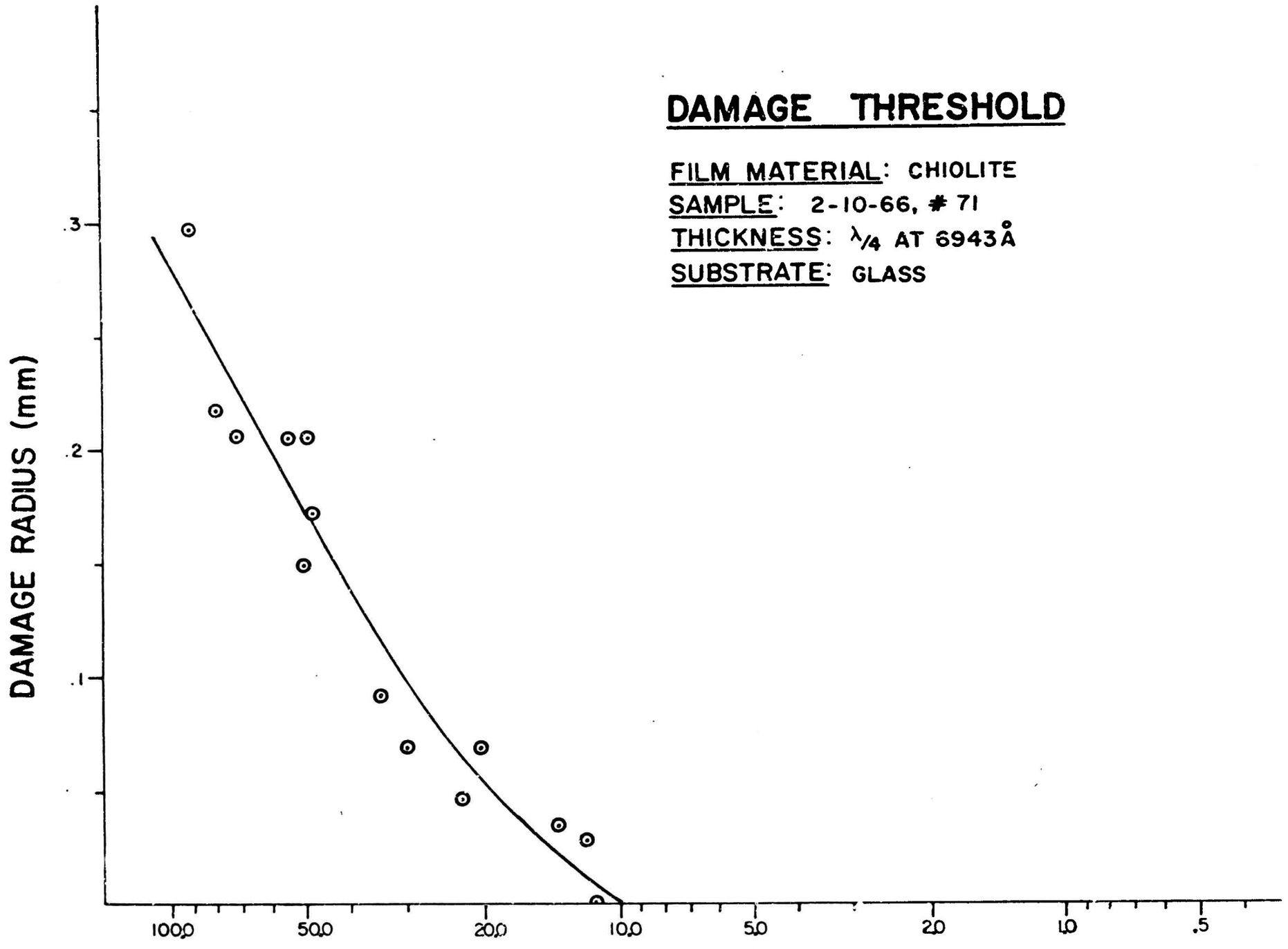
DAMAGE THRESHOLD
FILM MATERIAL: CHIOLITE
SAMPLE: 2-10-66, # 71
THICKNESS: λ/4 AT 6943Å
SUBSTRATE: GLASS
DAMAGE RADIUS (mm)
.3
.2
.1
100.0
50.0
20.0
10.0
5.0
2.0
1.0
.5
PEAK ENERGY DENSITY (joules/cm²)

FIG. 20

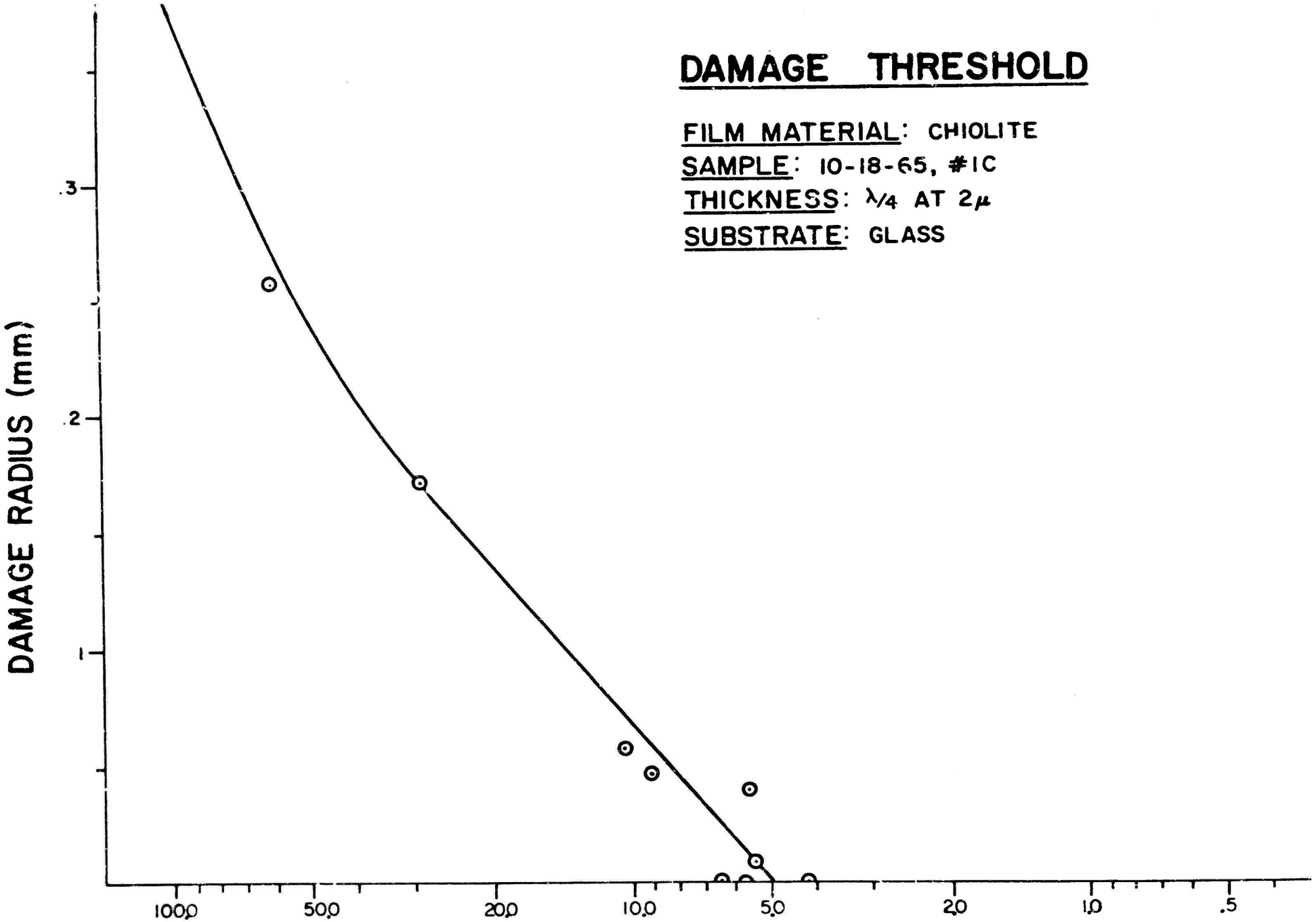
DAMAGE THRESHOLD
FILM MATERIAL: CHIOLITE
SAMPLE: 10-18-65, #1C
THICKNESS: λ/4 AT 2μ
SUBSTRATE: GLASS
DAMAGE RADIUS (mm)
.3
.2
1
100.0
50.0
20.0
10.0
5.0
2.0
1.0
.5
PEAK ENERGY DENSITY (joules/cm²)

FIG. 21

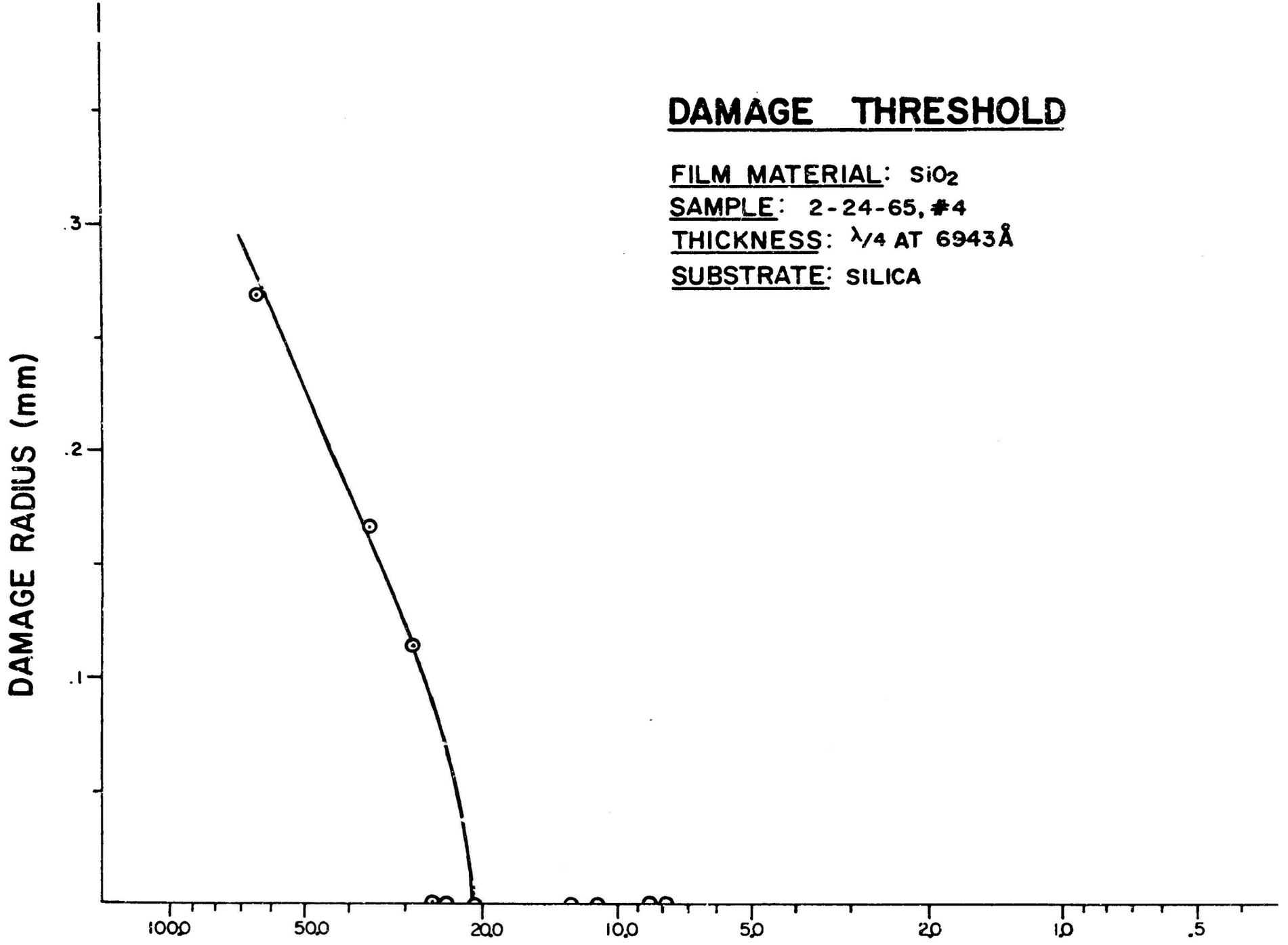
DAMAGE THRESHOLD
FILM MATERIAL: SiO_2
SAMPLE: 2-24-65, #4
THICKNESS: λ/4 AT 6943Å
SUBSTRATE: SILICA
DAMAGE RADIUS (mm)
.3
.2
.1
100.0
50.0
20.0
10.0
5.0
2.0
1.0
.5
PEAK ENERGY DENSITY (joules/cm²)

FIG. 22

DAMAGE THRESHOLD

FILM MATERIAL: SiO_2
SAMPLE: 12-28-65, #1
THICKNESS: $\lambda/2$ AT 6943Å
SUBSTRATE: SILICA

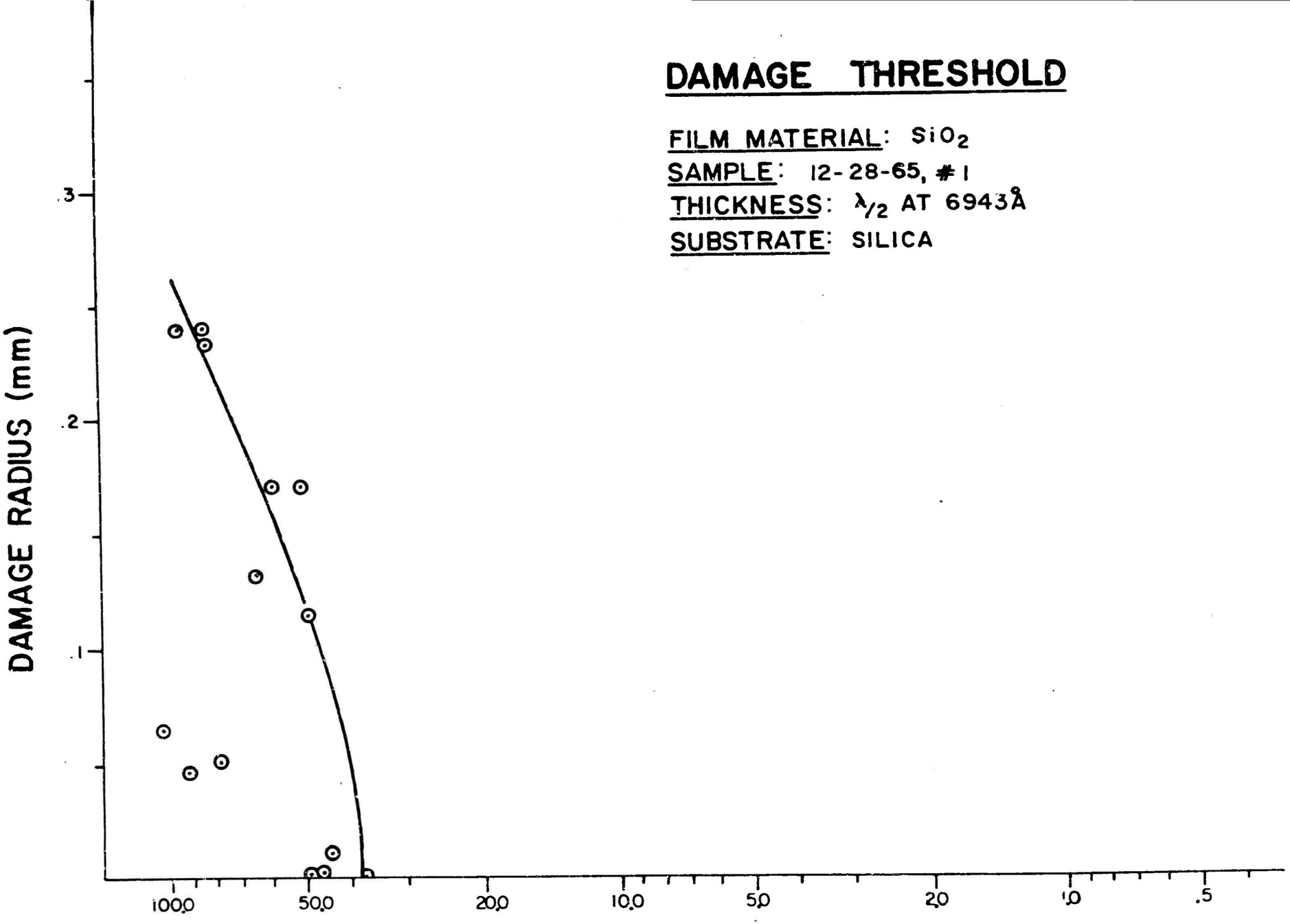

FIG. 23

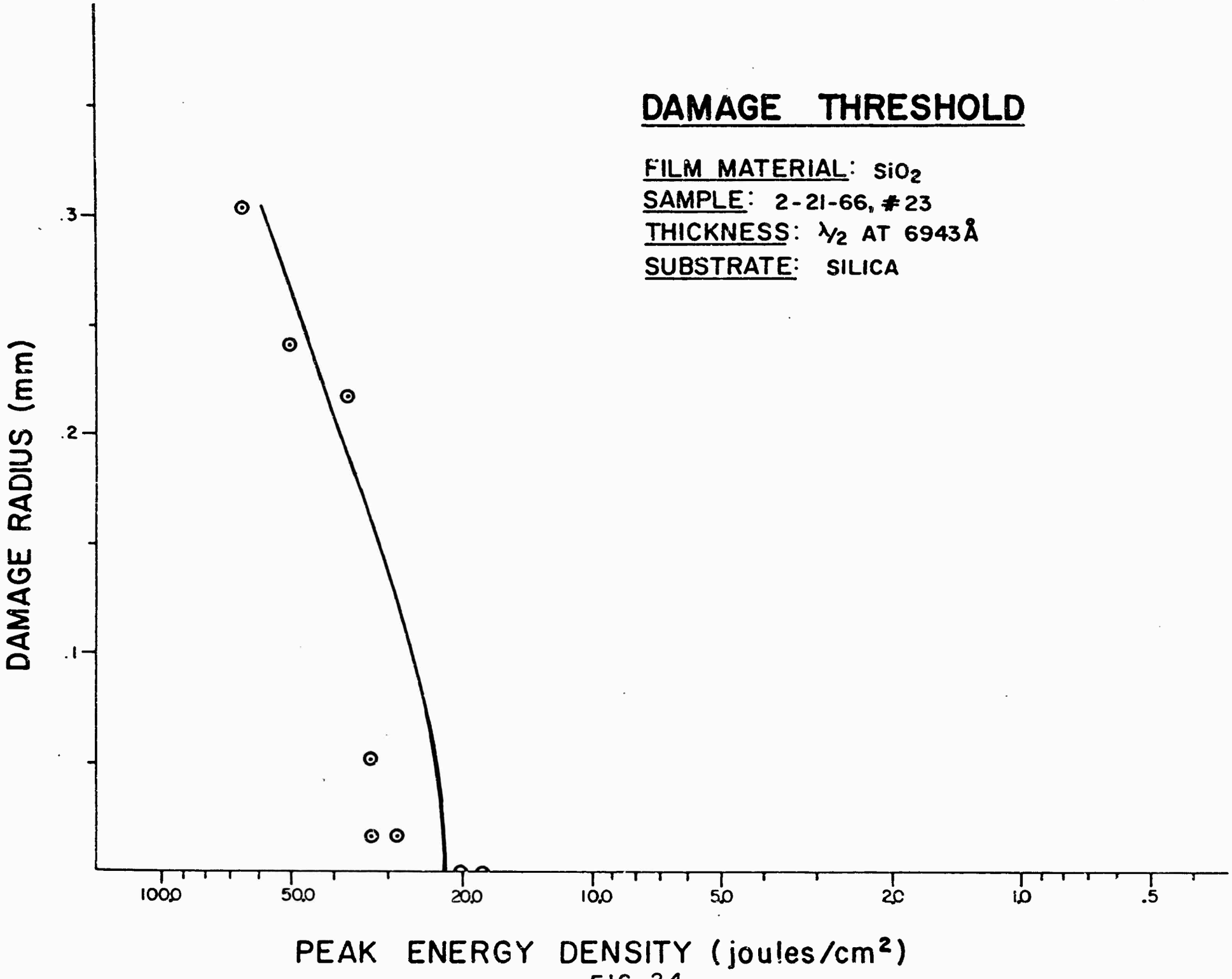
DAMAGE THRESHOLD
FILM MATERIAL: SiO_2
SAMPLE: 2-21-66, #23
THICKNESS: $\lambda/2$ AT 6943Å
SUBSTRATE: SILICA
DAMAGE RADIUS (mm)
.3
.2
.1
100.0
50.0
20.0
10.0
5.0
2.0
1.0
.5
PEAK ENERGY DENSITY (joules/cm²)

FIG. 24

DAMAGE THRESHOLD

FILM MATERIAL: ZrO_2
SAMPLE: 6-10-65, #1
THICKNESS: $\lambda/4$ AT 6943Å
SUBSTRATE: GLASS

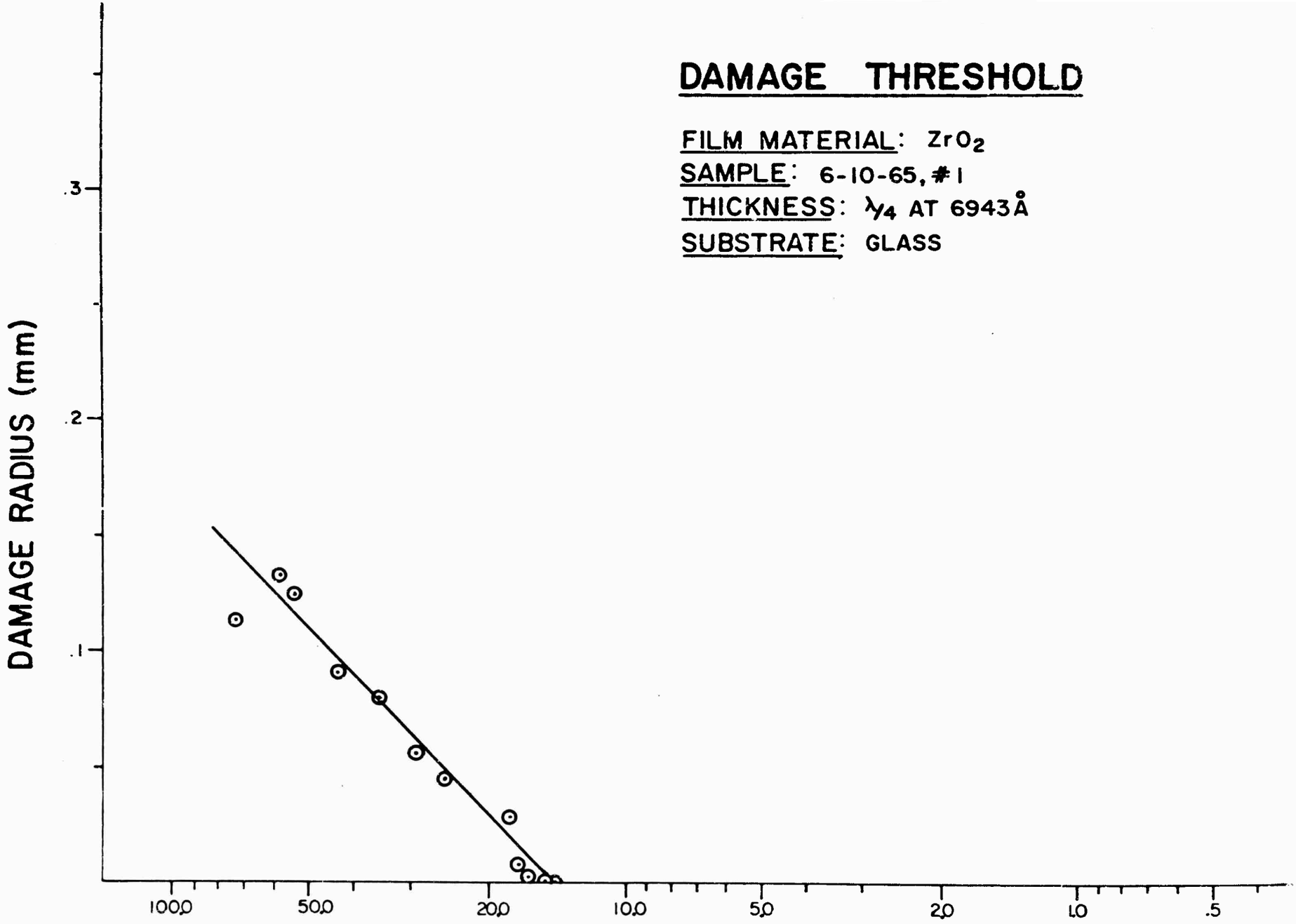

FIG. 25

DAMAGE THRESHOLD

FILM MATERIAL: ZrO_2
SAMPLE: 6-25-65, #1
THICKNESS: $\lambda/4$ AT 6943Å
SUBSTRATE: SILIC

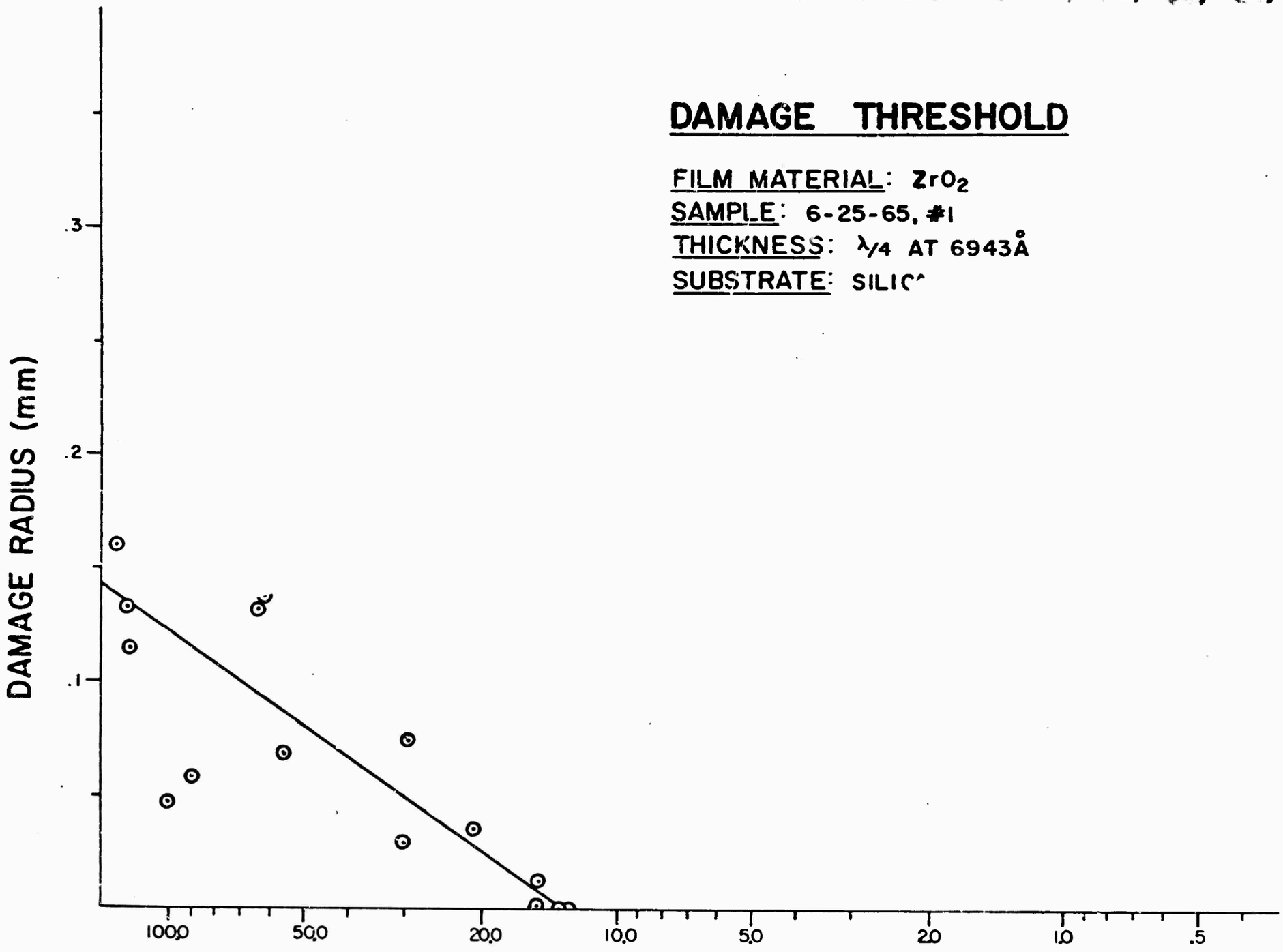

FIG. 26

DAMAGE THRESHOLD

FILM MATERIAL: ZrO_2
SAMPLE: 2-22-66, #34
THICKNESS: $\lambda/2$ AT 6943Å
SUBSTRATE: SILICA

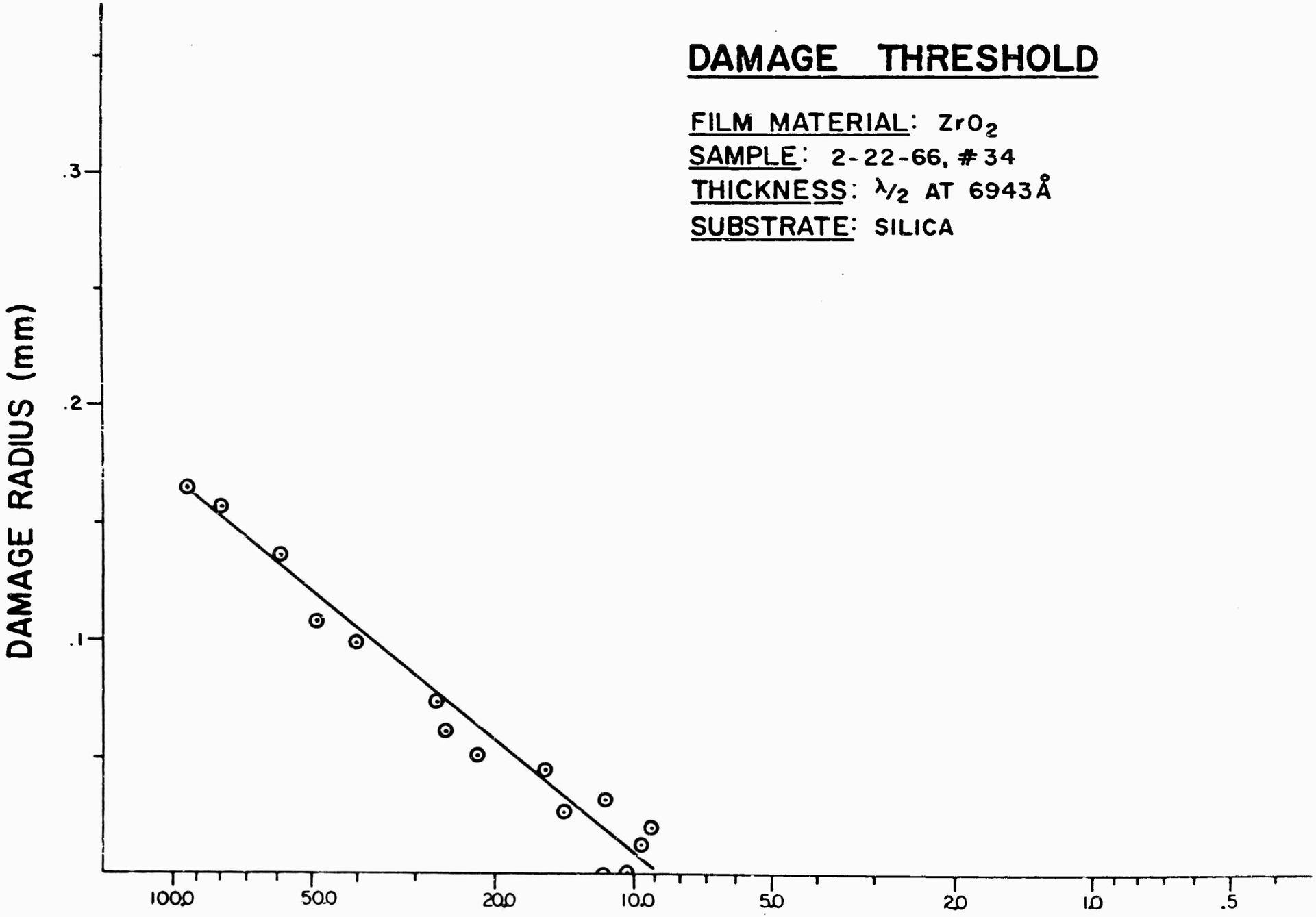

FIG. 27

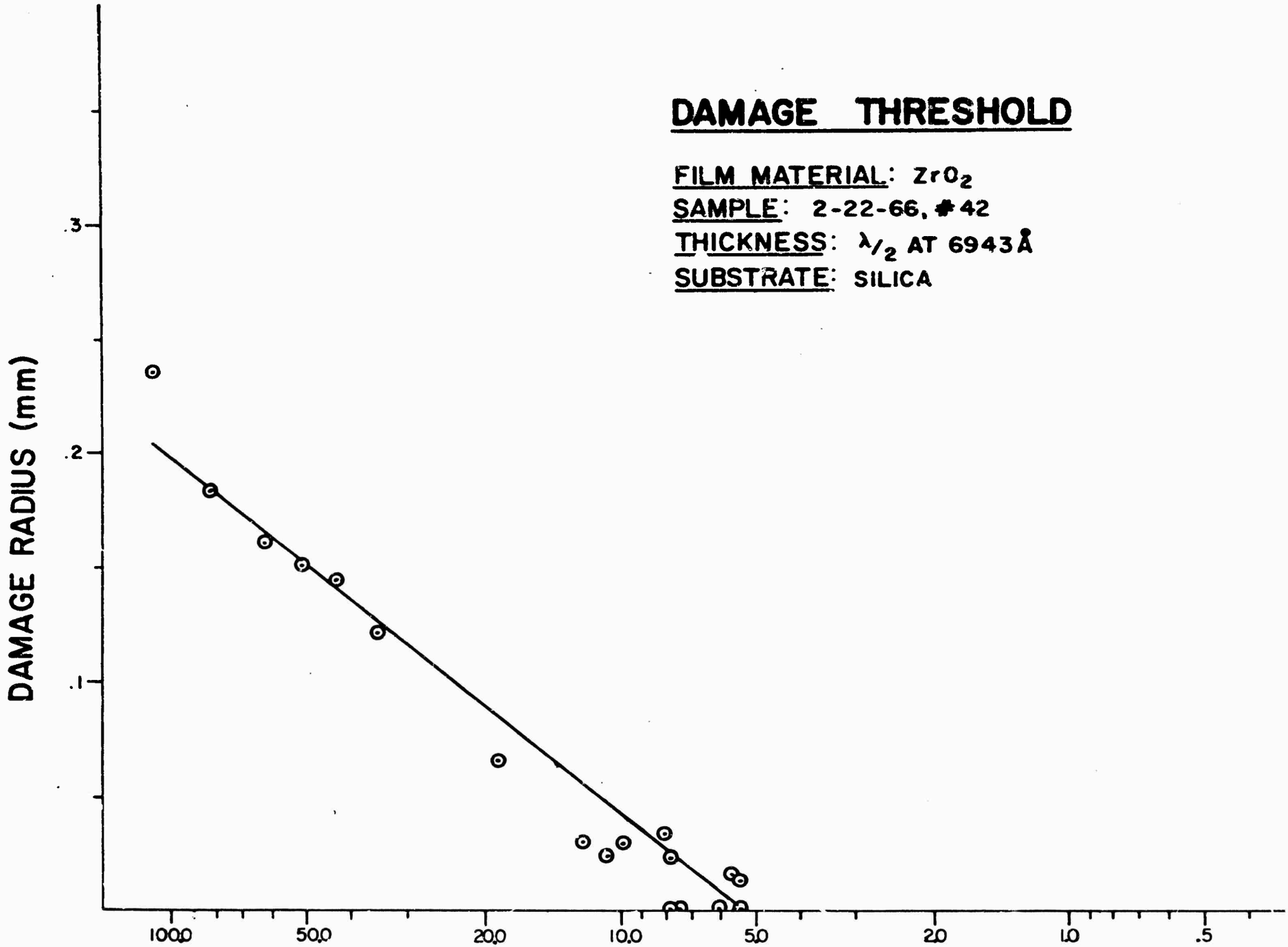
DAMAGE THRESHOLD
FILM MATERIAL: ZrO_2
SAMPLE: 2-22-66, #42
THICKNESS: $\lambda/2$ AT 6943Å
SUBSTRATE: SILICA
DAMAGE RADIUS (mm)
.3
.2
.1
100.0
50.0
20.0
10.0
5.0
2.0
1.0
.5
PEAK ENERGY DENSITY (joules/cm²)

FIG. 28

DAMAGE THRESHOLD

FILM MATERIAL: TiO_2
SAMPLE: 12-23-65, #3 & #3A
THICKNESS: $\lambda/2$ AT 6943Å
SUBSTRATE: GLASS

⊙ - #3 NOT BAKED
⊡ - #3A BAKED FOR 5 HRS. AT 800° F.

SAMPLE WAS INITIALLY ABSORBING AT 6943 Å, BUT SHOWED NO ABSORTION AT THAT WAVELENGTH. AFTER BAKING.

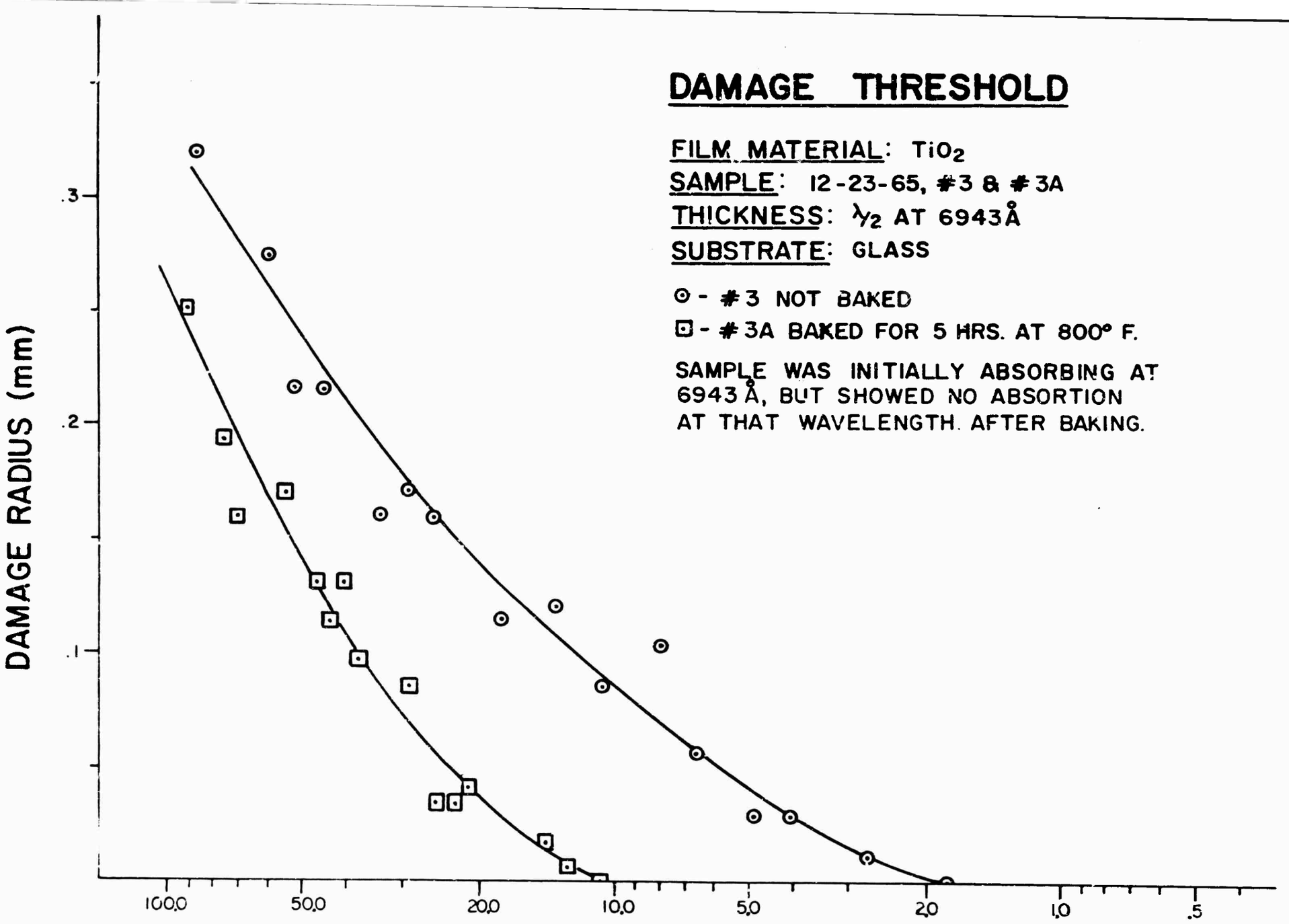

FIG. 29

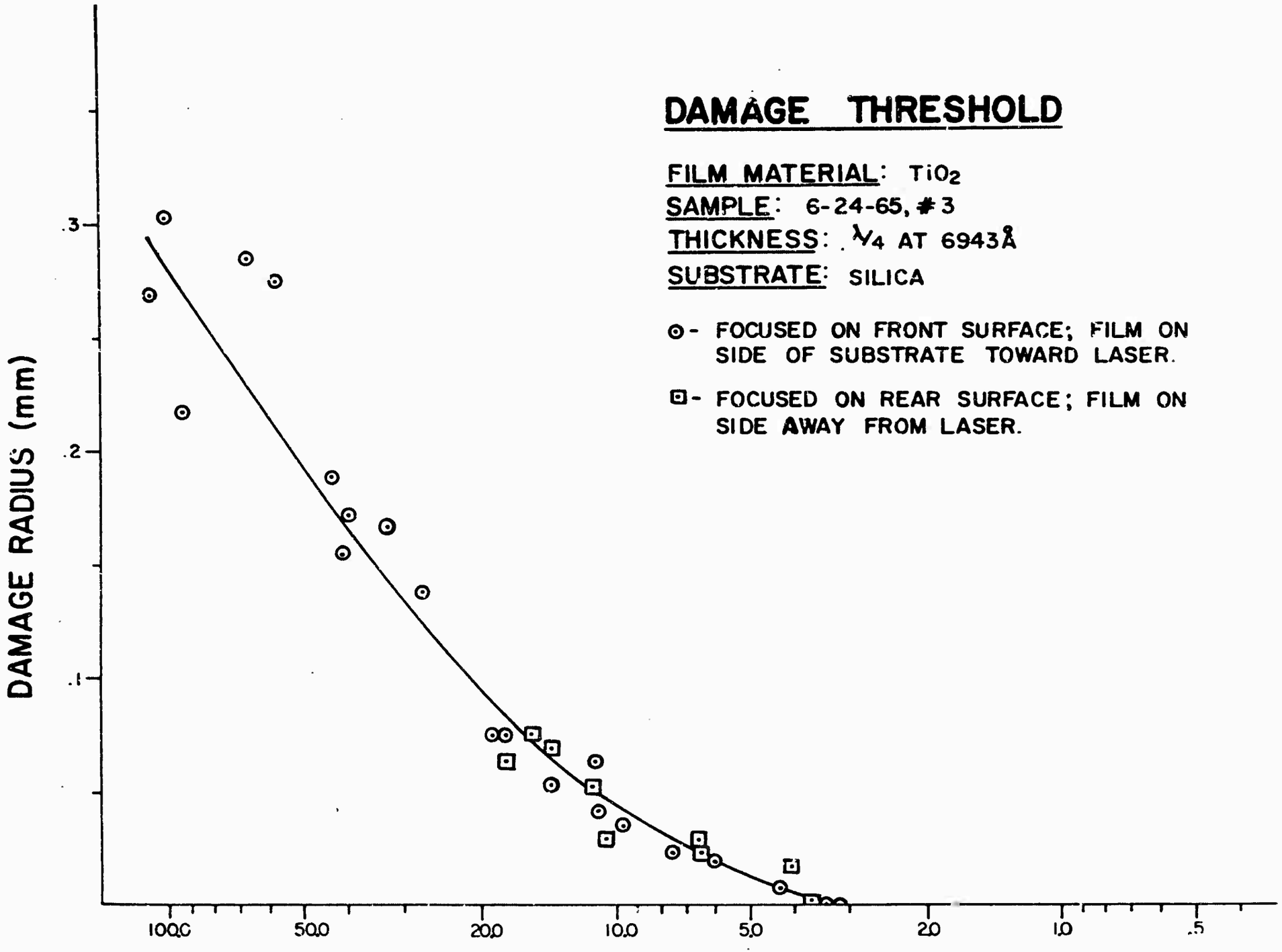
DAMAGE THRESHOLD
FILM MATERIAL: TiO_2
SAMPLE: 6-24-65, #3
THICKNESS: $\lambda/4$ AT 6943Å
SUBSTRATE: SILICA
⊙- FOCUSED ON FRONT SURFACE; FILM ON SIDE OF SUBSTRATE TOWARD LASER.
⊡- FOCUSED ON REAR SURFACE; FILM ON SIDE AWAY FROM LASER.
DAMAGE RADIUS (mm)
.3
.2
.1
100.0
50.0
20.0
10.0
5.0
2.0
1.0
.5
PEAK ENERGY DENSITY (joules/cm²)

FIG. 30

FIG. 30

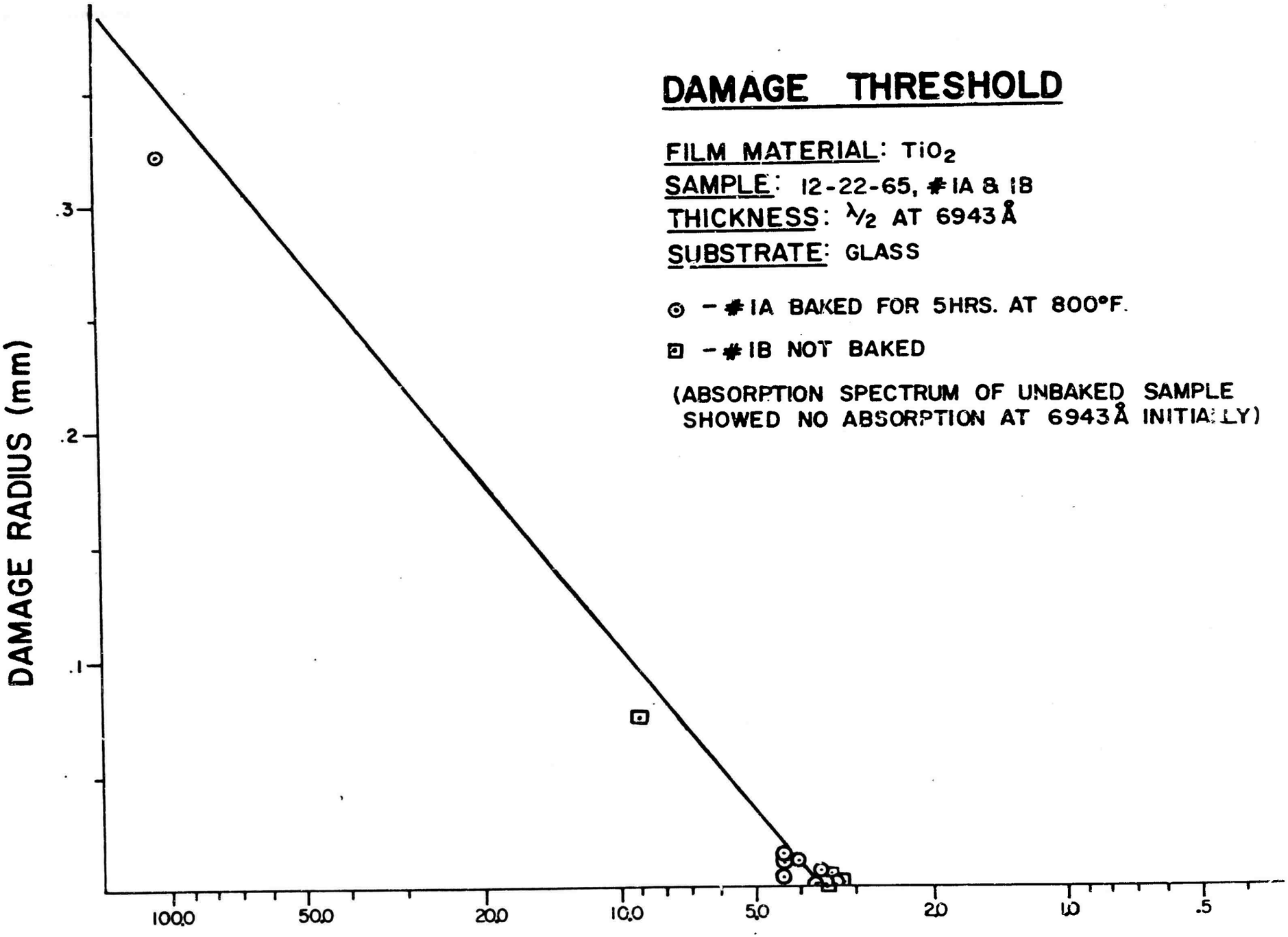
DAMAGE THRESHOLD
FILM MATERIAL: TiO_2
SAMPLE: 12-22-65, #1A & 1B
THICKNESS: $\lambda/2$ AT 6943 Å
SUBSTRATE: GLASS
⊙ – #1A BAKED FOR 5HRS. AT 800°F.
⊡ – #1B NOT BAKED
(ABSORPTION SPECTRUM OF UNBAKED SAMPLE SHOWED NO ABSORPTION AT 6943 Å INITIALLY)
DAMAGE RADIUS (mm)
.3
.2
.1
100.0
50.0
20.0
10.0
5.0
2.0
1.0
.5
PEAK ENERGY DENSITY (joules/cm²)

FIG. 31

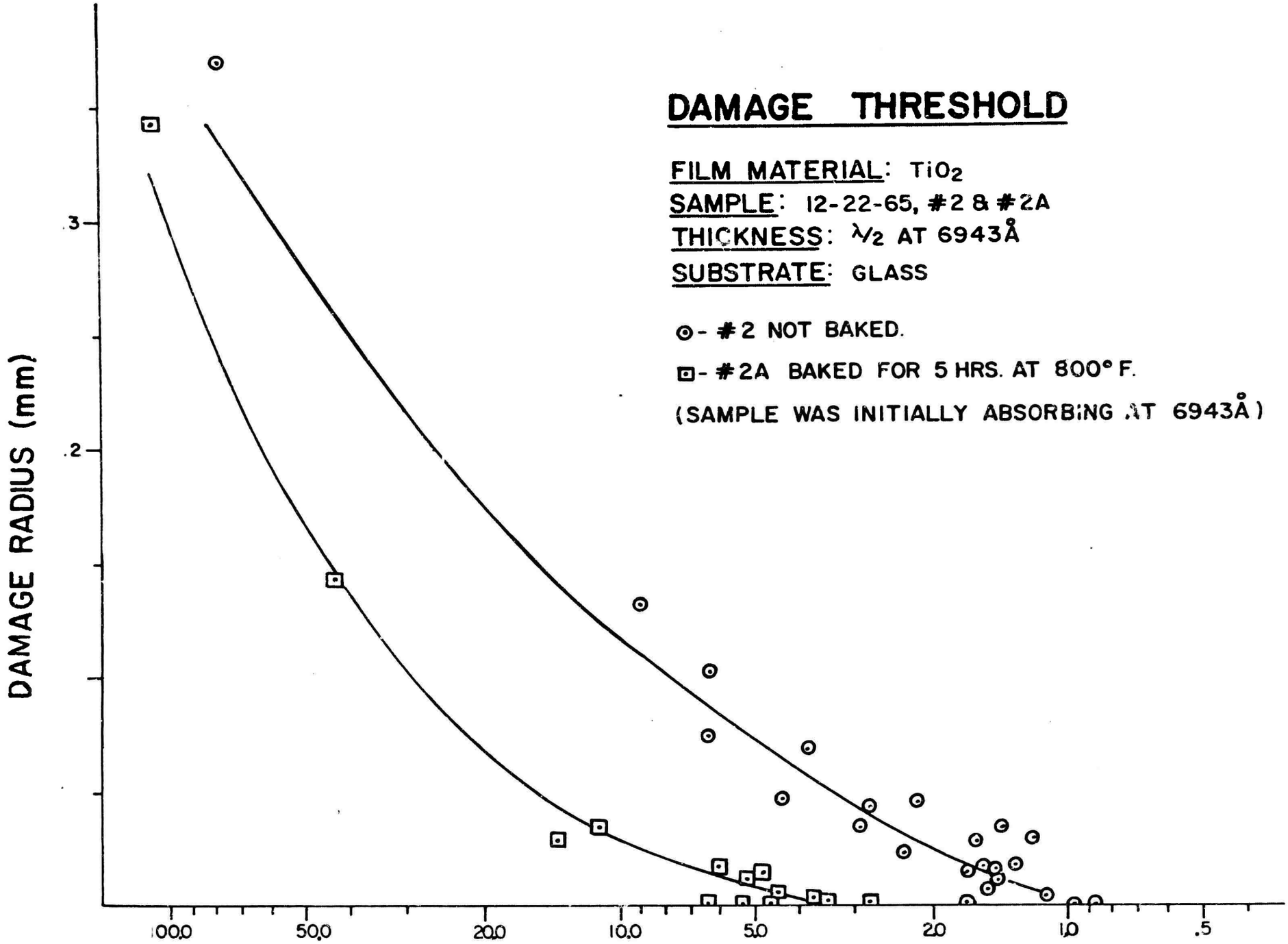
DAMAGE THRESHOLD
FILM MATERIAL: TiO2
SAMPLE: 12-22-65, #2 & #2A
THICKNESS: λ/2 AT 6943Å
SUBSTRATE: GLASS
⊙- #2 NOT BAKED.
⊡- #2A BAKED FOR 5 HRS. AT 800° F.
(SAMPLE WAS INITIALLY ABSORBING AT 6943Å)
DAMAGE RADIUS (mm)
.3
.2
100.0
50.0
20.0
10.0
5.0
2.0
1.0
.5
PEAK ENERGY DENSITY (joules/cm²)

FIG. 32

DAMAGE THRESHOLD

FILM MATERIAL: TiO_2
SAMPLE: 2-16-66, #54
THICKNESS: $\lambda/2$ AT 6943Å
SUBSTRATE: SILICA

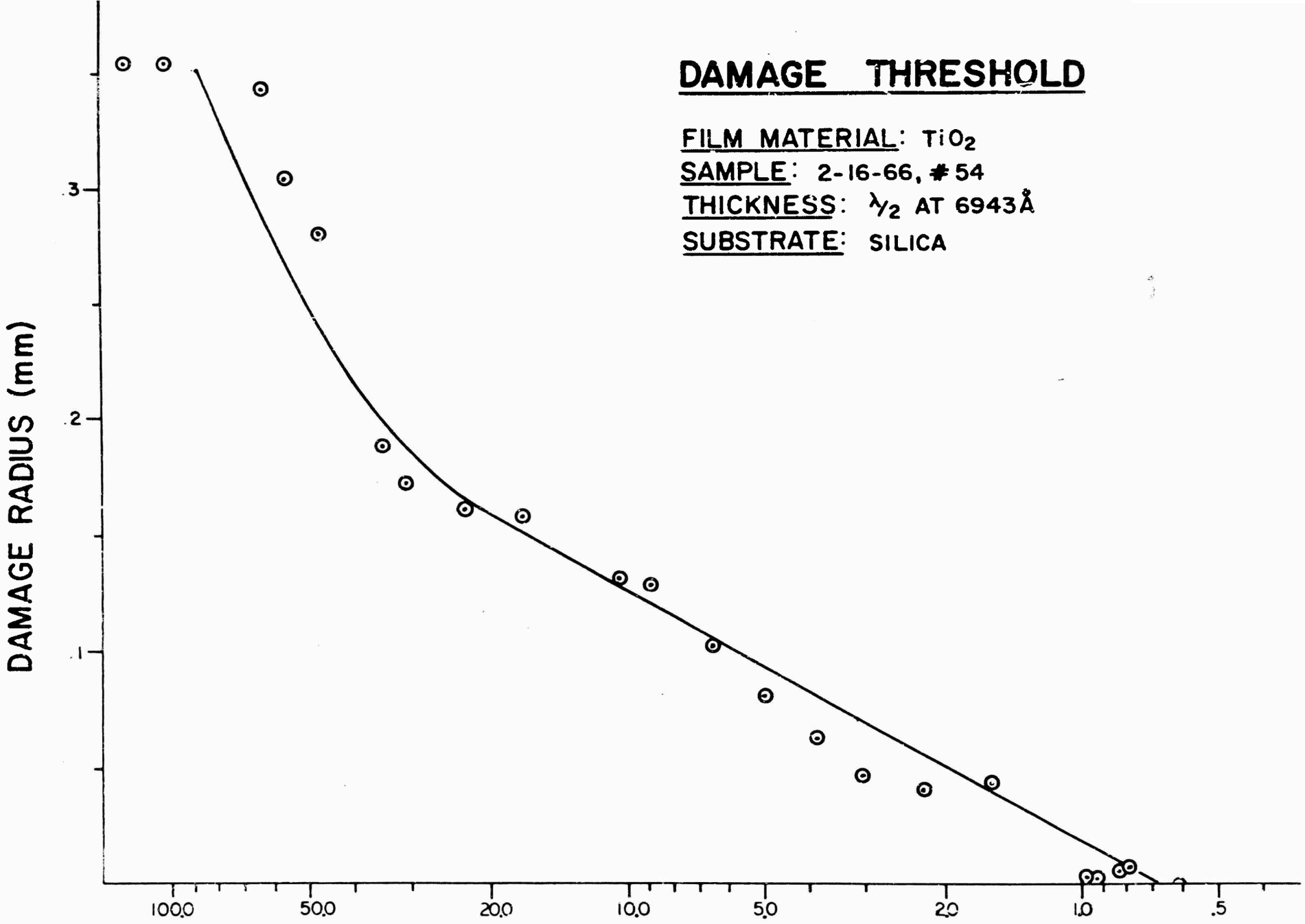

FIG. 33

DAMAGE THRESHOLD

FILM MATERIAL: CeO_2
SAMPLE: 6-11-65, #1
THICKNESS: $\lambda/4$ AT 6943 Å
SUBSTRATE: GLASS

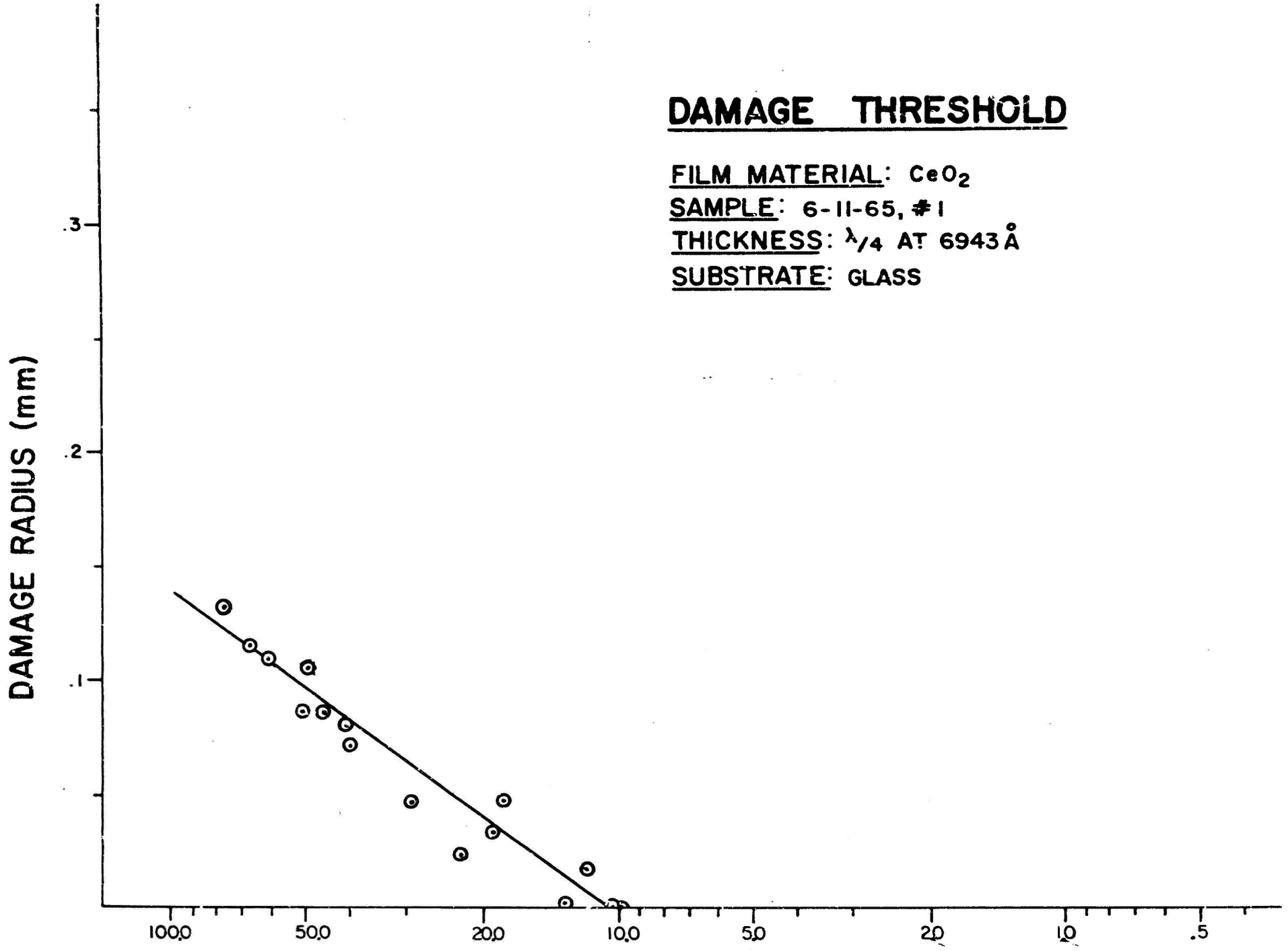

FIG. 34

FIG. 34

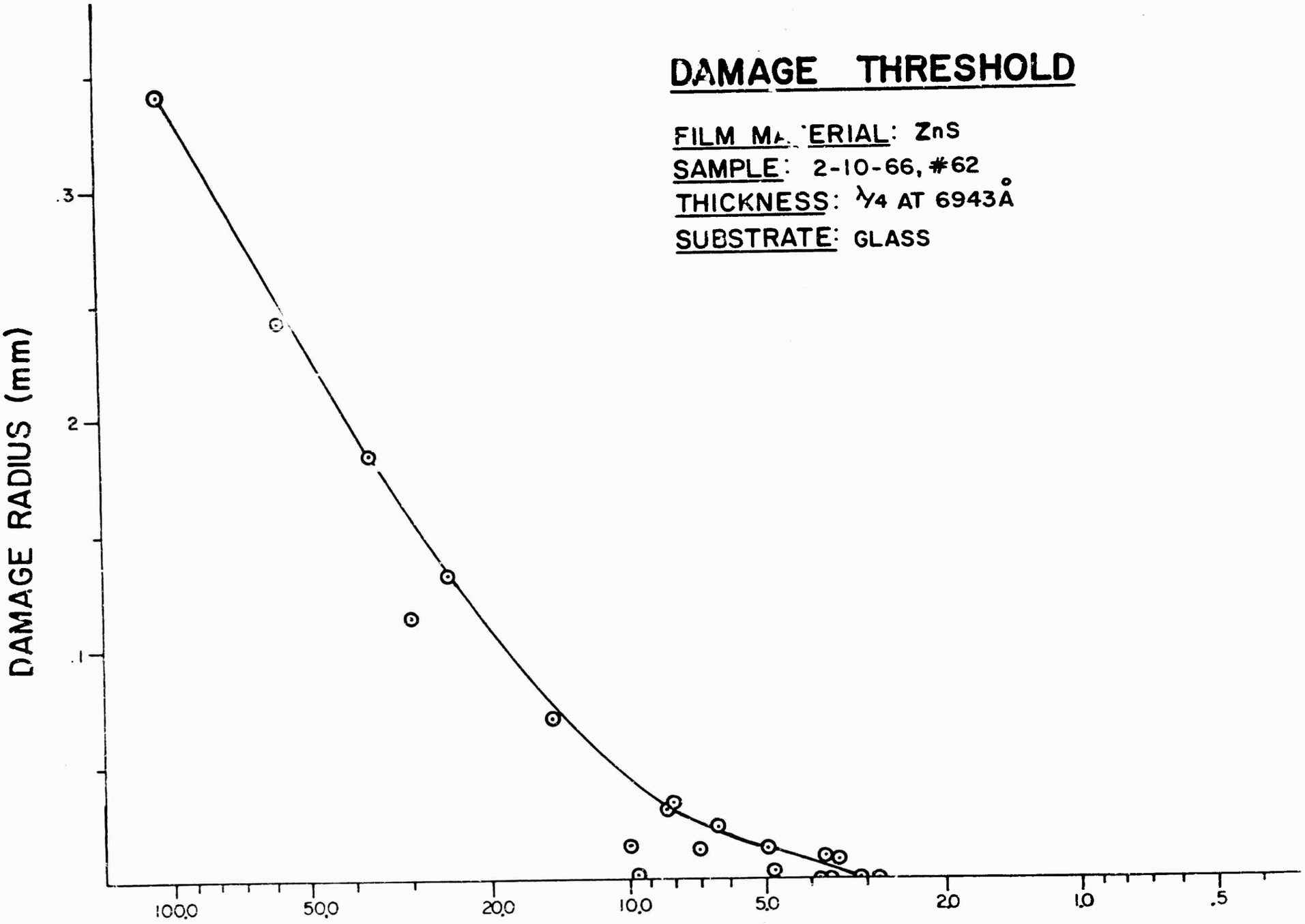
DAMAGE THRESHOLD
FILM MATERIAL: ZnS
SAMPLE: 2-10-66, #62
THICKNESS: λ/4 AT 6943Å
SUBSTRATE: GLASS
DAMAGE RADIUS (mm)
.3
2
.1
100.0
50.0
20.0
10.0
5.0
2.0
1.0
.5
PEAK ENERGY DENSITY (joules/cm²)

FIG. 35

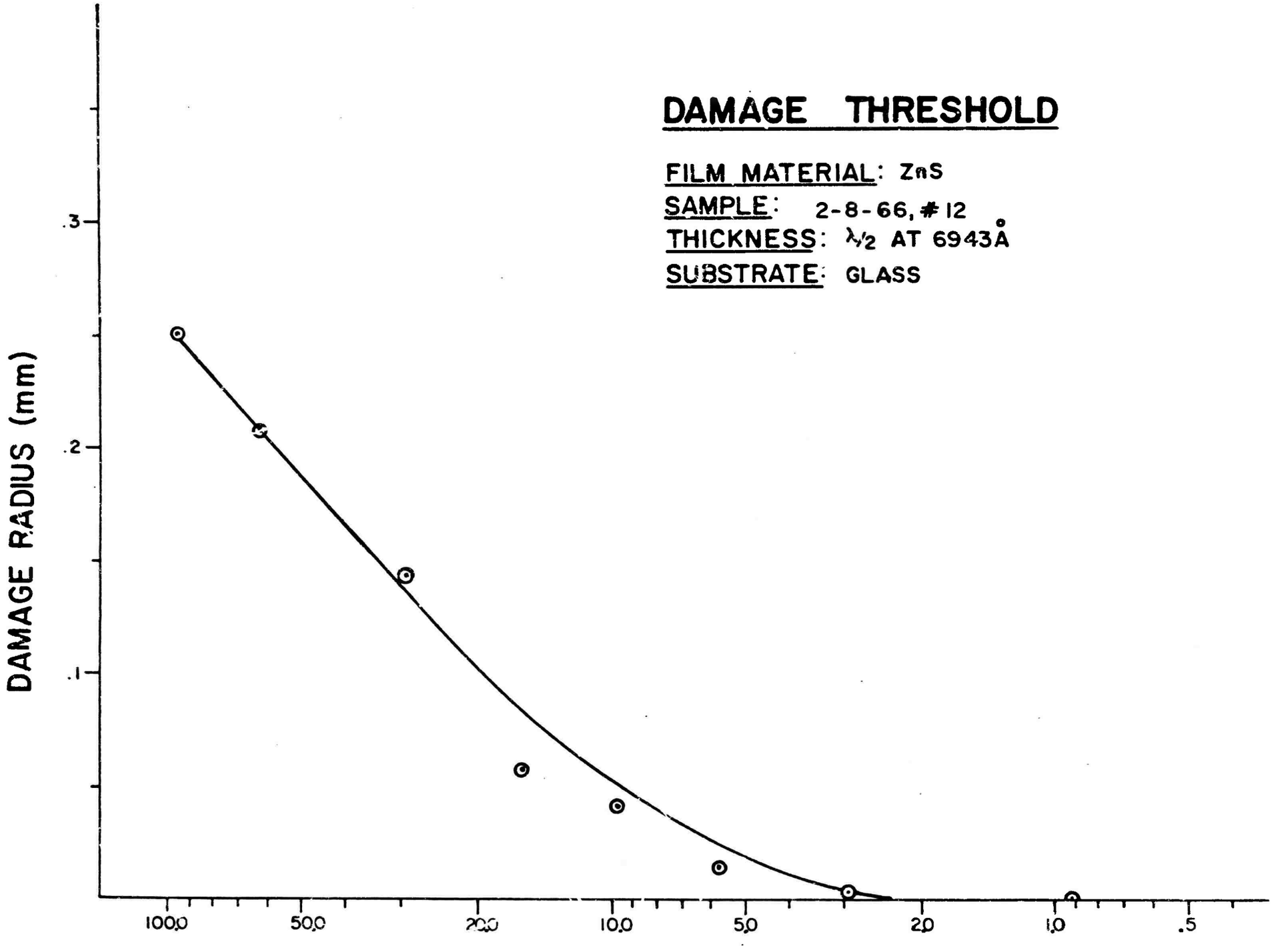
DAMAGE THRESHOLD
FILM MATERIAL: ZnS
SAMPLE: 2-8-66, #12
THICKNESS: λ/2 AT 6943Å
SUBSTRATE: GLASS
DAMAGE RADIUS (mm)
.3
.2
.1
100.0
50.0
20.0
10.0
5.0
2.0
1.0
.5
PEAK ENERGY DENSITY (joules/cm²)

FIG. 36

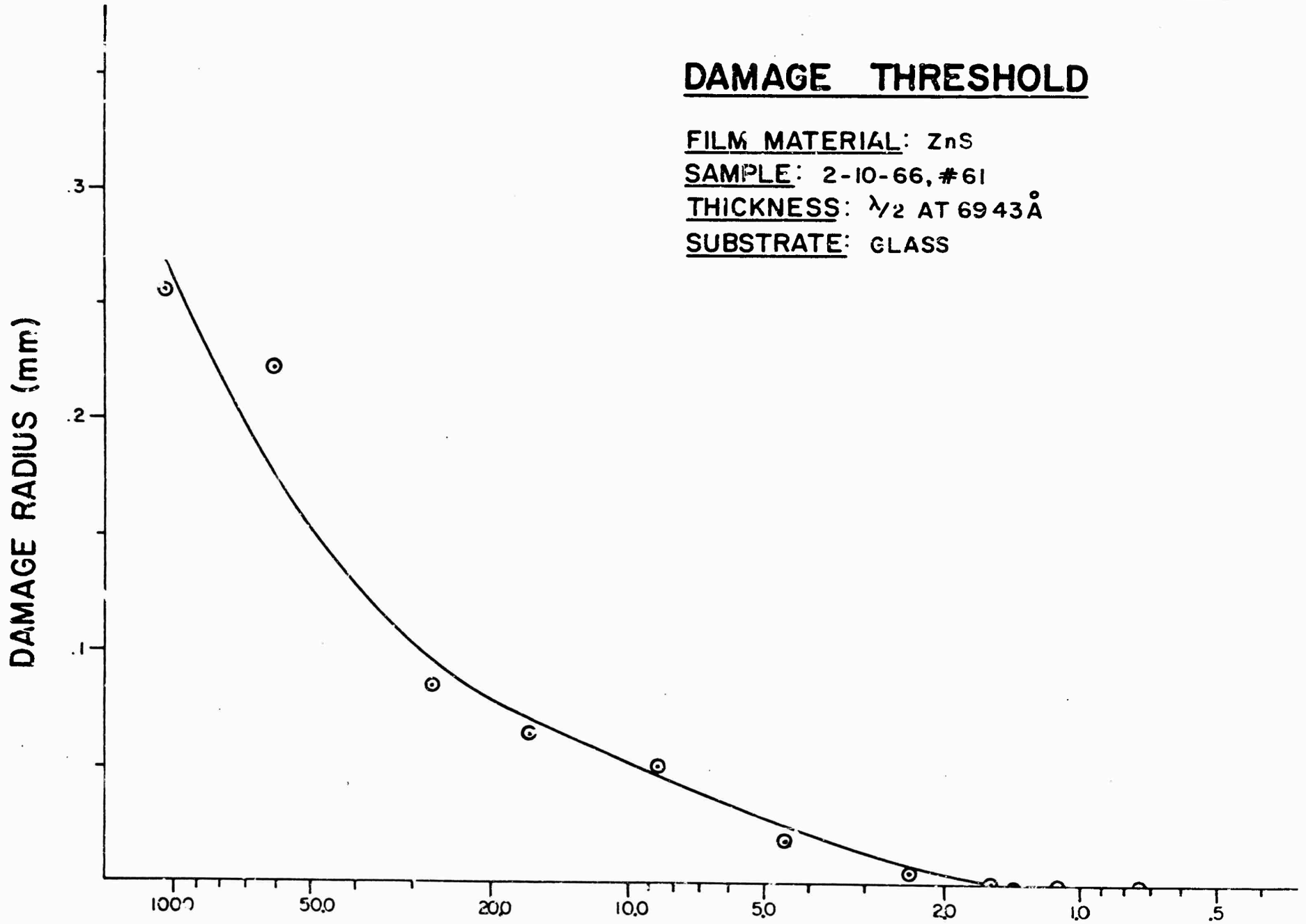
DAMAGE THRESHOLD
FILM MATERIAL: ZnS
SAMPLE: 2-10-66, #61
THICKNESS: λ/2 AT 6943Å
SUBSTRATE: GLASS
DAMAGE RADIUS (mm)
.3
.2
.1
100.0
50.0
20.0
10.0
5.0
2.0
1.0
.5
PEAK ENERGY DENSITY (joules/cm²)

FIG. 37

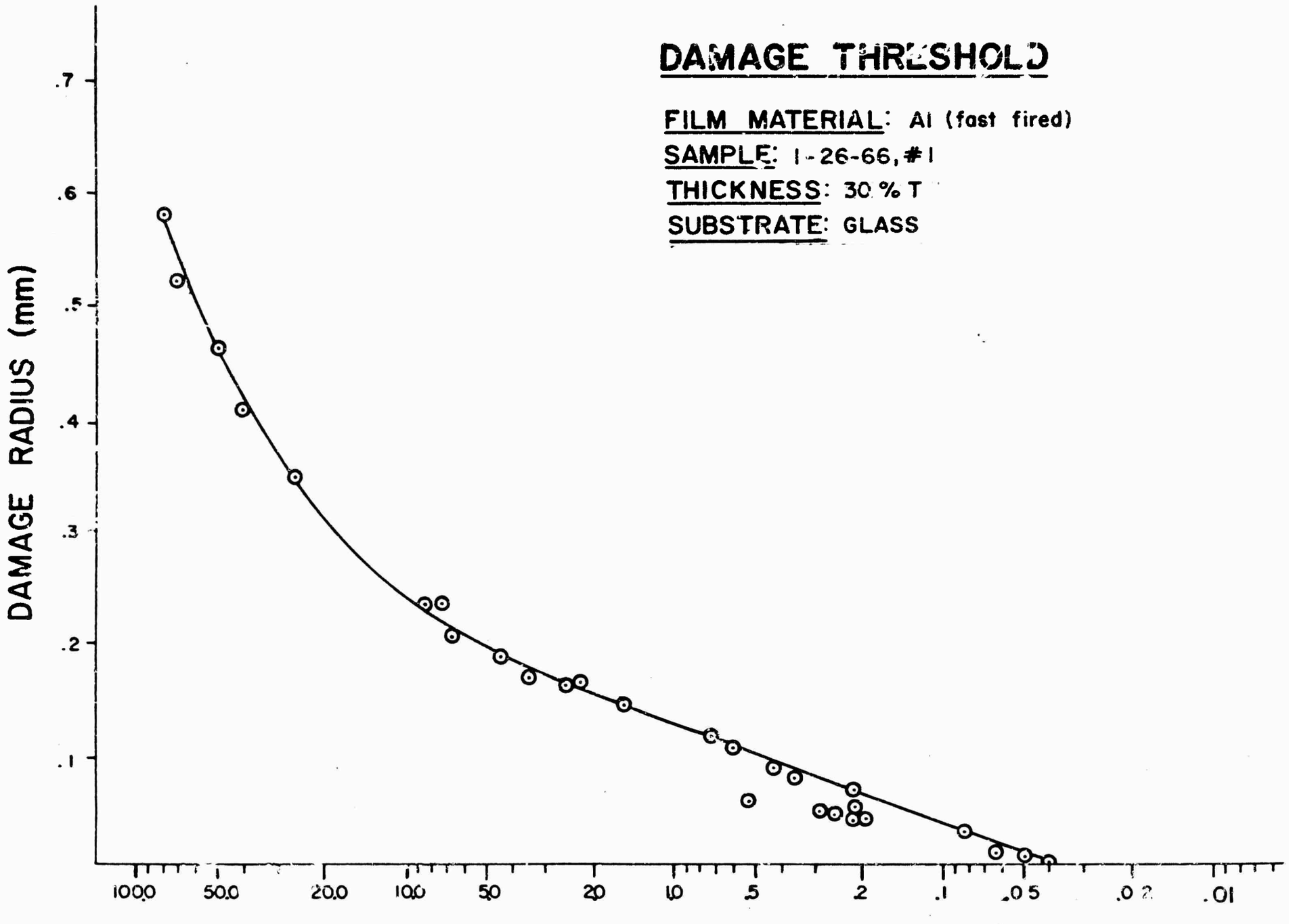
DAMAGE THRESHOLD
FILM MATERIAL: Al (fast fired)
SAMPLE: 1-26-66, #1
THICKNESS: 30 % T
SUBSTRATE: GLASS
DAMAGE RADIUS (mm)
.7
.6
.5
.4
.3
.2
.1
100.0
50.0
20.0
10.0
5.0
2.0
1.0
.5
.2
.1
.05
.02
.01
PEAK ENERGY DENSITY (joules/cm²)

FIG. 38

DAMAGE THRESHOLD

FILM MATERIAL: INCONEL
SAMPLE: 2-23-66, #2 In
THICKNESS: 7.0%T
SUBSTRATE: GLASS

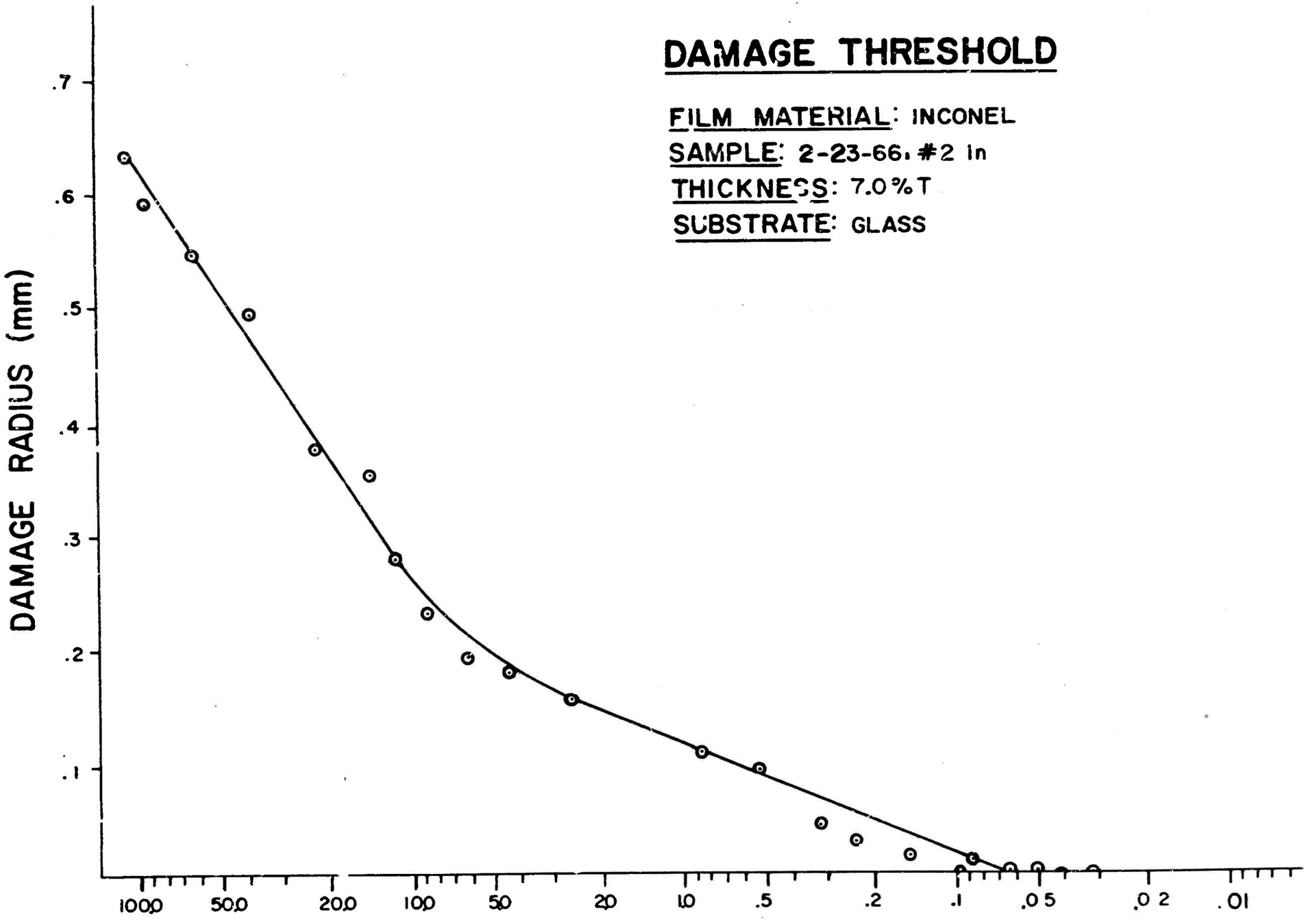

FIG. 39

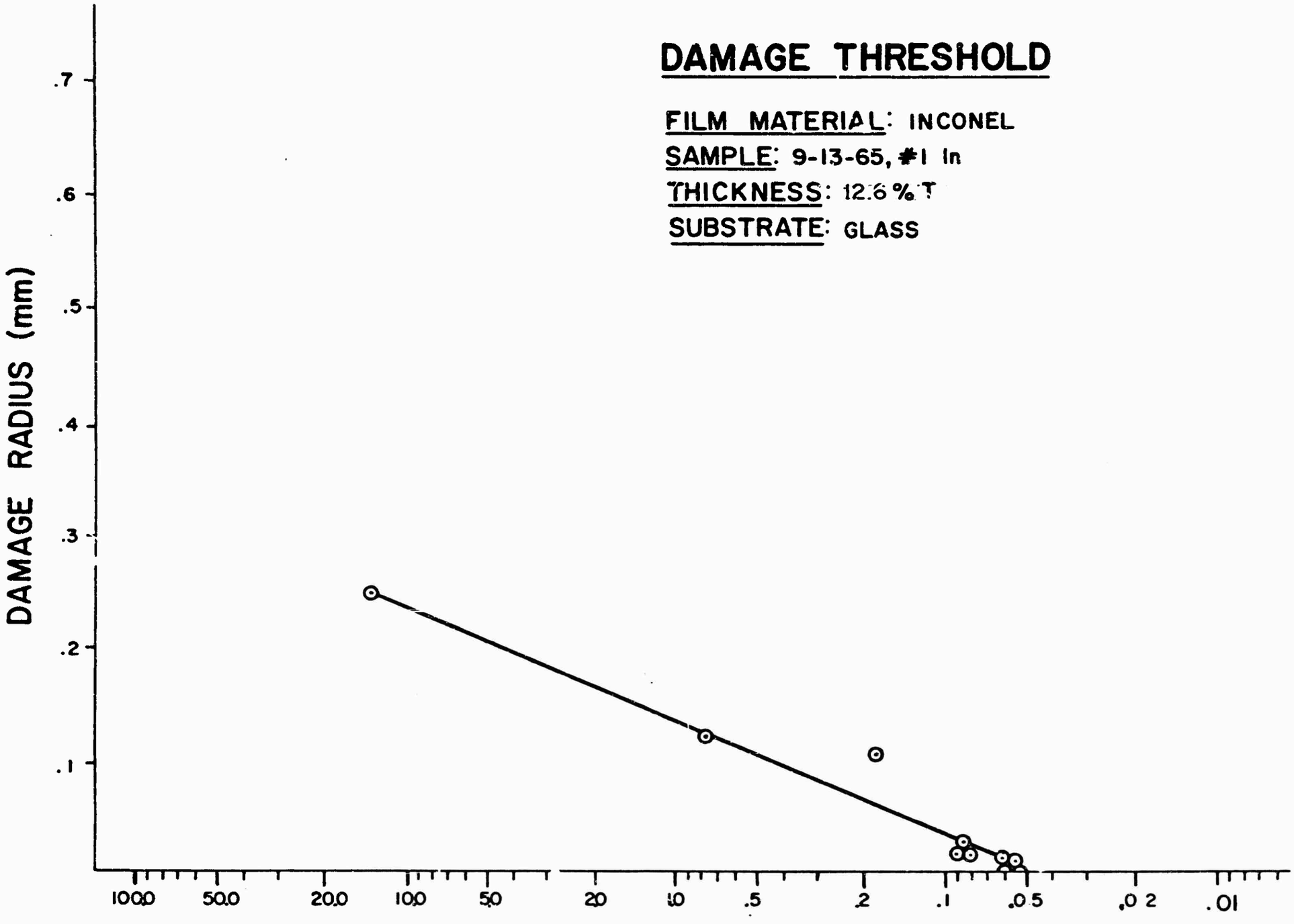
DAMAGE THRESHOLD
FILM MATERIAL: INCONEL
SAMPLE: 9-13-65, #1 In
THICKNESS: 12.6% T
SUBSTRATE: GLASS
DAMAGE RADIUS (mm)
.7
.6
.5
.4
.3
.2
.1
1000
500
200
100
50
20
10
5
2
1
.5
.2
.1
.05
.02
.01
PEAK ENERGY DENSITY (joules/cm²)

FIG. 40

THRESHOLDS OF VARIOUS FILMS OF λ/4 THICKNESS

(COMPARED WITH ALUMINUM AND INCONEL FILMS)

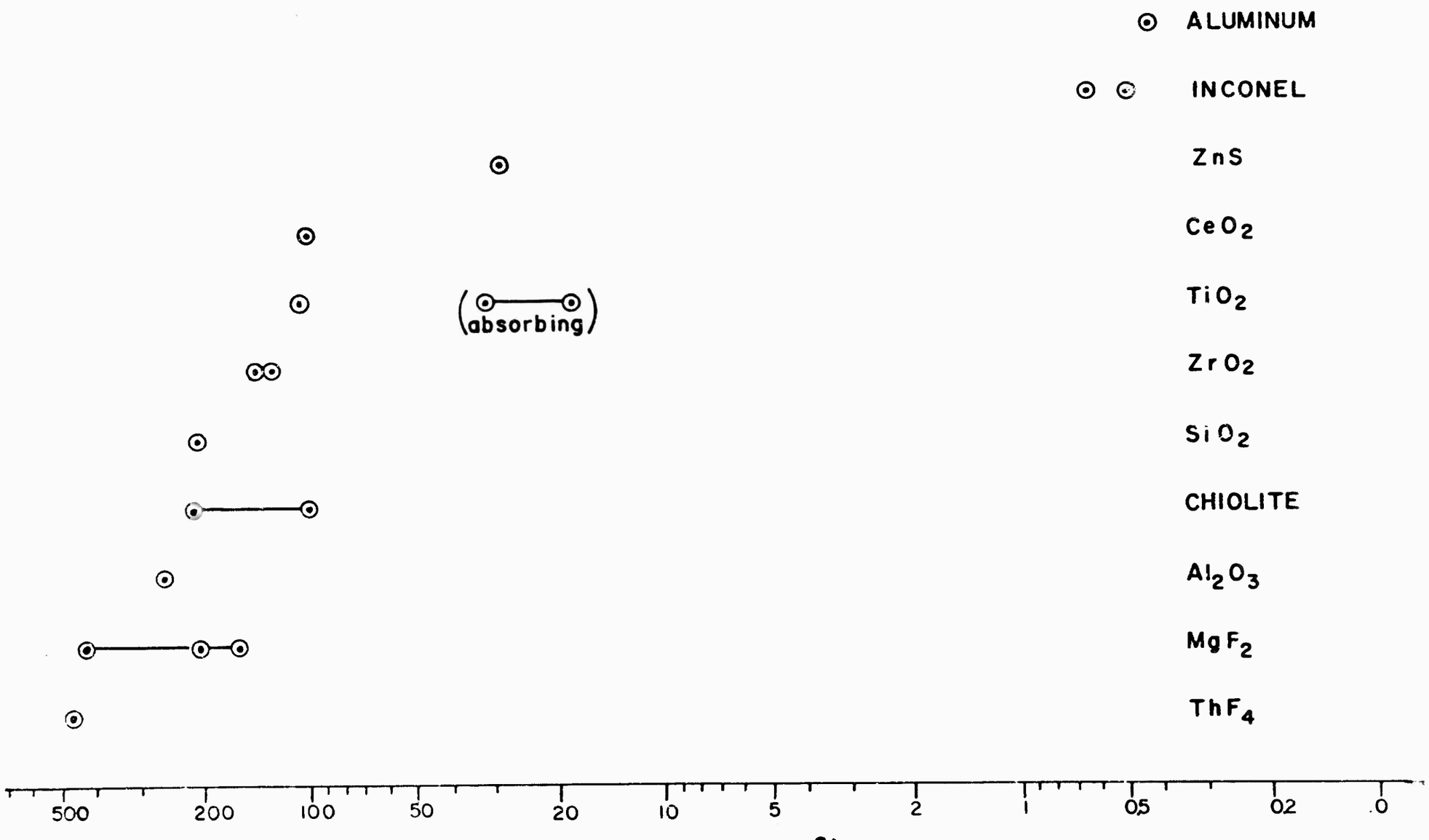

FIG. 41

THRESHOLDS OF VARIOUS FILMS OF $\lambda/2$ THICKNESS

(COMPARED WITH ALUMINUM AND INCONEL FILMS)

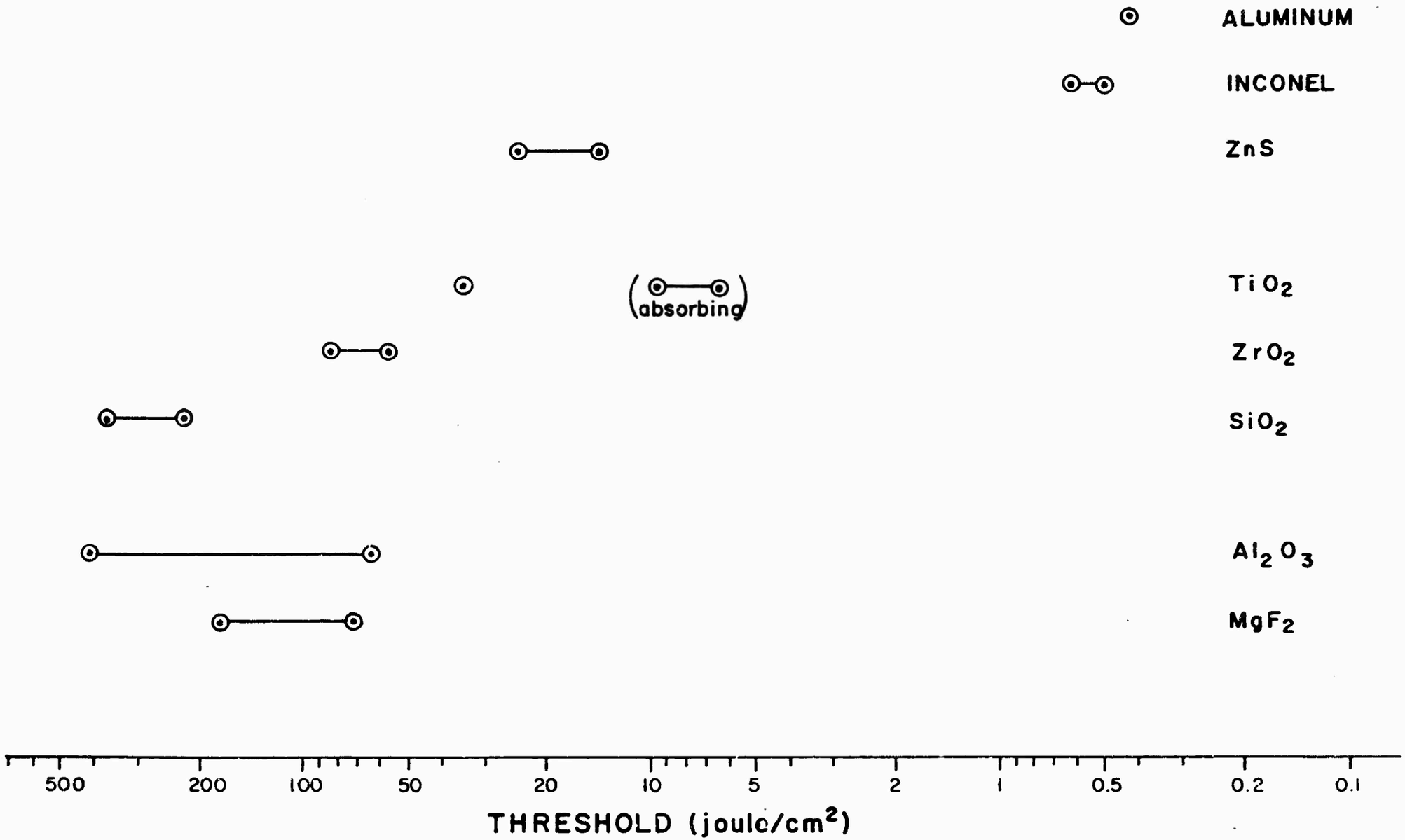

FIG. 42

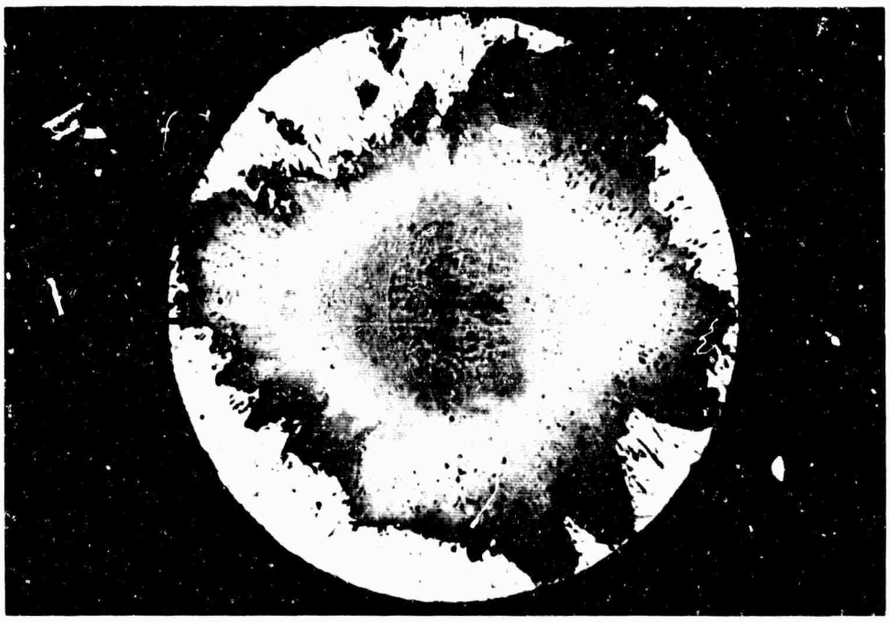

SCALE:

100μ/cm

FILM MATERIAL: TiO_2
SAMPLE: 12-22-65, # 2
THICKNESS: λ/2 at 6943 Å
INCIDENT ENERGY: .11 Joules

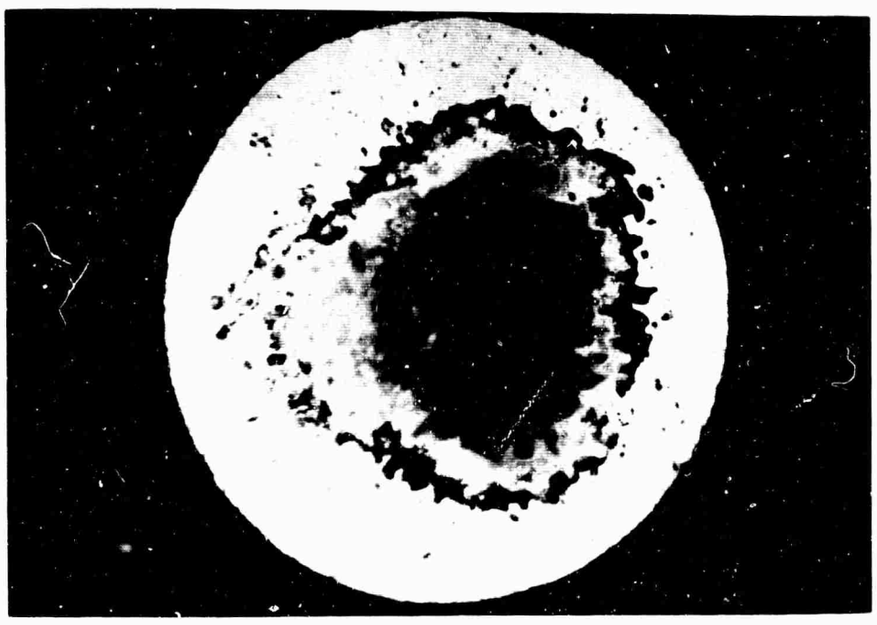

SCALE:

50μ/cm

FILM MATERIAL: TiO_2
SAMPLE: 12-22-65, # 2 (not baked)
THICKNESS: λ/2 at 6943 Å
INCIDENT ENERGY: .012 Joules

FIGURE 43

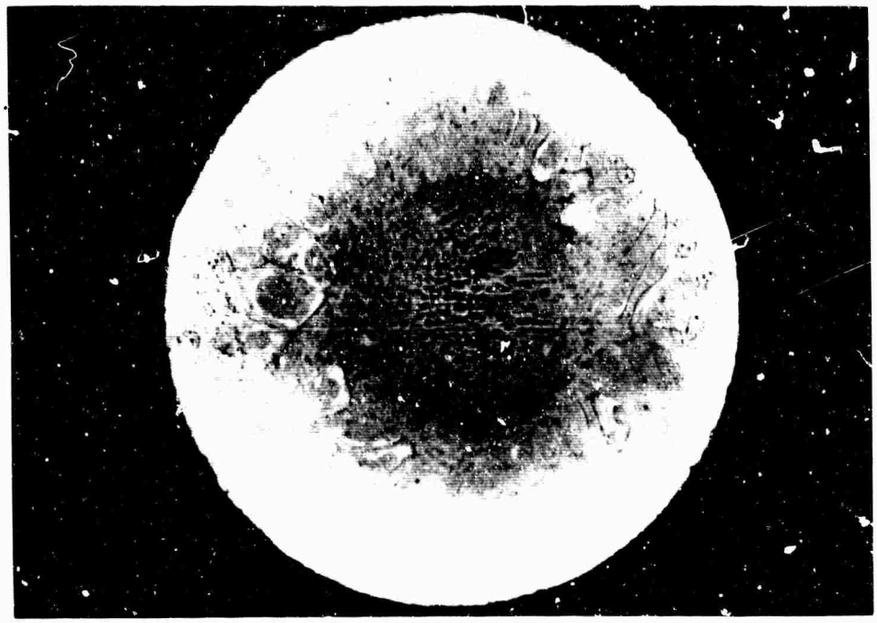

SCALE:

100μ/cm

FILM MATERIAL: TiO_2
SAMPLE: 12-22-65, # 2A (baked)
THICKNESS: λ/2 at 6943 Å
INCIDENT ENERGY: .15 joules

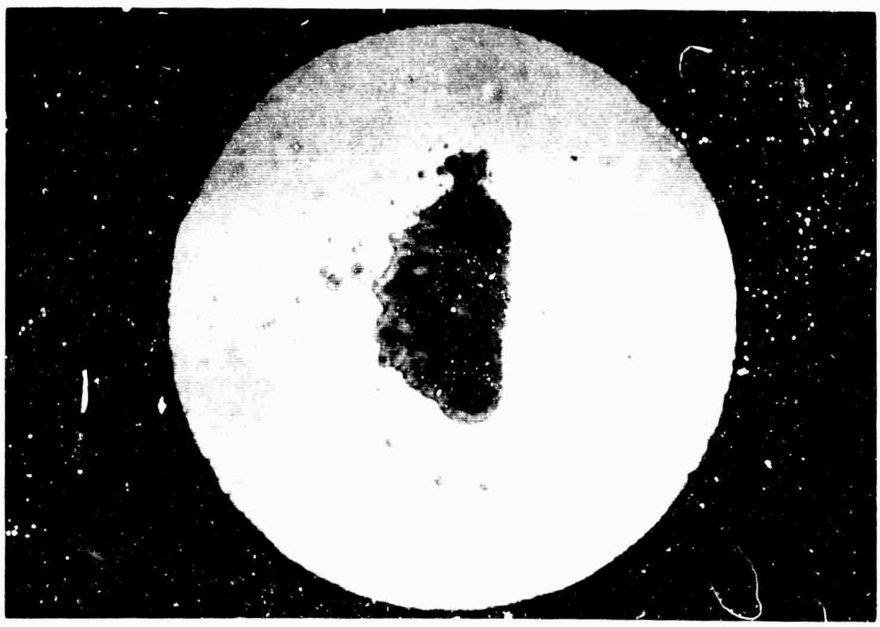

SCALE:

50μ/cm

FILM MATERIAL: TiO_2
SAMPLE: 12-22-65, #2A (baked)
THICKNESS: λ/2 at 6943 Å
INCIDENT ENERGY: .015 joules

FIGURE 44

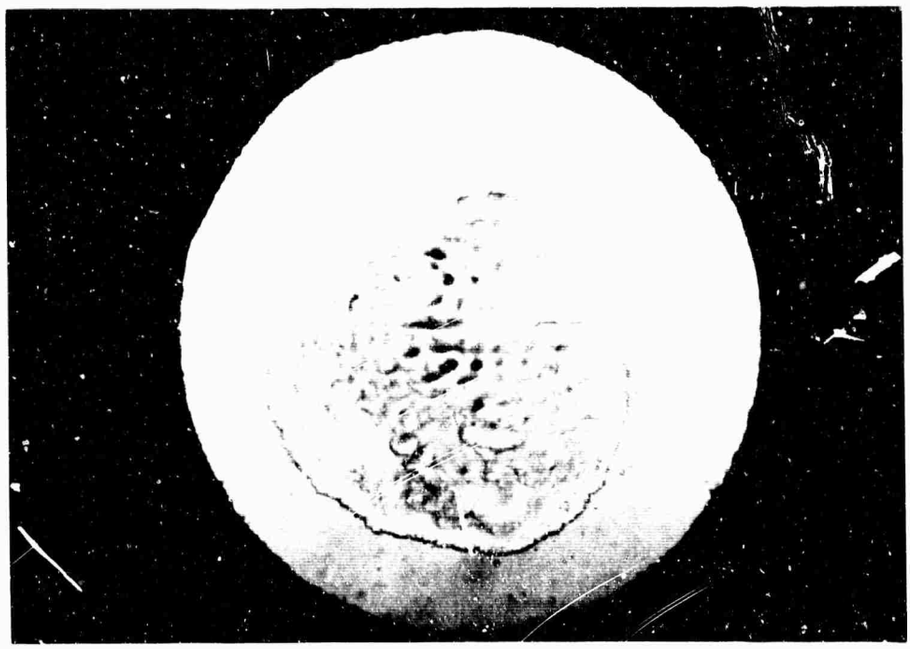

SCALE:

50 μ / cm

FILM MATERIAL: ZrO_2
SAMPLE: 6-10-65, # 1
THICKNESS: λ/4 at 6943 Å
INCIDENT ENERGY: .10 joules

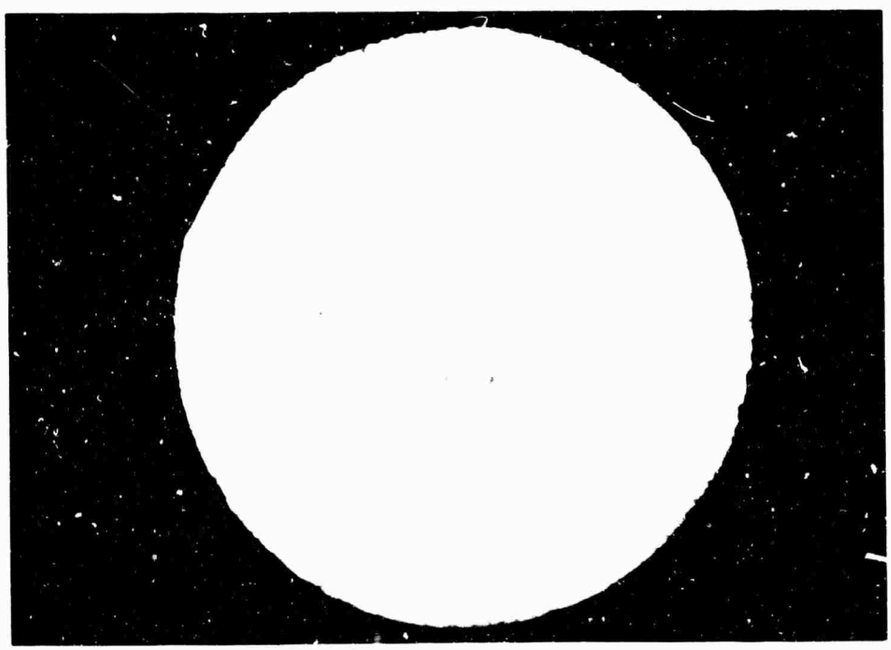

SCALE:

50 μ / cm

FILM MATERIAL: ZrO_2
SAMPLE: 6-10-65, # 1
THICKNESS: λ/4 at 6943 Å
INCIDENT ENERGY: .025 joules

FIGURE 45

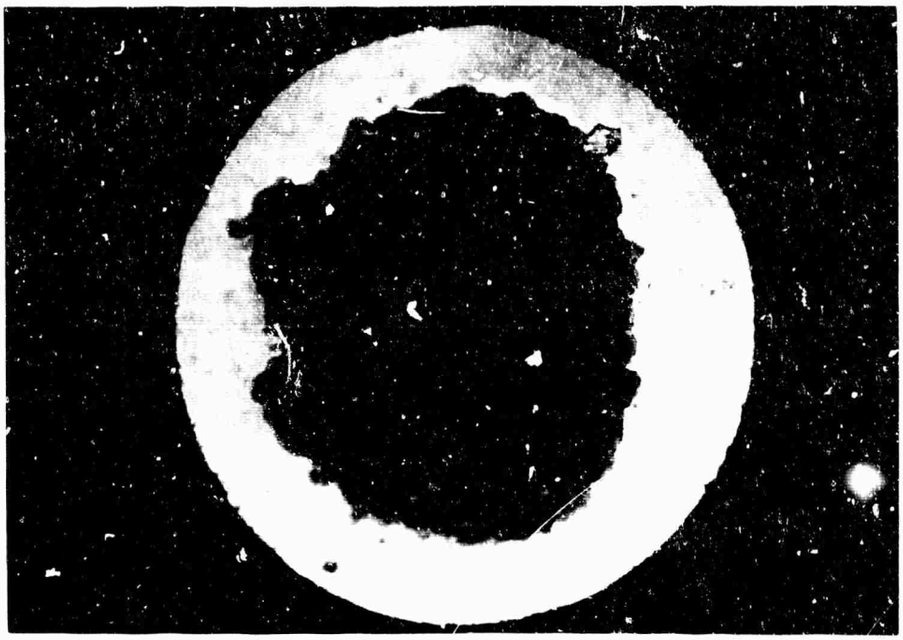

SCALE:

50 μ / cm

FILM MATERIAL: CeO_2
SAMPLE: 6-11-65, # 1
FILM THICKNESS: λ/4 at 6943 Å
INCIDENT ENERGY: 11 joules

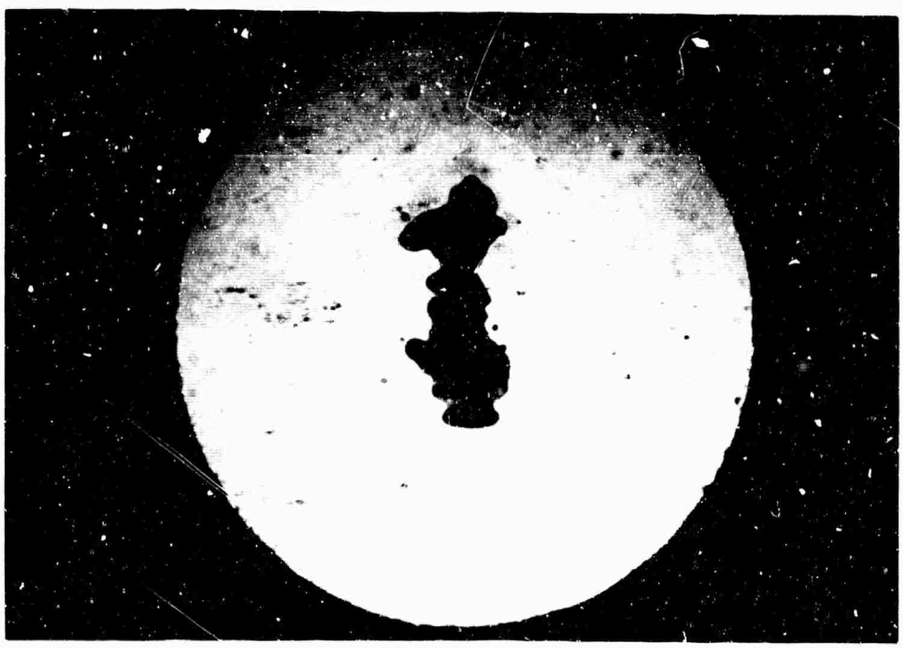

SCALE:

50 μ/cm

FILM MATERIAL: CeO_2
SAMPLE: 6-11-65, # 1
THICKNESS: λ/4 at 6943 Å
INCIDENT ENERGY: .032 joules

FIGURE 46

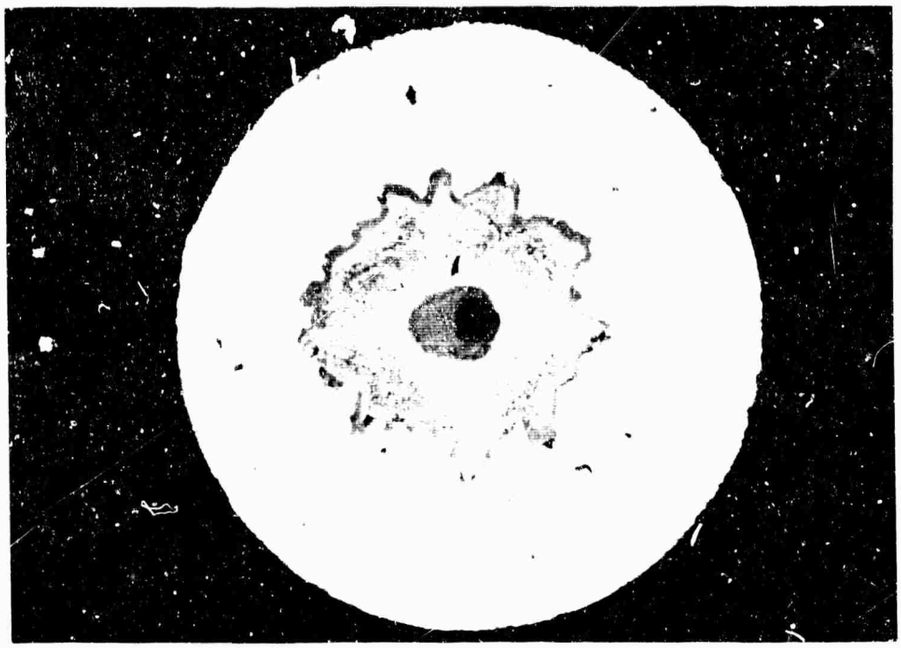

SCALE:

260 μ/cm

FILM MATERIAL: ZnS
SAMPLE: 2-10-66, # 62
THICKNESS: λ/4 at 6943 Å
INCIDENT ENERGY: .085 joules

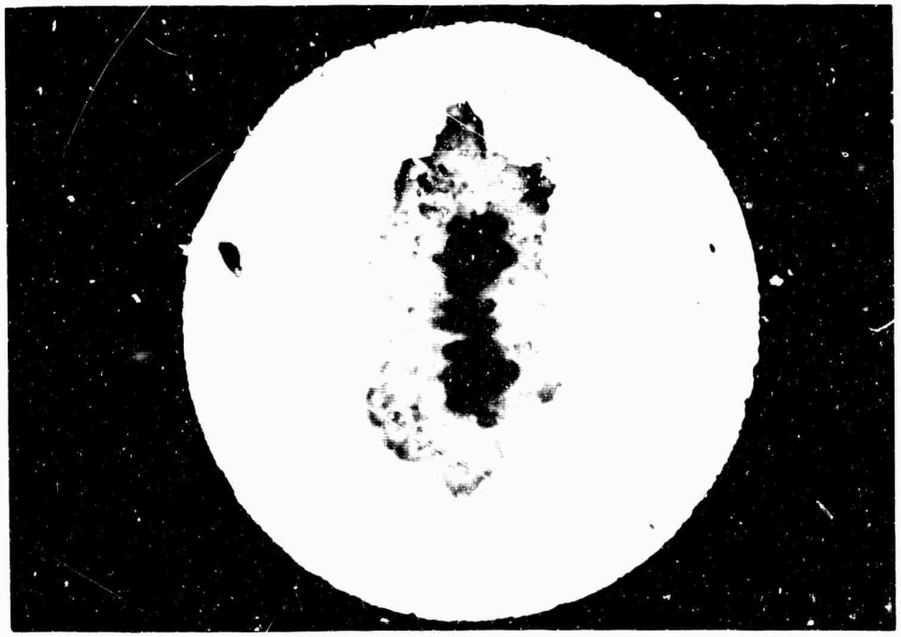

SCALE:

50 μ/cm

FILM MATERIAL: ZnS
SAMPLE: 2-10-66, # 62
THICKNESS: λ/4 at 6943 Å
INCIDENT ENERGY: .011 joules

FIGURE 47

SCALE:

100 μ/cm

FILM MATERIAL: ThF_4
SAMPLE: 6-11-65, # 3A
THICKNESS: λ/4 at 6943 Å
INCIDENT ENERGY: .12 joules

SCALE:

50 μ/cm

FILM MATERIAL: ThF_4
SAMPLE: 6-11-65, # 3A
THICKNESS: λ/4 at 6943 Å
INCIDENT ENERGY: .053 joules

FIGURE 48

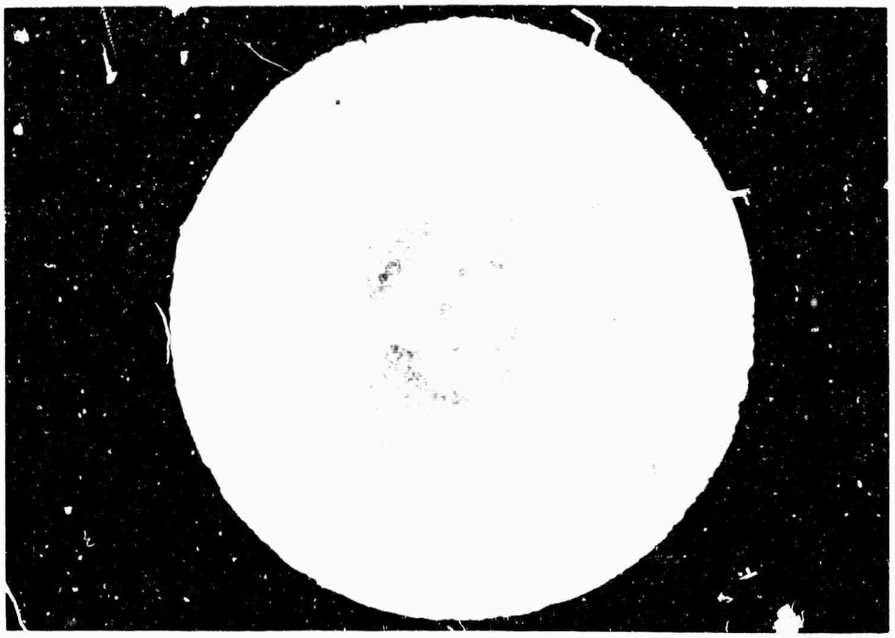

SCALE:

100 μ/cm

FILM MATERIAL: Al_2O_3
SAMPLE: 2-21-66, # 34
THICKNESS: λ/2 at 6943 Å
INCIDENT ENERGY: .082 joules

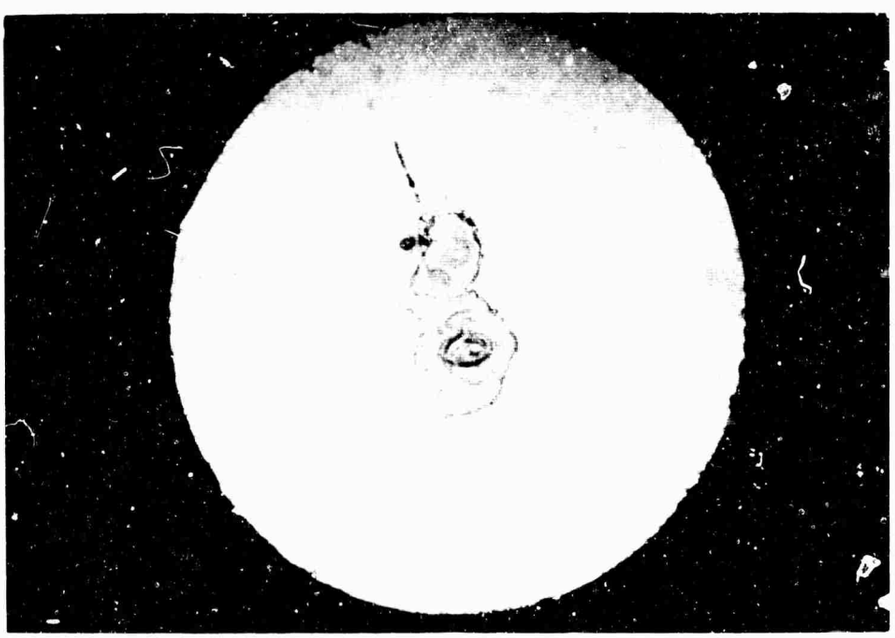

SCALE:

50 μ/cm

FILM MATERIAL: Al_2O_3
SAMPLE: 2-21-66, #34
THICKNESS: λ/2 at 6943 Å
INCIDENT ENERGY: .035 joules

FIGURE 49

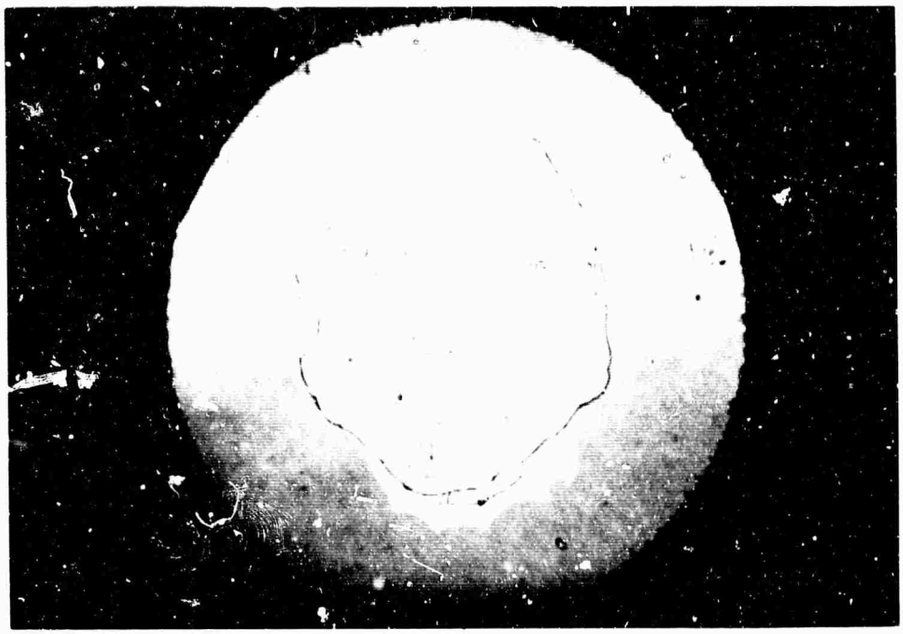

SCALE:

100 μ/cm

FILM MATERIAL: CHIOLITE
SAMPLE: 10-18-65, # 1C
THICKNESS: λ/4 at 2u
INCIDENT ENERGY: .12 joules

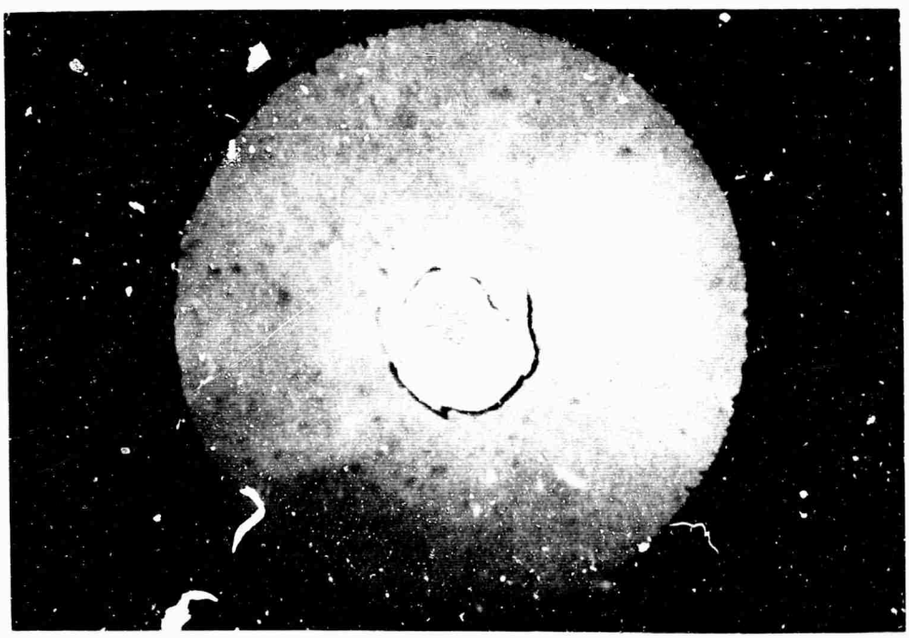

SCALE:

50 μ/cm

FILM MATERIAL: CHIOLITE
SAMPLE: 10-18-65, # 1C
THICKNESS: λ/4 at 2u
INCIDENT ENERGY: .089 joules

FIGURE 50

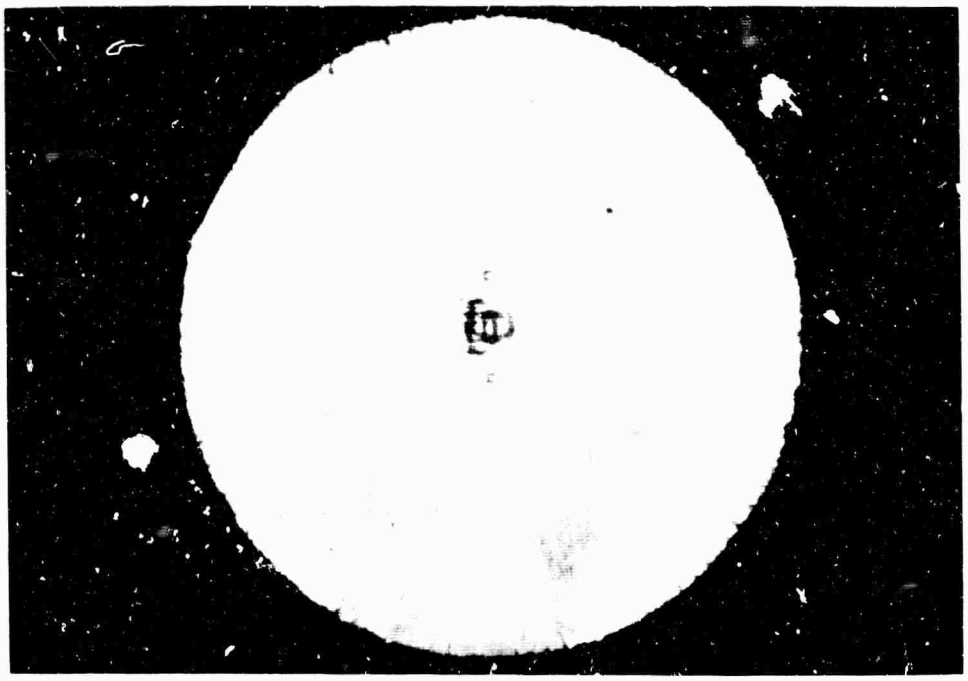

SCALE:

100 μ / cm

FILM MATERIAL : MgF_2
SAMPLE: 2-17-66, # 52
THICKNESS: λ/2 at 6943 Å
INCIDENT ENERGY : .054 joules

SCALE:

50 μ / cm

FILM MATERIAL : SiO_2
SAMPLE : 2-21-66, #23
THICKNESS : λ/2 at 6943 Å
INCIDENT ENERGY : .046 joules

FIGURE 51